AD-A111 886 CONSTRUCTION ENGINEERING RESEARCH LAB (ARMY) CHAMPAIGN IL F/G 11/6
WELDABILITY CHARACTERISTICS OF CONSTRUCTION STEELS A36, A514, A--ETC(U)
DEC 81 R A WEBER
UNCLASSIFIED CERL-TR-M-302 NL

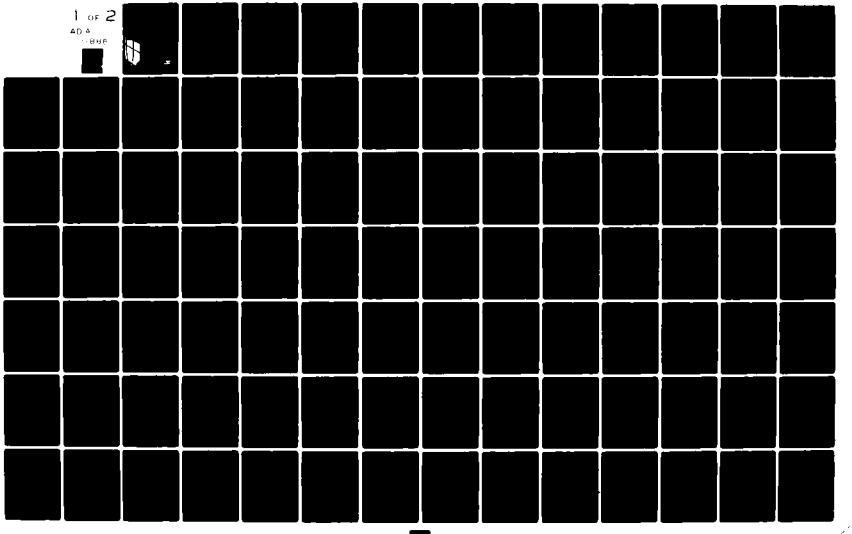

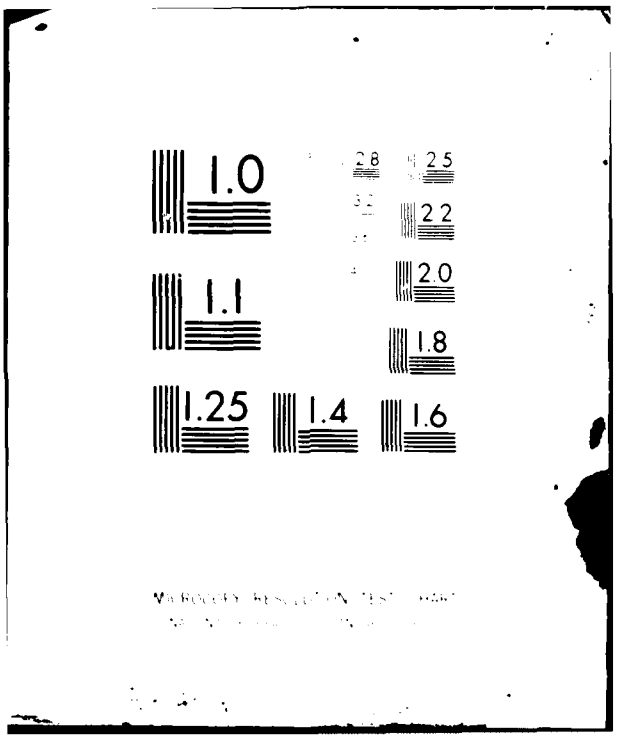
1.0
1.1
1.25
1.4
1.6
1.8
2.0
2.2
2.5

(12)

construction
engineering
research
laboratory

United States Army
Corps of Engineers
...Serving the Army
...Serving the Nation

TECHNICAL REPORT M-302
December 1981
Welding Criteria for Construction Welding
Based on Process Variables and Flaw Criticality

WELDABILITY CHARACTERISTICS OF CONSTRUCTION STEELS A36, A514, AND A516

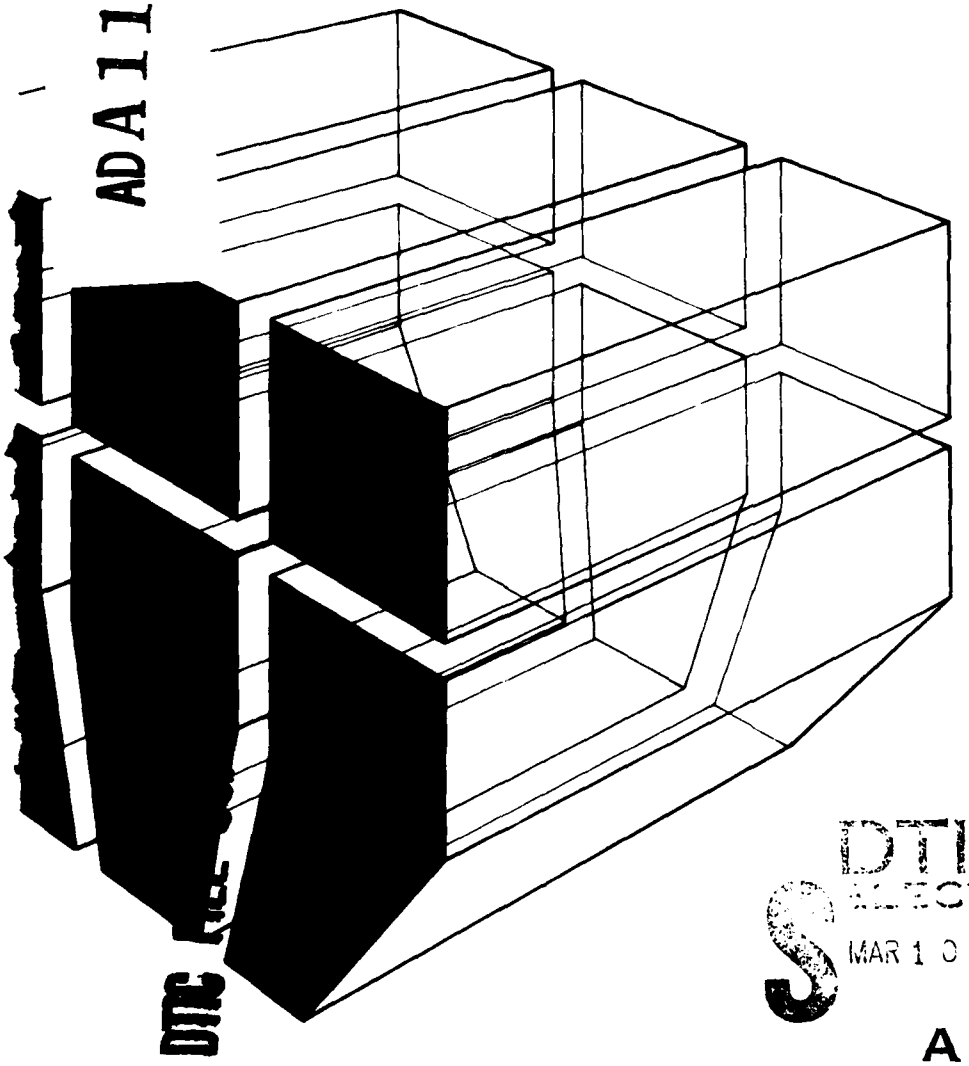

by
R. A. Weber

REPORT DOCUMENTATION PAGE

READ INSTRUCTIONS BEFORE COMPLETING FORM

1. REPORT NUMBER: CERL-TR-M-302	2. GOVT ACCESSION NO.
3. RECIPIENT'S CATALOG NUMBER	
4. TITLE (and Subtitle): WELDABILITY CHARACTERISTICS OF CONSTRUCTION STEELS A36, A514, AND A516	5. TYPE OF REPORT & PERIOD COVERED: FINAL
6. PERFORMING ORG. REPORT NUMBER	
7. AUTHOR(s): R. A. Weber	8. CONTRACT OR GRANT NUMBER(s)
9. PERFORMING ORGANIZATION NAME AND ADDRESS: U. S. ARMY CONSTRUCTION ENGINEERING RESEARCH LABORATORY P.O. Box 4005, Champaign, IL 61820	10. PROGRAM ELEMENT, PROJECT, TASK AREA & WORK UNIT NUMBERS: 4A762731AT41-C-030
11. CONTROLLING OFFICE NAME AND ADDRESS	12. REPORT DATE: December 1981
	13. NUMBER OF PAGES: 97
14. MONITORING AGENCY NAME & ADDRESS(if different from Controlling Office)	15. SECURITY CLASS. (of this report): Unclassified
	15a. DECLASSIFICATION/DOWNGRADING SCHEDULE

16. DISTRIBUTION STATEMENT (of this Report)

Approved for public release; distribution unlimited.

17. DISTRIBUTION STATEMENT (of the abstract entered in Block 20, if different from Report)

18. SUPPLEMENTARY NOTES

Copies are obtainable from the National Technical Information Service
Springfield, VA 22151

19. KEY WORDS (Continue on reverse side if necessary and identify by block number)

structural steel
weldability

20. ABSTRACT (Continue on reverse side if necessary and identify by block number)

This study determined the voltage, current, and travel speed limits necessary to ensure proper weld strength levels for three construction steels: American Society for Testing and Materials (ASTM) A36, A516, and A514.

To achieve the objective of this study, the U.S. Army Construction Engineering Research Laboratory defined voltage, current, and travel speed limits through bead-on-plate

Block 20 continued.

tests and tests to determine the tensile and impact properties of butt joint welds produced with fully automatic gas metal-arc welding and manual shielded metal-arc welding. Then the limits were refined by using the results of fabricating butt joints under high restraint conditions.

FOREWORD

This investigation was performed for the Directorate of Military Programs, Office of the Chief of Engineers (OCE), under Project Number 4A762731AT41, "Military Facilities Engineering Technology"; Work Unit 030 "Welding Criteria for Construction Welding Based on Process Variables and Flaw Criticality." The applicable QCR is 3.07.024. The OCE Technical Monitors were Mr. I. A. Schwartz, DAEN-MPE-T, and Messrs. G. Matsumura and Schneider, DAEN-MPE-B.

This investigation was performed by the Engineering and Materials (EM) Division, U.S. Army Construction Engineering Research Laboratory (CERL). CERL personnel directly involved in the study were Mr. F. H. Kisters, Ms. R. E. Tegler, and Dr. P. A. Howdyshell. Dr. R. Quattrone is Chief of EM.

COL Louis J. Circeo is Commander and Director of CERL, and Dr. L. R. Shaffer is Technical Director.

CONTENTS

TABLES

FIGURES

FIGURES (cont'd)

FIGURES (cont'd)

FIGURES (cont'd)

FIGURES (cont'd)

FIGURES (cont'd)

WELDABILITY CHARACTERISTICS OF CONSTRUCTION STEELS A36, A514, AND A516

1 INTRODUCTION

Background

For many years, the U.S. armed services have used American Society for Testing and Materials (ASTM) specification A36. This covers structural quality carbon steel shapes, plates, and bars for general and welded construction of bridges and buildings.[1] The specification restricts use of A36 very little from the standpoint of weldability – even though the carbon content of the steel may range as high as 0.29 to 0.33 percent, depending on plate thickness. These percentages are somewhat high for guaranteed adequate weldability. In addition, manganese content, another indication of weldability, is not specified in thin sections; a maximum of 1.25 percent is permitted in plates over 3/4-in. (19.1-mm) thick.

Steels other than A36 may provide better structures at an equal or lower final cost to the customer since some of these steels may be used at higher levels of design loading, thus providing a lower weight structure. The higher quality plate steels include ASTM A441, a high-strength, low-alloy structural manganese-vanadium steel plate suitable for welding; ASTM A516, a carbon steel plate for moderate and lower temperature pressure vessels; and ASTM A514, a high-strength, low-alloy structural steel with 100,000 psi (689 MPa) minimum yield strength.

In many structures built recently, the U.S. Army Corps of Engineers has taken advantage of some of the physical and mechanical property improvements under these additional specifications. However, adequate weldability safeguards are required when structures are built under special provisions for the use of higher quality steels. Weld-related failures can include structural failures attributed to lamellar tearing of plates as a result of welding, failures of structural beams caused by misapplication of the shielded metal-arc welding (SMAW) process, and failures in high temperature hot water distribution systems because of overstress caused by lack-of-penetration defects.

[1] *Steel, Structural*, ASTM A36 (American Society for Testing and Materials [ASTM], 14 August 1979).

SMAW and gas metal-arc welding (GMAW) are the predominant forms of electric arc welding used today. SMAW is used about twice as often as GMAW for both field and shop fabrication. For many years, the only way to control these welding processes has been to limit the heat input (measured in Joules per linear inch of weld). Heat input is determined by using the simple relation:

$$\text{Heat input} = \frac{\text{voltage} \times \text{current}}{\text{travel speed}} \qquad \text{[Eq 1]}$$

The heat input limit was generally set to a maximum of 55 kJ/in. (2167 J/mm). Dorschu, and Schultz and Jackson have shown that for a given set of parameters the strength of the weld can vary considerably.[2] Dorschu devised a method for correlating the strength of weldments to the cooling rate of the weld beads. To calculate the cooling rate, he developed a formula that includes the variables of heat input, plate thickness, and initial plate temperature. In general form, this relation is:

$$\text{Cooling rate} = \frac{\text{thickness} \times [\text{test temperature} - \text{plate temperature}]}{\text{heat input}} \qquad \text{[Eq 2]}$$

Dorschu has shown that with ASTM A201 mild steel up to 2-in. (50.8-mm) thick, the yield strength of the weld metal is proportional to the cooling rates; at high cooling rates, yield strengths can be increased from 15 to 20 ksi (103.4 to 137.9 MPa). Schultz and Jackson have gone one step further and determined that for a 5 Ni-Cr-Mo-V steel the arc voltage has no significant effect on the cooling rate, which appears to be determined by the current and travel speed only. Schultz and Jackson conclude that there is a clear relationship between cooling rate and nugget area which, therefore, becomes a useful indicator of weld metal mechanical properties under the influence of weld cooling rate. Schultz and Jackson define nugget area as the cross section of a single weld bead. This nugget area equation is:

$$\text{Nugget area} = \text{constant} \times \frac{\text{arc current}^{1.55}}{\text{travel speed}^{0.903}} \qquad \text{[Eq 3]}$$

[2] K. E. Dorschu, "Control of Cooling Rates in Steel Weld Metal," *Welding Journal*, Vol 47 (February 1968), Research Supplement; B. L. Schultz and C. E. Jackson, "Influence of Weld Bead Areas on Weld Mechanical Properties," *Welding Journal*, Vol 53 (June 1974), Research Supplement.

Unfortunately, Schultz and Jackson do not describe the way to determine the voltage, current, and travel speed limits that will ensure proper weld strength levels.

The U.S. Army Construction Engineering Research Laboratory (CERL) has conducted a three-part research program to determine these limits for various plate steels and welding electrodes. In the first part of the study, the limits on voltage, current, and electrode travel speed were determined on the basis of bead-on-plate welds examined for quality.[3] The second part of the study was intended to refine these limits using their interrelationship with nugget area and heat input based on butt weld mechanical properties. This work, detailed in CERL Technical Report M-278, concentrated on the limits for SMAW and GMAW electrodes combined with a carbon steel (A36), a pressure vessel steel (A516), and a high-strength, low-alloy steel (A514).[4] The third part of the study was intended to refine these limits by looking at effects of high restraint on the weld joint; the effects on mechanical properties as well as the problem of cracking in the weld joint under the influence of high restraint were to be investigated.

This report documents additional data from SMAW and GMAW butt weld tests in the second part of the study, and presents data collected during the third part.

Objective

The objective of the portion of the study reported here was to determine the voltage, current, and travel speed limits necessary to ensure proper weld strength levels for construction steels.

Mode of Technology Transfer

The information in this report is part of a research effort designed to maintain Corps of Engineers Guide Specifications 05141 and 15116 and Army Technical Manuals (TM) 5-805-7 and 9-237.[5]

[3] R. A. Weber, *Determination of Arc Voltage, Amperage, and Travel Speed Limits by Bead-on-Plate Welding*, Technical Report M-197/ADA033684 (U.S. Army Construction Engineering Research Laboratory [CERL], December 1976).

[4] R. A. Weber, *Determination of the Effect of Current and Travel Speed of Gas Metal-Arc Welding on the Mechanical Properties of A36, A516, and A514 Steels*, Technical Report M-278/ADA085342 (CERL, May 1980).

[5] *Welding, Structural*, Corps of Engineers Guide Specification (CEGS) 05141 (Department of the Army [DA], Office of the Chief of Engineers [OCE]; *Welding, Mechanical*, CEGS 15116 (DA, OCE, October 1974); *Welding: Design, Procedures, and Inspection*, Technical Manual (TM) 5-805-7 (Headquarters [HQ], DA, March 1968); *Operator Manual: Welding Theory and Application*, TM 9-237 (HQ, DA, October 1976).

2 APPROACH

CERL achieved the objective of this study by defining voltage, current, and travel speed limits through bead-on-plate tests and tests to determine the tensile and impact properties of butt joint welds produced with fully automatic GMAW and manual SMAW in carbon steel (A36), pressure vessel steel (A516), and high-strength, low-alloy steel (A514). Then the limits were refined by using the results of fabricating butt joints under high restraint conditions.

Materials

Electrode technology has been improved to the point where many types of electrodes are now available to respond to a wide variety of welding problems. The American Welding Society (AWS) has developed a classification system for steel welding electrodes based on some of the electrodes' characteristics. The SMAW classification codes are made up of an E and four or five numbers (EXXYZ). The E designates that the material is an electrode. The first two numbers, XX, give the deposited weld metal tensile strength in thousands of pounds per square inch (ksi). That is, an electrode with an E60YZ classification would have a minimum deposited tensile strength of 60,000 psi (4.13 MPa). This tensile strength designation can be 60, 70, 80, 100 or 110. The number represented by Y – either 1 or 2 – indicates the welding position in which the electrode can be used. A 1 means that the electrode can be used in all positions – flat, horizontal, vertical, and overhead; a 2 indicates that usage is limited to flat or horizontal fillet welds. The last term in the classification, Z, can be any number from 0 through 8. These numbers indicate major coating constituents and welding current limitations as shown in Table 1.

Table 1
Coatings and Current Designation

Z	Coating Types	Current Types
0	High cellulose sodium*	dc, reversed polarity
1	High cellulose potassium	ac or dc, reversed polarity
2	High titania sodium	ac or dc, straight polarity
3	High titania potassium	ac or dc, either polarity
4	Iron powder titania	ac or dc, either polarity
5	Low hydrogen sodium	dc, reversed polarity
6	Low hydrogen potassium	ac or dc, reversed polarity
7	Iron powder, iron oxide	ac or dc, either polarity**
8	Iron powder, low hydrogen	ac or dc, reversed polarity

*Except when preceded by a 2; in that case, it is high iron oxide, ac or dc, either polarity.
**Reversed polarity is not recommended for horizontal fillets.

The classification system for GMAW electrodes is somewhat simpler. The first three or four characters, EXX or EXXX, have the same meaning as in the SMAW code; the only difference is that the tensile strength designations for GMAW wires range from 70 to 120. The next digit is either an S or U. An S means that the electrode has no coating and is a solid wire. A U means that the solid wire has an emissive coating. The final digit can be any number from 1 through 6, or the letter G. The numbers refer to different chemical compositions – in particular, carbon and silicon contents. The G represents a general classification which has no chemistry restrictions, except that nickel, chromium, molybdenum, or vanadium cannot be intentionally added.

The plate steels (by ASTM code numbers) and the electrodes (by AWS code numbers) used in the bead-on-plate investigation are identified in Table 2. Selection of electrode types for each plate material was based on the AWS *Structural Welding Code*, D1.1.[6] Table 3 identifies the three plate materials and four electrode types used for the butt weld and the high restraint joint investigations, which concentrated on one steel type from each of three categories frequently used in Corps construction:

1. Carbon steel (ASTM A36)
2. Pressure vessel steel (ASTM A516)
3. High-strength, low-alloy steel (ASTM A514)

The tensile properties for these three steel plates are listed in Table 4. The results of dynamic tear impact tests are presented in Figures 1, 2, and 3. The electrode types were selected for use with these plate steels based on AWS D1.1, and the common usage for Corps construction. The tensile requirements for the four types of electrodes used are presented in Table 5.

Table 2
Materials Used in Bead-on-Plate Study

Plate Material (ASTM No.)	Electrodes (AWS No.)	
	GMAW	SMAW
A36	E70S-2, E70S-3 E70S-4, E70S-6	E6010, E6011 E6013, E7018, E7024
A242	E70S-2, E70S-3 E70S-4, E70S-6	E7018, E7024
A441	E70S-2, E70S-3 E70S-4, E70S-6	E7018, E7024
A514	E120S-1	E11018
A527	E70S-2, E70S-3 E70S-4, E70S-6	E7018, E7024
A588	E70S-2, E70S-3 E70S-4, E70S-6	E7018, E7024
A710	--	E8018

Experimental Procedures

The investigation was divided into three parts. The first was a series of bead-on-plate welds. For this work, all plate material was cut to approximately 12 by 18 in. (300 by 500 mm) using an oxyacetylene cutting apparatus. The surface to be welded was sandblasted and wirebrushed to remove oxides and paints. The deposited weld beads were visually inspected for bead contour and shape and then sectioned for macroscopic examination. The macrospecimens were polished and etched with 5 percent Nitol and examined for penetration, reinforcement, undercut, and porosity. From all these observations, limits of voltage, current, and travel speed were determined.

The second part of this investigation involved the fabrication of V-groove butt joints and testing for mechanical properties. The weld joint used was a 60-degree included angle, single-V butt joint with a 1/8-in. (3.2-mm) root opening (Figure 4). The larger than normal joint cross-section was used to accommodate the test specimens. The weld length was approximately 30 in. (762 mm). The completed test plate was about 12 by 30 in. (305 by 762 mm). All plate material was cut and beveled using an oxyacetylene cutting apparatus, and then surface ground to remove oxides and slag from the joint area. X-ray radiography, based on Military Specification MIL-R-11468, was used to nondestructively examine each completed weldment for soundness.

One macrospecimen, three tensile specimens, and 12 impact (dynamic tear) specimens were machined from each completed sound weld. Figure 5 is a schematic of the specimen locations as machined from the weldments. The impact specimens were machined so that half were notched in weld metal and half were notched next to the weld in the heat affected zone (HAZ). They were then tested at temperatures ranging from −60 to +50°C, according to ASTM standards.[7]

[6] *Structural Welding Code*, D1.1 (American Welding Society [AWS], 1979).

[7] "ASTM Proposed Method for 5/8-in. (16-mm) Dynamic Tear Test of Metallic Materials," *1980 Annual Book of ASTM Standards*, Part 10 (ASTM, 1980).

Table 3
Materials Used for Butt Welds and Restrained Joint Welds

ASTM No.	Plate Material Thickness, in. (mm)	Electrode	Diameter, in. (mm)
A36	3/4 (19)	E7018	1/8 (3.2)
		E70S-3	1/16 (1.6)
A516, Grade 70	1 (25.4)	E7018	1/8 (3.2)
		E70S-3	1/16 (1.6)
A514	3/4 (19)	E11018	1/8 (3.2)
		E120S-1	1/16 (1.6)

Table 4
Tensile Properties of the Plate Material Used for the Single-V Butt Joints and the Restrained Joints

Plate Type	Yield Strength, ksi (MPa)	Ultimate Tensile Strength, ksi (MPa)	Elongation, Percent	Reduction in Area, Percent
A36	35.6 (245.5)	70.5 (486.1)	34.8	54.0
	34.8 (239.9)	70.0 (482.6)	33.8	60.7
Specification	36 Minimum (248.2)	58-80 (399.9 - 551.6)	23 Minimum	Not specified
A516, Grade 70	39.9 (275.1)	74.8 (515.7)	33.0	54.5
	40.5 (279.2)	75.2 (518.5)	30.9	53.9
Specification	38 Minimum (262)	70-90 (482.6 - 620.5)	21 Minimum	Not specified
A514	121.3 (836.3)	124.7 (859.8)	20.9	69.1
	121.3 (836.3)	124.3 (857.0)	21.1	70.0
Specification	100 Minimum (689.5)	110-130 (758.4 - 896.3)	18 Minimum	40 Minimum

Table 5
Tensile Property Requirements for Electrodes

Electrode	Specification	Yield Strength, ksi (MPa)	Ultimate Tensile Strength, ksi (MPa)
E7018	A5.1-69	60 (413.7)	72 (496.4)
E11018	A5.5-69	97 (668.8)	110 (758.4)
E70S-3	A5.18-69	60 (413.7)	72 (496.4)
E120S to 1	A5.28-79	105-122 (724.0 - 841.2)	120 (827.4)

Two of the tensile specimens were machined from the weld metal. The third was machined from the HAZ. All the tensile specimens were tested at ambient temperature according to Military Standard (MIL-STD) 418C.[8] The tensile test results include the yield strength, ultimate tensile strength, the true fracture stress and the true fracture strain.* These results were compared to the heat input and nugget area to determine if either quantity was a better indicator of strength. The macrospecimens were polished and etched using 5 percent Nitol etchant and visually examined for small flaws not shown by radiography. The nugget area was determined using a nomograph presented by Schultz and Jackson (Figure 6).

The restraint joint part of this investigation required the same type of weld joint and specimen testing shown in Figure 4, except the plate was welded to an *HY-80 strong back plate 2-in. thick by 36 by 36 in.* (50.8 by 914.4 by 914.4 mm). Figure 7 shows a schematic layout of the highly restrained weld joints.

Welding Procedure

The bead-on-plate welding was performed with manual SMAW and fully automatic GMAW systems using reverse polarity (electrode positive) direct current. Individual weld beads were deposited with preset values of the welding variables – voltage, amperage, and travel speed. In subsequent beads, each variable was changed to find the maximum and minimum tolerable limits. Two types of shielding gases were used with the GMAW: a mixture of argon and oxygen, and carbon dioxide. Tests with the E70S-2 and E70S-3 electrodes were shielded with both gases, while E70S-4 and E70S-6 were shielded with carbon dioxide only; the E120S-1 electrode was shielded with argon and 2 percent oxygen only. The welding parameters used in this part of the investigation are presented in Table 6.

The arc voltage, current, and travel speed for the butt welds were selected based on the results of the bead-on-plate study. Table 7 shows the welding variables for weldments using 1/8-in. (3.2-mm) diameter E7018 and E11018 SMAW electrodes, and using 1/16-in. (1.6-mm) diameter E70S-3 and E120S-1 GMAW electrodes with direct current, reverse polarity (electrode positive).

Table 6
Welding Parameters of Bead-on-Plate Welds

Plate Material (ASTM No.)	Current, A	Voltage, V	Travel Speed, *in./min* (mm/min)
	E6010 (1/8-in. [3.2-mm] diameter)		
A36	75	28	7.5 (191)
	75	32	7.7 (196)
	75	28	6.0 (152)
	100	29	8.3 (211)
	100	29	14.1 (358)
	100	34	9.8 (249)
	125	30	11.7 (297)
	125	28	21.7 (551)
	125	38	13.3 (338)
	E6011 (1/8-in. [3.2-mm] diameter)		
A36	75	28	9.6 (244)
	75	34	8.7 (221)
	75	30	8.0 (203)
	75	30	6.0 (152)
	100	28	11.4 (290)
	100	28	8.0 (203)
	100	35	10.0 (254)
	125	30	8.2 (208)
	125	30	13.7 (348)
	125	28	7.2 (183)
	E6013 (1/8-in. [3.2-mm] diameter)		
A36	130	22	8.3 (211)
	130	23	16.0 (406)
	130	27	9.6 (244)
	150	26	10.0 (254)
	150	27	17.8 (452)
	150	22	7.2 (183)
	150	24	9.4 (239)
	E7018 (1/8-in. [3.2-mm] diameter)		
A36	115	25	8.7 (221)
	115	25	15.0 (381)
	115	25	8.0 (203)
	140	26	10.2 (259)
	140	25	20.0 (508)
	140	26	8.3 (211)
	165	27	12.0 (305)
	165	28	15.5 (394)
	165	28	7.5 (191)
A242	115	26	6.5 (165)
	115	25	8.4 (213)
	115	25	12.0 (305)
	115	25	16.6 (422)
	140	26	8.0 (203)
	140	27	12.0 (305)
	140	26	16.0 (406)
	165	28	8.0 (203)
	165	27	12.0 (305)
	165	27	17.0 (434)

*The true fracture strain, which is the natural logarithm of the initial area divided by the final area, was used to indicate the ductility exhibited by the tensile specimen. It is a dimensionless number and shows increasing ductility with higher numbers.

[8]Military Standard, *Mechanical Tests for Welded Joints*, MIL-STD-418C (June 1972).

Table 6 (cont'd)

Plate Material (ASTM No.)	Current, A	Voltage, V	Travel Speed, in./min (mm/min)
A441	115	25	6.3 (160)
	115	38	6.4 (163)
	115	28	6.7 (170)
	115	26	8.9 (226)
	115	25	12.3 (312)
	115	24	15.5 (394)
	115	25	17.1 (434)
	135	26	6.7 (170)
	135	32	7.0 (178)
	140	26	12.0 (305)
	140	26	8.0 (203)
	140	26	18.5 (470)
	150	26	7.5 (191)
	150	35	8.1 (206)
	150	32	8.5 (216)
	165	27	8.2 (208)
	165	36	8.7 (221)
	165	33	8.6 (218)
	165	26	10.4 (264)
	165	26	16.6 (422)
	165	26	22.9 (582)
A572	115	26	8.7 (221)
	115	25	16.6 (422)
	115	26	10.4 (264)
	140	26	8.0 (203)
	140	26	20.0 (508)
	140	26	13.0 (330)
	165	29	12.0 (305)
	165	28	16.0 (406)
	165	27	8.7 (221)
A588	115	26	8.0 (203)
	115	25	14.6 (371)
	115	26	9.8 (249)
	140	26	8.0 (203)
	140	26	18.5 (470)
	140	27	10.7 (272)
	165	28	8.5 (216)
	165	*30*	*20.0 (508)*
	165	32	9.8 (229)
E7024 (1/8-in. [3.2-mm] diameter)			
A36	140	29	12.3 (312)
	140	30	21.8 (554)
	140	30	7.7 (196)
	170	31	10.7 (272)
	170	32	20.0 (508)
	170	31	7.0 (178)
	190	34	12.6 (320)
	190	34	20.9 (531)
	190	32	7.8 (198)
A242	140	26	22.9 (582)
	140	27	12.0 (305)
	140	27	8.0 (203)
	170	30	19.2 (488)
	170	30	12.0 (305)

Table 6 (cont'd)

Plate Material (ASTM No.)	Current, A	Voltage, V	Travel Speed, in./min (mm/min)
	170	30	8.3 (211)
	190	32	20.9 (531)
	190	32	12.0 (305)
	190	32	8.0 (203)
A441	140	26	21.8 (554)
	140	28	12.0 (305)
	140	28	8.0 (203)
	140	32	8.3 (211)
	140	40	8.1 (206)
	170	31	9.4 (239)
	170	40	11.2 (284)
	190	32	11.2 (284)
	190	42	11.2 (284)
	190	33	22.9 (582)
	190	33	16.0 (406)
A572	140	28	10.4 (264)
	140	30	22.9 (582)
	140	29	8.0 (203)
	170	29	9.8 (249)
	170	31	20.9 (531)
	170	30	8.0 (203)
	190	31	10.9 (277)
	190	33	24.0 (610)
	190	32	10.4 (264)
A588	140	28	10.9 (277)
	140	27	25.3 (643)
	140	28	7.7 (196)
	170	32	15.0 (381)
	170	31	26.7 (678)
	170	31	7.8 (198)
	190	33	12.6 (320)
	190	33	24.0 (610)
	190	33	7.8 (198)
E8018 (5/32-in. [4.0-mm] diameter)			
A710	150	22	13.0 (330)
	150	27	13.7 (348)
	150	25	8.0 (203)
	185	26	12.0 (305)
	185	26	19.5 (495)
	185	30	10.4 (264)
	185	26	8.0 (203)
	220	28	12.0 (305)
	220	36	12.0 (305)
	220	30	20.0 (508)
	220	29	8.2 (208)
E11018 (1/8-in. [3.2-mm] diameter)			
A514	115	25	8.0 (203)
	115	32	8.0 (203)
	115	27	8.0 (203)
	115	25	11.4 (290)
	115	25	6.3 (160)
	115	25	17.1 (434)

Table 6 (cont'd)

Plate Material (ASTM No.)	Current, A	Voltage, V	Travel Speed, in./min (mm/min)
	140	26	17.1 (434)
	140	25	12.0 (305)
	140	25	7.5 (191)
	140	28	8.4 (213)
	140	34	10.2 (259)
	165	27	10.9 (277)
	165	35	9.4 (239)
	165	30	10.9 (277)
	165	26	17.8 (452)
	165	26	10.0 (254)
	165	26	8.5 (127)
E70S-2 (1/16-in. [1.5-mm] diameter) (argon with 2 percent oxygen addition)			
A36	360	25	15 (381)
	350	25	15 (381)
	300	26	15 (381)
	400	23	15 (381)
	370	20	15 (381)
	315	22	15 (381)
	295	22	15 (381)
	270	23	15 (381)
	260	25	15 (381)
	200	20	15 (381)
	250	20	15 (381)
	275	19	15 (381)
	310	18	15 (381)
	360	33	15 (381)
	430	32	15 (381)
	470	31	15 (381)
	370	24	30 (762)
	380	24	25 (635)
	350	25	20 (508)
	350	25	10 (254)
	305	25	5 (127)
	320	18	10 (254)
	310	18	20 (508)
	315	18	25 (635)
	320	18	30 (762)
	500	29	30 (762)
A242	365	25	35 (889)
	365	25	25 (635)
	390	25	15 (381)
	390	25	10 (254)
A441	360	25	35 (889)
	360	25	35 (889)
	385	25	15 (381)
	385	25	10 (254)
A572	365	25	15 (381)
	380	25	25 (635)
	380	25	35 (889)
A588	390	25	35 (889)
	390	25	25 (635)
	390	25	15 (381)
	390	25	10 (254)

Table 6 (cont'd)

Plate Material (ASTM No.)	Current, A	Voltage, V	Travel Speed, in./min (mm/min)
A70S-2 (1/16-in. [1.5-mm] diameter) (carbon dioxide)			
A36	300	35	10 (254)
	350	34	10 (254)
	390	34	10 (254)
	430	33	15 (381)
	430	32	15 (381)
	450	32	15 (381)
	380	25	15 (381)
	365	25	15 (381)
	360	27	15 (381)
	345	26	15 (381)
	280	27	15 (381)
	330	20	15 (381)
	280	20	15 (381)
	210	22	15 (381)
	170	22	15 (381)
	380	26	35 (889)
	380	25	30 (762)
	380	26	5 (127)
A242	375	25	35 (889)
	375	25	25 (635)
	360	26	15 (381)
	360	26	10 (254)
A441	360	26	35 (889)
	360	26	25 (635)
	370	25	15 (381)
	370	25	10 (254)
A572	370	25	35 (889)
	365	25	25 (635)
	360	25	15 (381)
A588	360	26	35 (889)
	360	26	25 (635)
	360	26	15 (381)
	360	26	10 (254)
E70S-3 (1/16-in. [1.5-mm] diameter) (argon with 2 percent oxygen addition)			
A36	400	28	15 (381)
	445	27	15 (381)
	465	28	15 (381)
	400	20	15 (381)
	370	20	15 (381)
	350	21	15 (381)
	355	21	15 (381)
	300	22	15 (381)
	275	23	15 (381)
	150	18	15 (381)
	230	24	15 (381)
	200	17	15 (381)
	250	16	15 (381)
	340	16	15 (381)
	280	16	15 (381)
	285	16	25 (635)

Table 6 (cont'd)

Plate Material (ASTM No.)	Current, A	Voltage, V	Travel Speed, in./min (mm/min)
	280	16	30 (762)
	280	16	20 (508)
	250	17	10 (254)
	410	27	10 (254)
	410	27	20 (508)
	410	27	25 (635)
	390	28	30 (762)
	415	27	5 (127)
	410	27	35 (889)
A242	380	25	35 (889)
	380	25	25 (635)
	375	25	15 (381)
	375	25	10 (254)
A441	380	25	35 (889)
	380	25	25 (635)
	370	25	15 (381)
	370	25	10 (254)
	370	25	35 (889)
A572	370	25	25 (635)
	360	25	15 (381)
A588	370	26	35 (889)
	370	26	25 (635)
	375	25	15 (381)
	375	25	10 (254)
E70S-3 (1/16-in. [1.5-mm] diameter) (carbon dioxide)			
A36	180	22	10 (254)
	230	21	15 (381)
	270	20	15 (381)
	310	19	15 (381)
	300	27	15 (381)
	325	26	15 (381)
	350	26	15 (381)
	380	26	15 (381)
	400	25	15 (381)
	420	24	15 (381)
	365	33	15 (381)
	415	32	15 (381)
	440	32	15 (381)
	480	31	15 (381)
	365	26	35 (889)
	395	25	35 (889)
	385	25	25 (635)
	385	25	10 (254)
A242	370	26	35 (889)
	370	26	25 (635)
	350	26	15 (381)
	350	26	10 (254)
A441	350	26	35 (889)
	350	26	25 (635)
	360	26	15 (381)
	360	26	10 (254)

Table 6 (cont'd)

Plate Material (ASTM No.)	Current, A	Voltage, V	Travel Speed, in./min (mm/min)
A572	350	26	35 (889)
	350	26	25 (635)
	350	26	15 (381)
	340	26	10 (254)
A588	370	26	35 (889)
	370	26	25 (635)
	360	26	15 (381)
	360	26	10 (254)
E70S-4 (1/16-in. [1.5-mm] diameter) (carbon dioxide)			
A36	140	22	20 (508)
	230	21	15 (381)
	280	20	15 (381)
	360	19	15 (381)
	220	29	15 (381)
	300	28	15 (381)
	350	26	15 (381)
	370	25	15 (381)
	300	34	15 (381)
	375	33	15 (381)
	420	32	15 (381)
	450	32	15 (381)
	360	26	35 (889)
	350	26	25 (635)
	335	26	10 (254)
A242	360	26	35 (889)
	360	26	25 (635)
	360	26	15 (381)
	350	26	10 (254)
A441	360	26	35 (889)
	360	26	25 (635)
	360	26	15 (381)
	350	26	10 (254)
A572	340	26	35 (889)
	340	26	25 (635)
	330	26	15 (381)
A588	360	26	35 (889)
	360	26	25 (635)
	360	26	15 (381)
	360	26	10 (254)
E70S-6 (1/16-in. [1.5-mm] diameter) (carbon dioxide)			
A36	340	34	15 (381)
	440	32	15 (381)
	440	32	15 (381)
	400	25	15 (381)
	360	26	15 (381)
	340	26	15 (381)
	280	27	15 (381)
	315	19	15 (381)
	270	20	15 (381)
	220	21	15 (381)

Table 6 (cont'd)

Plate Material (ASTM No.)	Current, A	Voltage, V	Travel Speed, in./min (mm/min)
	140	22	15 (381)
	340	26	35 (889)
	340	26	25 (635)
	340	26	5 (127)
A242	340	26	35 (889)
	340	26	25 (635)
	320	26	15 (381)
	320	26	10 (254)
A441	340	26	35 (889)
	340	26	25 (635)
	365	26	15 (381)
	365	26	10 (254)
A572	340	26	35 (889)
	350	26	25 (635)
	360	26	15 (381)
	350	26	10 (254)
A588	320	26	35 (889)
	325	26	25 (635)
	335	26	15 (381)
E110S (1/16-in. [1.5-mm] diameter) (argon with 2 percent oxygen addition)			
A514	225	20	15 (381)
	280	20	15 (381)
	330	19	15 (381)
	370	18	15 (381)
	390	25	15 (381)
	425	24	15 (381)
	455	24	15 (381)
	465	24	15 (381)
	500	30	15 (381)
	120	15	15 (381)
	225	14	15 (381)
	245	14	15 (381)
	300	20	35 (889)
	300	20	25 (635)
	300	20	10 (254)

In the third phase of this investigation, all weldments were fabricated under restraint conditions with the base plate secured by fillet welding to a 2-in. (50.8-mm)-thick HY-80 steel restraint plate, as shown in Figure 7. Welding parameters used for fabricating each weldment were based on limits established by the butt weld portion (Table 8). During welding, magnetic particle inspection was performed on each deposited layer of weld metal. Each weldment was left secured to the restraint plate for 7 days after completion of welding to allow time for cracking to occur. Then magnetic particle and radiographic inspection were done.

Following nondestructive testing, welds representing the highest and lowest heat input condition successfully welded were sectioned for mechanical property testing. Figure 5 shows sectioning of a typical weld.

3 DATA ANALYSIS AND DISCUSSION

Bead-on-Plate Welds

SMAW Welds

For the SMAW electrodes, AWS A5.1 current limits, which are based on wire diameter and coating composition, were used in this study to establish the voltage and travel speed limitations.[9] The current limits, as defined by AWS A5.1, are the extreme values for each electrode noted in Table 6; these limits are discussed below with each SMAW electrode. Table 9 presents the voltage limits established for the SMAW electrodes. Voltage, which is directly related to the arc length, affects both bead width and shielding characteristics; i.e., long arc length (high voltage) produces a wide bead and could cause porosity in the weld by allowing the aspiration of air into the arc atmosphere. Short arc lengths (low voltage) present operational difficulties such as short circuiting.

Figures 8 through 14 are graphs of travel speed and current for the individual SMAW electrodes; the dashed lines are the travel speed limits at various current levels. These limits were determined by bead shape and amount of undercut. Undercutting is caused by a combination of factors, but primarily by a rate of travel speed too high for a particular current level. A large area is melted and drawn to the center; the arc passes by too quickly to allow enough weld metal to be deposited in the welded area. At slow travel speeds other problems arise – weld bead roll-over (lack of fusion) and slag entrapment, for example.

E6010. The E6010 is a high-cellulose electrode which has many uses in welded fabrication. It produces a forceful, spray-type arc which gives deep penetration. Slag cover on the weld bead is thin and easily removed.

AWS A5.1 gives a current range of 75 to 125 A for this electrode. The voltage was varied from 28 to 34 V, and the travel speed used ranged from 6 to 21.7 in./minute (152 to 551 mm/minute).

[9] *Specification for Mild Steel Covered Arc Welding Electrodes*, AWS A5.1 (1969).

Table 7
Welding Parameters for Butt Welds

	Specimen	Volts	Current	Travel Speed (in./min)*	Heat Input (kJ/in.)*	Nugget Area (sq in.)*	Plate Thickness (in.)*
	B4	24	160	15.7	12.8	0.020	0.75
	B7	22	115	11.5	13.2	0.019	0.75
	B8	25	160	15.6	15.4	0.024	0.75
Steel: A36	B9	23	115	9.1	17.4	0.024	0.75
Electrode: E7018 SMAW	B6	26	165	13.5	19.1	0.029	0.75
	B3	24	140	10.3	19.6	0.029	0.75
	C2	25	165	8.0	31.1	0.045	0.75
	C1	28	165	6.6	42.0	0.055	0.75
	D6	25	165	4.8	51.2	0.074	0.75
	B10	23	115	10.1	15.7	0.022	1.0
	B11	23.5	140	10.8	18.3	0.028	1.0
	B12	26	165	11.4	22.6	0.034	1.0
Steel: A516	B14	23	140	8.4	23.0	0.035	1.0
Electrode: 7018 SMAW	B13	22	115	6.3	24.1	0.033	1.0
	B15	26	160	8.6	29.0	0.042	1.0
	C3	24	150	6.5	33.1	0.044	1.0
	D5	25	155	5.6	41.4	0.055	1.0
	C4	25	165	4.8	51.5	0.074	1.0
	B16	22	115	7.7	19.7	0.028	0.75
	B17	23	140	8.6	22.5	0.034	0.75
	B18	25	165	8.7	28.5	0.044	0.75
Steel: A514	B19	22	115	5.3	28.6	0.039	0.75
Electrode: E11018 SMAW	B20	23	140	6.2	31.2	0.046	0.75
	C6	25	165	7.0	35.4	0.050	0.75
	B21	25	165	6.0	41.3	0.061	0.75
	C5	25	165	5.2	48.0	0.068	0.75
	D7	25	165	4.3	57.2	0.080	0.75
	B25	25	300	30	15	0.035	0.75
	B26	25	300	20	22	0.050	0.75
Steel: A36	B24	30	400	30	24	0.055	0.75
Electrode: E70S-3 GMAW	B23	30	400	20	36	0.080	0.75
	B27	25	300	10	45	0.095	0.75
	D4	25	250	6.9	52.8	0.100	0.75
	B22	30	400	10	72	0.150	0.75
	B30	25	300	30	15	0.035	1.0
	B29	25	300	22	22	0.050	1.0
	B31	30	400	30	24	0.055	1.0
Steel: A516	D3	25	250	10.8	34.7	0.067	1.0
Electrode: E70S-3 GMAW	B32	30	400	20	36	0.080	1.0
	B28	25	300	10	45	0.095	1.0
	D2	25	250	6.4	58.6	0.098	1.0
	B33	30	400	10	72	0.150	1.0
	B39	20	250	30	10.0	0.027	0.75
	B38	20	250	20	15	0.038	0.75
Steel: A514	B36	24	350	30	16.8	0.045	0.75
Electrode: E120S-1 GMAW	B35	24	350	20	25.2	0.065	0.75
	B37	20	250	10	30	0.070	0.75
	D1	23	320	11	40.1	0.097	0.75
	B34	24	350	10	50.4	0.130	0.75

*Metric conversion factors:
1 in./min = 1524 mm/sec
1 kJ/in. = 39.37 J/mm
1 sq in. = 645.16 mm^2
1 in. = 25.4 mm

Table 8
Welding Parameters for the Restrained Joints

	Specimen Code	Volts	Current	Travel Speed (in./min)*	Heat Input (kJ/in.)*	Nugget Area (sq in.)*	Plate Thickness (in.)*
Steel: A36	T	22	140	3	61.6	0.087	0.75
Electrode: E7018 SMAW	M	23	140	7.5	25.8	0.038	0.75
	S	24	90	6.5	19.9	0.024	0.75
Steel: A516	R	22	140	3	61.6	0.087	1
Electrode: E7018 SMAW	Q	22	125	11	15.5	0.023	1
Steel: A514	P	21	130	4	40.9	0.059	0.75
Electrode: E11018 SMAW	O	20	125	9.5	15.8	0.026	0.75
Steel: A36	K	31	320	12	49.6	0.090	0.75
Electrode: E70S-3 GMAW	L	31	350	26	25.0	0.051	0.75
Steel: A516	I	30	300	11	49.1	0.088	1
Electrode: E70S-3 GMAW	W	29	320	25	24.2	0.046	1
Steel: A514	V	27	320	10	51.8	0.110	0.75
Electrode: E120S-1 GMAW	U	26	275	27	15.9	0.034	0.75
	J	28	400	27	24.9	0.060	0.75

*Metric conversion factors:
1 in./min = 1524 mm/sec
1 kJ/in. = 39.37 J/mm
1 sq in. = 645.16 mm^2
1 in. = 25.4 mm

The lower limit for voltage was determined to be 28 V; the arc could not be maintained at lower voltages because it tended to short circuit. The higher limit of 32 V was based on visual inspection of the external surface and macrospecimen, and on the handling characteristics of the electrode with long arc lengths. Figure 8 shows the limit for travel speed determined by bead shape and the amount of undercut.

E6011. The E6011 electrode is quite similar to E6010 in arc characteristics, but sodium is used in place of potassium, which allows the electrode to be used with alternating as well as direct current. Current range for this electrode is also 75 to 125 A. At the lower end of the current range, the penetration was minimal, and overall the penetration was less than that of the E6010 electrode.

The voltage was varied between 28 and 35 V. Based on the same criteria used for the E6010 electrode, the voltage range was determined to be 28 to 32 V. Travel speed was varied between 6 and 11.4 in./minute (152 and 290 mm/minute). Figure 9 shows the limits of travel speed determined by bead shape and the amount of undercut.

E6013. The E6013 electrode was originally designed for light gauge sheet metal, although larger electrode diameters are used for single pass, high speed, horizontal fillet welds. The electrode can be used for welding sheet metal in a vertical down position.

The current range for this electrode is 130 to 150 A. The voltage used ranged from 22 to 27 V; the voltage limits were 22 to 26 V. The travel speed was varied from 7.2 to 17.8 in./minute (97 to 452 mm/minute). Figure 10 shows the limits on travel speed for this electrode.

E7018. The E7018 electrode has a smooth, quiet arc with small amounts of spatter and low penetration. Very high welding speed can be used with this electrode. The coating contains between 25 and 40 percent iron powder. This low-hydrogen electrode is used where other types of electrodes could cause underbead or delayed cracking, which is usually attributed to hydrogen pickup from the arc atmosphere. The current range for this electrode is 115 to 165 A. The test welds were made with voltages between 25 and 38 V. Based on the bead shape, porosity content, and usability, the

Table 9
Bead-on-Plate Established Voltage Limits

Electrode	Voltage Limits, V
E6010	28 to 32
E6011	28 to 32
E6013	22 to 26
E7018	25 to 28
E7024	26 to 32
E8018	22 to 28
E11018	25 to 30

limits on voltage were determined to be 25 and 28 V. The travel speed was varied between 6.3 and 22.9 in./minute (160 and 582 mm/minute). Figure 11 shows the travel speed limits for the E7018 electrode.

Weld beads produced with E7018 on the different types of steel plate showed no differences that were related to the plate. Therefore, to determine the tolerable limits of voltage and travel speed, all welds made with the E7018 electrode were grouped together – as were the welds produced with the E7024 electrode.

E7024. The E7024 electrode's heavy coating, which contains high percentages of iron powder, makes up about 50 percent of the total electrode weight. E7024, which is manufactured specifically for flat position and horizontal fillet welding, has a smooth, quiet arc with very small amounts of spatter. This electrode generally has minimal penetration and can be used with high lineal speed.

The current range for this electrode is 115 to 165 A. Weld beads were produced with voltages from 26 to 42 V and travel speeds from 7 to 26.7 in./minute (178 to 678 mm/minute). The usable range for voltage was determined to be 26 to 32 V. Figure 12 shows the travel speed for this electrode.

E8018. E8018, used with high strength steel, is a low-hydrogen electrode with arc characteristics similar to E7018. The electrode provides shallow penetration with a smooth, quiet arc and small amounts of spatter.

The current range for E8018 is 150 to 220 A. The voltage used for this electrode ranged from 22 to 36 V, and the travel speed ranged from 8 to 20 in./minute (203 to 508 mm/minute). The usable voltage range was determined to be 22 to 28 V. Figure 13 shows the travel speed limits at various current levels.

E11018. The E11018 electrode is also a low-hydrogen electrode used for high-strength, low-alloy steels. The arc characteristics are similar to the E7018 and E8018 electrodes. The current range for E11018 is 115 to 165 A. The voltage range was 25 to 35 V, and the travel speed ranged from 6.3 to 17.8 in./minute (160 to 452 mm/minute). The voltage range for this electrode was determined to be 25 to 30 V. Above 30 V, porosity and spatter became a problem, and below 25 V usability dropped off because of short circuiting. Figure 14 shows the travel speed limits for the E11018 electrode.

GMAW Welds

The travel speed, voltage, and current limits for the GMAW electrodes could not be delineated as clearly as for the SMAW electrodes. Arc voltage and current level combinations can be adjusted to give several types of metal transfer. With the use of argon and 2 to 5 percent oxygen addition, transfer can be by large droplets (globular) at low power levels, or by a fine spray at high power levels. There is a definite transition to spray transfer, which is the method normally used with argon-oxygen shielded GMAW.

With carbon dioxide shield gas, three types of transfer – short circuit, repelled, and projected – can be obtained, depending on the levels of current and voltage. The short circuiting transfer method (which was developed for thin materials and welding in the vertical and overhead position) involves transfer of weld metal from the electrode tip by repetitive short circuits through contact of the molten electrode and the work piece. The diameters recommended for short circuiting welding are 0.030 in. (0.8 mm) or 0.045 in. (1.1 mm). The 0.062-in.-diameter (1.6-mm) wire used in this investigation is not normally used in short circuiting transfer because of the high currents required to melt an electrode of this size. Higher current and voltage cause droplets to form at the end of the electrode. As these droplets enlarge, they begin to detach from the electrode by gravity. Forces in the center of the arc give the drop an initial acceleration that repells it from the weld pool. With increased current levels, the electromagnetic forces pinch the drop off and project it toward the weld pool. The projected transfer mode is most frequently used because it gives better penetration and less spatter and the repelled transfer mode.

Figures 15 through 21 are graphs of voltage versus current levels for the GMAW electrodes used in this study. The lines on these graphs represent the boundaries between types of metal transfer. In Figure 17, the two points at the lower left are from arcs that exhibited

short circuiting characteristics but were very erratic and had minimal usability; settings in these arcs are not recommended when a shield gas of argon with 2 percent oxygen addition is used. The spray transfer region was established for the three electrodes which can be used with argon-oxygen shield gas (Figures 15, 17, and 21).

The four electrodes shielded with carbon dioxide gas – E70S-2, E70S-3, E70S-4 and E70S-6 – exhibited the three types of weld metal transfer. Figures 16, 18, 19, and 20 show the limits of the three transfer modes.

The travel speed for each electrode ranged from 5 to 35 in./minute (127 to 889 mm/minute). Except for the E70S-2 electrodes shielded with argon-2 percent oxygen addition and A36 steel, no significant undercutting was present at the toe of weld. Further examination of the A36 welds showed that the problem of undercut was caused by a cast in the weld wire that forced the arc to one side, leaving an undercut toe on the opposite side. The usable range of travel speed was 10 to 35 in./minute (254 to 889 mm/minute). Below 10 in./minute (254 mm/minute) the weld crown became too high, exceeding the 1/8-in. (3.2-mm) limit specified in AWS D1.1. A few isolated weld beads other than those deposited at slow travel speeds exceeded the maximum. These were attributed to short arc lengths and high current levels that did not allow the weld metal to spread out, causing tall, narrow weld beads.

A36 SMAW Butt Welds

Tensile Test Results

Table 10 and Figures 22 and 23 present the tensile test results for the E7018 weld metal and the A36 HAZ specimens over the ranges of heat input and nugget area tested. The weld metal yield strengths are spread over a 15.2 ksi (104.8 MPa) range. Figures 22 and 23 show the weld metal strength data plotted against heat input and calculated nugget area, respectively. Both figures show a trend of weld metal yield strengths decreasing as heat input and nugget area increase. To determine which parameter, heat input or nugget area, was a more sensitive predictor of yield strength, linear correlation coefficients (r) were computed for both.* The coefficients for heat input ($r = -0.399$) and nugget area ($r = -0.392$) were not significant and indicated that for the test conditions under study, both were equally poor predictors of yield strength under straight-line conditions.

The HAZ yield strengths varied widely from 46.2 to 69.0 ksi (318.5 to 475.5 MPa). The yield strength did not correlate significantly with either nugget area ($r = 0.280$) or heat input ($r = 0.262$); therefore, neither could be used to predict HAZ yield strength. Review of the HAZ yield strength data shows increasing yield strength with increasing heat input up to approximately 30 kJ/in. (1181.1 J/mm) heat input. Then yield strength decreases with increasing heat input. In other words, the data indicate that the HAZ yield strength peaks somewhere between 30 and 35 kJ/in. (1181.1 and 1378 J/mm). Even at the lowest strength levels of the HAZ, the material is still significantly stronger than the unaffected base plates surrounding the weld joints.

The ultimate tensile strength (UTS) of the weld metal specimens varied between 73.9 and 89.6 ksi (509.5 and 617.8 MPa); increasing heat inputs and nugget areas were associated with decreasing UTS. The linear correlation coefficients for the UTS of the weld metal versus heat input and nugget area were −0.819 and −0.807, respectively. The trends observed in weld metal UTS results are similar to those observed for the yield strength data. None of the heat input or nugget area conditions used in this investigation produced a UTS below the specification minimum of 72 ksi (496.4 MPa).

The UTS of the HAZ specimens varied between 70.6 and 83.4 ksi (486.8 and 575.0 MPa). As with the yield strengths, the HAZ UTS did not correlate significantly with either heat input ($r = 0.539$) or nugget area ($r = 0.594$); therefore neither could be used to predict HAZ tensile strength. The trend of increasing tensile strength with increased heat input and nugget area is similar to that found in the yield strength data, although the HAZ tensile strength data did not peak at 30 to 35 kJ/in. (1181.1 to 1378 J/mm), but steadily increased through the range of heat inputs and nugget areas tested.

The true fracture stress and the true strain at fracture were calculated to provide information on strength and ductility of the weldments. There was no significant correlation between either heat input or nugget area with these two quantities.

Impact Test Results

Figures 24 through 32 graph the impact energy versus test temperature for each weldment. The figures

*The correlation coefficient is the ratio of the explained variation to the total variation. For zero explained variation, the correlation coefficient is 0. For completely explained variation, the coefficient is ±1. All other coefficients vary between +1 and −1, with increasingly explained variations approaching ±1.

contain the all-weld metal impact results and the associated HAZ impact results. The impact energy at a given temperature for the HAZ specimens in most cases is lower than that of the all-weld metal specimens. Because of the shrinkage stresses of the weld metal, some of these weldments were so warped that dynamic tear test specimens could not be machined from the plates. Consequently, each dynamic tear specimen was converted to three Charpy V-notch (CVN) specimens.

The upper shelf energy level for all the weldments tested was considerably lower for the HAZ specimens than for the all-weld metal specimens. The transition temperatures for the CVN and the dynamic tear test specimens cannot be correlated with each other and cannot be used together to generate a correlation coefficient with either the heat input or the nugget area. In one weldment (C2), the energy curves for the HAZ and the all-weld metal specimens cross, indicating that the transition temperature for the HAZ was lower than that for the all-weld metal specimens. In either case, transition was well below 0°C. The transition temperature for all the weld specimens being measured with the CVN specimen or the dynamic test specimens was a maximum of 0°C. The transition temperatures for the HAZs were a maximum of 0°C. Two of the HAZ energy curves, specimens B4 and B3, were very flat. There appear to be no trends in the transition temperatures for the HAZ or the weld metal specimens tested.

Analysis of Mechanical Properties

In a general analysis of the mechanical properties of the A36 SMAW weldments, it is important to com-

Table 10
All-Weld and HAZ Tensile Data for A36 SMAW Butt Welds Using E7018 Electrodes

Specimen Code	Yield Strength (ksi)*	Ultimate Tensile Strength (ksi)	True Stress at Fracture (ksi)	True Fracture Strain
		All-Weld Metal Specimens		
B4	77.4	89.3	185.5	1.21
	73.2	89.0	193.7	1.23
B7	72.4	86.7	188.5	1.29
	75.0	87.6	189.3	1.23
B8	67.4	81.7	190.8	1.35
	74.8	86.9	185.2	1.20
B9	70.2	84.7	191.8	1.29
	78.4	89.6	185.9	1.11
B6	69.5	86.1	183.7	1.15
	76.6	89.3	191.1	1.26
B3	72.2	86.1	191.1	1.27
	63.7	85.9	181.5	1.23
C2	73.7	86.9	154.3	0.94
	63.7	81.2	213.9	1.44
C1	71.9	81.1	120.6	0.71
	63.2	75.8	164.7	1.19
D6	73.4	80.8	184.5	1.36
	65.6	73.9	94.2	0.31 (defect)
		HAZ Specimens		
B4	49.8	74.2	141.7	0.92
B7	46.2	70.6	146.3	1.04
B8	66.6	81.9	169.2	1.01
B9	52.3	74.7	145.3	0.92
B6	59.5	78.3	157.7	0.97
B3	62.2	80.1	159.7	0.99
C2	69.0	81.6	145.9	0.85
C1	60.1	76.8	156.8	1.04
D6	56.0	83.4	155.9	0.92

*1 ksi = 6.89 MPa

pare the properties of the weld metal and the HAZ to those required for the base plate and the electrodes. Table 5 indicates that the AWS A5.1 minimum yield strength for the E7018 electrode is 60 ksi (414 MPa); Table 4 indicates that the minimum A36 yield strength is 36 ksi (248 MPa). As shown in Figures 22 and 23, all the HAZ yield strengths significantly exceeded both this specified minimum and the yield strength in Table 4 for the A36 base plate over the ranges of heat input and nugget area investigated. The weld metal yield strength met or exceeded the minimum of 60 ksi (414 MPa) for the electrode in all heat inputs and nugget areas investigated.

One-third of the HAZ specimens' UTSs were above the 58 to 80 ksi (399.9 to 551.6 MPa) range for A36 steel, and all were higher than the unaffected base plate at 66 to 67 ksi (455 to 462 MPa). The UTS of the all-weld metal specimens exceeded the 72 ksi (496.4 MPa) minimum requirements. However, at the highest heat input (51.2 kJ/in. [2015.8 J/mm]) and the largest nugget area (0.074 sq in. [47.7 mm^2]), the UTS of the weld metal declined almost to the minimum requirement.

The A36 base plate and the E7018 electrode do not have specified dynamic tear impact requirements. However, results of base plate testing (Figure 1) show that the transition temperature for A36 steel is about −5°C. The transition temperatures for all weldments except B8 and C2 are significantly higher than the value in Figure 1. These two weldments have transition temperatures at or just below the reported value. Thus, the transition temperature of welded A36 steel should be considered in design and fabrication if impact resistance is a critical factor.

During test plate fabrication, side wall fusion and depth of penetration become increasingly difficult to control at heat input and nugget areas less than 20 kJ/in. (787.4 J/mm) and 0.03 sq in. (19.4 mm^2), respectively. This, when coupled with the above criteria for weld metal yield strength, places the acceptable range for heat input at 20 to 55 kJ/in. (787.4 to 2165.4 J/mm), and nugget area at 0.03 to 0.08 sq in. (19.4 to 51.6 mm^2) for the SMAW process using the E7018 electrodes on A36 steel.

A516 SMAW Butt Weldments

Tensile Test Results

Table 11 and Figures 33 and 34 present the tensile test results for the E7018 weld metal and the A516 HAZ specimens. The weld metal yield strengths are spread over a 13.1 ksi (90.3 MPa) range varying from 63.7 to 76.8 ksi (439.2 to 529.5 MPa). The weld metal yield strengths per heat input or nugget area for the A516 weldments with the E7018 electrode are nearly identical to those for the A36 weldments with the same electrode. Figures 33 and 34 show the weld metal yield strength data plotted against heat input and nugget area. Both figures show a trend of decreasing weld metal yield strength as heat input and nugget area increase. The linear correlation coefficient for the weld metal yield strength versus heat input is −0.429; for the weld metal yield strength versus nugget area it is −0.472, and is only marginally significant.

The HAZ yield strengths varied between 53.3 and 73.9 ksi (367.5 and 509.5 MPa), with increasing heat inputs and nugget areas producing lower yield strengths (Figures 33 and 34). The linear correlation coefficient for HAZ yield strength versus heat input was −0.271; the coefficient for HAZ yield strength versus nugget area was −0.287. These correlation coefficients are very low; therefore, neither quantity could be used to predict HAZ yield strength.

The UTSs of the weld metal specimens varied between 78.2 and 90.2 ksi (538.2 and 621.9 MPa), with increasing heat inputs and nugget areas associated with decreasing UTSs. As with the yield strengths, the UTSs of the A516 weldments were in the same range as the UTS for the A36 weldments with the same electrode. Linear correlation coefficients for the weld metal versus the heat input and nugget area were −0.292 and −0.322, respectively. The correlation coefficients were relatively low; therefore, nugget area and heat input cannot be used as a predictor of weld metal UTS.

The UTS of the A516 HAZ specimens varied between 75.2 and 87.6 ksi (518.5 and 604 MPa), with increasing heat inputs and nugget areas associated with decreasing UTS. The linear correlation coefficients for the HAZ UTS versus heat input and nugget area were −0.113 and −0.414, respectively. The correlation coefficient for the HAZ UTS versus nugget area is much higher than that for heat input, although still only marginally significant.

To indicate the strengths and ductility of the weldments, the true fracture stress and the true strain at fracture were calculated for all specimens tested. There was no significant correlation between either heat input or nugget areas with these two quantities.

Table 11
All-Weld and HAZ Tensile Data for A516 SMAW
Butt Welds Using E7018 Electrodes

Specimen Code	Yield Strength (ksi)*	Ultimate Tensile Strength (ksi)	True Stress at Fracture (ksi)	True Fracture Strain
		All-Weld Metal Specimens		
B10	69.6	81.9	198.5	1.39
	75.8	90.2	185.0	1.05
B11	68.7	82.8	181.6	1.25
	76.8	87.6	182.3	1.24
B12	68.4	81.8	188.7	1.33
	73.6	85.2	189.7	1.29
B14	66.7	81.7	182.5	1.31
	72.2	83.2	186.1	1.32
B13	68.4	82.2	190.4	1.35
	74.2	85.7	184.9	1.29
B15	63.7	78.2	186.5	1.38
	69.4	80.1	162.0	1.09
C3	74.4	87.0	188.6	1.23
	66.2	81.5	196.6	1.36
D5	76.4	84.2	177.8	1.23
C4	68.4	82.7	193.4	1.35
	57.6	81.2	184.4	1.25
		HAZ Specimens		
B10	73.9	87.6	188.5	1.20
B11	54.8	80.1	157.9	1.01
B12	53.3	76.5	168.0	1.11
B14	64.8	84.2	170.6	1.05
B13	69.3	84.5	190.7	1.24
B15	59.9	79.2	151.0	0.99
C3	54.6	75.4	153.2	1.06
D5	58.3	75.2	140.5	1.01
C4	61.1	81.1	160.1	1.02

*1 ksi = 6.89 MPa

Impact Test Results

Figures 35 through 43 graph the dynamic tear impact energy absorbed versus test temperature for each weldment for the range of heat input and nugget areas tested. Each figure contains the all-weld metal impact results and the associated HAZ impact results. As with the A36 impact results, the impact energy at a given temperature for the HAZ specimens is lower than that for the all-weld metal specimens (except the lower shelf of weldment C3), and the transition temperatures are generally spread from −20 to +20°C for all the heat inputs and nugget areas tested. The transition temperatures for the all-weld metal specimens were between −20 and +20°C – except for specimen C4, which had the highest heat input and nugget area. The transition temperature for specimen C4, with a heat input of 51.5 kJ/in. (2027.6 J/mm) and a nugget area of 0.074 sq in. (47.7 mm^2), was approximately −40°C. There is very little apparent correlation between the transition temperature and either heat input or nugget area.

Analysis of Mechanical Properties

The mechanical properties of the A516 weldments, when compared with the specification requirements, indicate that the yield strength of the E7018 electrode drops below the 60 ksi (413.7 MPa) minimum requirement at heat inputs and nugget areas near 51.5 kJ/in. and 0.074 sq in. (2027.6 J/mm and 47.7 mm^2), respectively (Figures 33 and 34). But none of the HAZ yield strengths drops below the 38 ksi (262 MPa) minimum specified for the base plate or the values recorded in Table 4 for unaffected base plate.

The UTSs of the weld metal specimens all met minimum requirements of AWS A5.1 at the heat inputs and nugget areas used in this investigation. The UTSs of the HAZ specimens were within the specified 70 to 90 ksi (482.6 to 620.5 MPa) range for ASTM A516, Grade 70 base plate.

Neither the A516 plate nor the E7018 electrode has specified dynamic tear impact requirements. Figure 2 shows the impact results from unaffected base plate. The transition temperature for the plate is −5°C; the HAZ specimen's transition temperature is higher than this. Thus, the impact resistance of the HAZ and the weld metal may be significantly less than that of the base plate and should be considered in the design and fabrication of A516 welded components if impact resistance is critical.

As with the A36 plate, side wall fusion and depth penetration became increasingly difficult to control at heat input and nugget areas less than 20 kJ/in. and 0.03 sq in. (787.4 J/mm and 19.4 mm^2), respectively. This, when coupled with the weld metal yield strength criteria, places the acceptable range for heat input at 20 to 50 kJ/in. (787.4 to 1968.5 J/mm), and the nugget area at 0.03 to 0.07 sq in. (19.4 to 45.6 mm^2) for the SMAW process using E7018 electrodes on A516, Grade 70 steel.

A514 SMAW Butt Weldments

Tensile Test Results

Table 12 and Figures 44 and 45 present the tensile test results for the E11018 weld metal and the A514 HAZ specimens over the range of heat input and nugget areas tested. Except for one tensile specimen (yield strength = 96.4 ksi [665 MPa]) with possible hydrogen damage, all the weld metal specimens were above the 97 ksi (668.8 MPa) minimum yield strength requirement for the weld metal. Figures 44 and 45 show the weld metal yield strength data plotted against heat input and nugget area. Both figures show a trend of decreasing weld metal yield strength as heat input and nugget area increase. The linear correlation coefficients for heat input ($r = -0.238$) and for nugget area ($r = -0.290$) were not significant; consequently, the heat input and nugget area are not linearly related to the yield strength results.

The HAZ yield strength varied between 100.6 and 121.8 ksi (693.6 and 839.8 MPa). The HAZ yield strength did not correlate very well with either heat input ($r = -0.347$) or nugget area ($r = 0.578$). The HAZ yield strength tended to decrease with increased heat input but was relatively flat when compared with nugget area. The HAZ yield strength also met the minimum specification requirements for the A514 steel, but was significantly lower for most specimens than the tabulated yield strength of the unaffected A514 base plate in Table 4 (121 ksi [834 MPa]).

The UTS of the weld metal, varying from 109.3 to 137.8 ksi (753.6 to 950.1 MPa), did not correlate very well with either the heat input ($r = -0.238$) or nugget area ($r = -0.290$). But as with yield strength, the UTS tended to decrease with increasing heat input and nugget area.

The UTS of the HAZ specimens varied between 112.3 and 129.1 ksi (774.3 and 890.1 MPa). As with the HAZ yield strength, the HAZ UTS did not correlate with either heat input ($r = 0.042$) or the nugget area ($r = 0.020$). Again the linear regression analysis was not effective in determining any trend between either heat input or nugget area and the UTS. All UTS specimens of the HAZ were within the 110 to 130 ksi (758.4 to 896.3 MPa) range specified by ASTM A514.

The true fracture stress and the true strain at fracture were calculated to provide information on the strength and ductility of the weldments. These two quantities did not correlate significantly with either heat input or nugget area.

Impact Test Results

Figures 46 through 54 graph the impact energy versus test temperature for each weldment. Each figure contains the all-weld metal impact results and the associated HAZ impact results. As with the A36 SMAW impact specimens, some of the weldments had warped so much that dynamic tear specimens could not be machined from the weldment; therefore, each was converted into three CVN impact specimens. Except for the C5 weldment, the all-weld metal specimens showed a higher impact energy at a particular temperature than did the HAZ specimens. Weldment C5 had HAZ energy in the transition zone somewhat above the all-weld metal energy, and had a lower transition temperature than did the weld metal. For the specimens tested, no trend can be identified in heat input or nugget area versus the transition temperatures. Some of the weldments do not show any transition temperature over the range of temperatures tested. Other weldments are apparently all at the upper range of temperatures, while still others show very definite transitions from −60 to 0°C.

Table 12
All-Weld and HAZ Tensile Data for A514 SMAW
Butt Welds Using E11018 Electrodes

Specimen Code	Yield Strength (ksi)*	Ultimate Tensile Strength (ksi)	True Stress at Fracture (ksi)	True Fracture Strain
		All-Weld Metal Specimens		
B16	113.4	123.8	199.3	0.83
	114.5	120.9	212.6	0.96
B17	114.4	124.5	215.6	0.90
	120.3	125.5	162.9	0.31 (defect)
B18	105.4	120.3	211.0	0.93
	106.9	115.6	206.5	0.97
B19	117.4	127.8	224.5	0.85
	127.8	137.8	247.0	0.80
B20	114.3	126.8	210.5	0.90
	110.3	120.7	205.5	0.79
C6	103.9	113.5	240.6	1.19
	107.1	127.3	238.9	0.98
B21	106.3	119.5	210.1	0.91
	96.4	109.3	185.0	0.75
C5	105.1	113.2	198.8	0.95
	108.0	126.1	208.3	0.84
D7	115.6	123.4	211.2	0.87
	110.3	121.8	164.9	0.31 (defect)
		HAZ Specimens		
B16	116.8	124.8	239.5	1.17
B17	109.9	118.8	235.5	1.21
B18	115.4	123.3	235.9	1.13
B19	100.6	119.7	207.3	0.78
B20	121.8	129.1	207.9	0.74
C6	114.6	123.1	203.0	0.77
B21	100.5	112.3	227.3	1.26
C5	117.4	125.5	204.2	0.72
D7	115.7	124.6	199.6	0.67

*1 ksi = 6.89 MPa

Analysis of Mechanical Properties

The mechanical properties of the A514 weldments, when compared with the specification requirements, indicate that the yield strength of the E11018 weld metal meets the requirements of 97 ksi (668.8 MPa) in all cases but one, where the yield strength was 96.4 ksi (664.6 MPa). The HAZ yield strengths met the base plate yield strength requirement of 100 ksi (689.5 MPa) minimum for all heat inputs and nugget areas used in this investigation. The weld metal UTS was above the 110 ksi (758.4 MPa) minimum required by AWS A5.1 – except for one specimen which had a UTS of 109.3 ksi (753.6 MPa). This was the same specimen that had the 96.4 ksi (664.7 MPa) yield strength. The HAZ UTS was within the base plate specification for UTS (110 to 130 ksi [758.4 to 896.3 MPa]) for all heat inputs and nugget areas used in this investigation.

As with the previous test series, neither the A514 plate nor the E11018 electrode had specified dynamic tear impact requirements. The transition temperature shown in Figure 3 for the A514 steel is −65°C; the impact test data indicate that the HAZ transition temperatures are all significantly higher (above −60°C). Some of the weldments did not show a transition temperature for the impact energy within the range tested; therefore, a qualitative statement cannot be made about the working temperature versus the impact properties of the A514 steel and the E11018 electrode.

As with the other tests, joint side wall fusion and depth of penetration become increasingly difficult to control at heat inputs and nugget areas below 20 kJ/in. (787.4 J/mm) and 0.03 sq in. (19.4 mm^2). The yield strength, when projected using the linear regression line, drops below the minimum requirement well above

60 kJ/in. (2362.2 J/mm), but this is not conclusive because the correlation coefficient for this line has a significantly low value ($r = -0.347$). The high heat input weld (57.2 kJ/in. [2257.0 J/mm] and nugget area of 0.080 sq in. [51.6 mm^2]) was difficult to produce because the combinations of high current and slow travel speed made control of the weld puddle difficult. Therefore, the traditional maximum heat input allowance of 55 kJ/in. (2165.4 J/mm) for this material should be used. This makes the acceptable range of heat input from 20 to 55 kJ/in. (787.4 to 2165.4 J/mm) and nugget area from 0.03 to 0.08 sq in. (19.4 to 51.6 mm^2) for SMAW using the E11018 electrode on A514 steel.

A36 GMAW Butt Weldments

Tensile Test Results

Table 13 and Figures 55 and 56 present the tensile test results for the E70S-3 weld metal and the A36 HAZ specimens over the ranges of heat input and nugget area tested. The weld metal yield strengths are spread over a 21.1 ksi (145 MPa) range. Figures 55 and 56 show the weld metal strength data plotted against heat input and calculated nugget area. Both figures show a highly correlated linear trend of weld metal yield strength decreasing as heat input and nugget area increase. The correlation coefficients for heat input ($r = -0.957$) and nugget area ($r = -0.937$) were not significantly different, indicating that for the test conditions under study both were equal predictors of yield strength.

The HAZ yield strengths were relatively uniform – between 44.1 and 58.3 ksi (304 and 402 MPa). The yield strength showed no trend in relation to area or heat input.

The UTS of the weld metal specimens varied between 68.2 and 88.2 ksi (470.2 and 608.1 MPa); increasing heat input and nugget areas were associated with decreasing UTS. The linear correlation coefficients for the UTS of the weld metal versus heat input and

Table 13
All-Weld and HAZ Tensile Data for A36 GMAW Butt Welds Using E70S-3 Electrodes

Specimen Code	Yield Strength (ksi)*	Ultimate Tensile Strength (ksi)	True Stress at Fracture (ksi)	True Fracture Strain
		All-Weld Metal Specimens		
B25	75.0	88.2	168.6	0.91
	70.2	83.4	162.0	0.91
B26	71.4	87.0	165.8	0.95
	69.7	84.4	156.2	0.86
B24	68.3	82.4	149.7	0.85
	67.1	80.6	137.5	0.74
B23	65.5	80.0	119.3	0.67
	62.0	77.4	157.0	1.06
B27	61.4	75.2	161.3	1.09
	61.2	76.0	147.0	0.96
D4	58.5	68.2	130.1	1.00
	54.5	69.4	88.1	0.53
B22	53.9	73.4	168.9	1.18
	54.1	72.0	160.5	1.20
		HAZ Specimens		
B25	56.0	75.2	143.1	0.97
B26	57.7	75.2	117.6	0.78
B24	49.6	71.0	163.1	1.18
B23	44.1	69.4	161.8	1.18
B27	49.1	70.0	145.3	1.06
D4	58.3	82.2	144.6	0.95
B22	53.1	74.2	150.8	1.02

*1 ksi = 6.89 MPa

nugget area were −0.864 and −0.820, respectively. The trends in the weld metal UTS results are similar to those for the yield strength data.

The UTS of the HAZ specimens varied between 69.4 and 82.2 ksi (478.5 and 566.8 MPa). As with the yield strengths, the HAZ UTS did not correlate significantly with either heat input (r = 0.198) or nugget area (r = 0.101); therefore, neither could be used to predict HAZ tensile strength.

The true fracture stress and strain at fracture were calculated to provide information on the strength and ductility of the weldments. There was no significant correlation between either heat input or nugget area with these two quantities.

Impact Test Results

Figures 57 through 63 graph the dynamic tear impact energy versus test temperature for each weldment. The figures give the all-weld metal impact results and the associated HAZ impact results. The impact energy at a given temperature for the HAZ specimens is lower than that for the all-weld metal specimens. The transition temperatures of the HAZ specimens were all above 20°C, whereas those for the all-weld metal specimens were below 12°C. The correlation coefficients of the weld metal transition temperatures and the HAZ transition temperatures versus heat input or nugget area were not significant.

Analysis of Mechanical Properties

In a general analysis of the mechanical properties of the A36 weldments, it is important to compare the properties of the weld metal and HAZ to those required for the base plate and electrodes. Table 5 indicates that the AWS A5.18 minimum yield strength for the E70S-3 electrode is 60 ksi (413.7 MPa); the A36 steel is 36 ksi (248.2 MPa), as shown in Table 4. Figures 55 and 56 indicate that over the ranges of heat input and nugget area investigated, all the HAZ yield strengths significantly exceeded the specified minimum and actual yield strengths reported in Table 5 for the A36 steel. At heat inputs for nugget areas greater than 50 kJ/in. (1968.5 J/mm) and 0.10 sq in. (64.5 mm^2), the weld metal yield strength fell below the 60 ksi (413.7 MPa) weld metal minimum.

The UTSs of all but one HAZ specimen were within the specified range of 58 to 80 ksi (400 to 551.6 MPa) for A36 steel, and all were significantly higher than the UTS of the base plate (66.2 to 67.2 ksi [456.4 to 463.3 MPa]) shown in Table 4. The UTS of the weld metal met the 72 ksi (496.4 MPa) minimum in all cases.

When comparing the results of the GMAW and SMAW weldments, note that the GMAW weldments are much more sensitive to changes in heat input and nugget area. The slopes of the best fit lines are much larger with GMAW than with SMAW. The HAZ results are about the same in both cases, indicating that the HAZ is somewhat process independent.

The mode of metal transfer used is the possible cause of the higher sensitivity of the GMAW weld metal to heat input and nugget area. With the GMAW system, all alloying agents and deoxidizers must be in the solid wire and must pass through the arc. Whereas with the SMAW system, the alloying agents, deoxidizers, and slag formers are all in the coating material. Therefore, the GMAW system uses a very fine particle spray where the molten electrode material is projected through the arc. With the SMAW process, large globules of metal form at the end of the electrode before being forced across the arc by the expanding gases from the coating. As a globule is forming, the metal picks up alloying materials and deoxidizers from the electrode's coating before being projected to the plate.

The A36 base plate and the E70S-3 electrode do not have specified dynamic tear impact requirements. However, results of tests on the base plate (Figure 1) show that the transition temperature for A36 steel is about −6°C. As stated earlier, the transition temperatures of the HAZ tests were all above +20°C, which is significantly higher than the −5°C value reported. Thus, the HAZ's impact resistance between +30 and −5°C is significantly less than the base plate's; this should be considered in the design and fabrication of A36 welded components if impact resistance is critical.

During test plate fabrication, sidewall fusion and depth of penetration became increasingly difficult to control at heat inputs and nugget areas less than 20 kJ/in. (787.4 J/mm) and 0.045 sq in. (29.0 mm^2), respectively. This, when coupled with the above weld metal yield strength criteria, places the acceptable range for heat input at 20 to 50 kJ/in. (787.4 to 1968.5 J/mm) and nugget area at 0.045 to 0.10 sq in. (29.0 to 64.5 mm^2) for the GMAW using the E70S-3 electrodes and carbon dioxide shield gas on A36 steel.

A516 GMAW Weldments

Tensile Test Results

Table 14 and Figures 64 and 65 present the tensile test results for the E70S-3 weld metal and the A516 HAZ specimens. The weld metal yield strengths are

spread over a 21.1 ksi (145.5 MPa) range, varying from 52.1 to 73.2 ksi (359.2 to 504.7 MPa). The weld metal yield strengths per heat input or nugget area for the A516 weldments with the E70S-3 electrodes are nearly identical to the strengths of A36 weldments with the same electrodes (Tables 13 and 14). Figures 64 and 65 show the weld metal yield strength data plotted against heat input and nugget area. Both figures show a linear trend of weld metal yield strength decreasing as heat input and nugget area increase. The linear correlation coefficient for the weld metal yield strength versus heat input is −0.877, and for the weld metal yield strength versus nugget area, −0.852. The A516 weldment test series uses the same range of nugget areas and heat inputs as the A36 series. Thus, the relative difference between nugget area and heat input values is too small to evaluate the sensitivities of the two parameters to the physical test results.

The HAZ yield strengths varied between 56.2 and 71.7 ksi (387.5 and 494.4 MPa), with increasing heat inputs and nugget areas producing lower yield strengths (Figures 64 and 65). The linear correlation coefficient for the HAZ yield strength versus heat input was −0.766; the linear correlation coefficient for HAZ yield strength versus nugget area was −0.720. Thus, the A516 weldments' HAZ yield strength data correlated more closely with heat input and nugget area than did the A36 specimens'.

The UTS of the weld metal specimens varied between 67 and 88.6 ksi (462 and 610.9 MPa), with increasing heat inputs and nugget areas associated with decreasing UTS. As with the yield strengths, the UTSs of the A516 weldments for each heat input or nugget area were nearly identical to those of the A36 weldments with the same electrodes. The linear correlation coefficients for the weld metal versus heat input and nugget area were −0.814 and −0.724, respectively, showing a relatively higher correlation with heat input.

Table 14
All-Weld and HAZ Tensile Data for A516 GMAW Butt Welds Using E70S-3 Electrodes

Specimen Code	Yield Strength (ksi)*	Ultimate Tensile Strength (ksi)	True Stress at Fracture (ksi)	True Fracture Strain
		All-Weld Metal Specimens		
B30	72.2	84.2	116.2	0.53
	72.4	85.8	165.0	0.88
B29	69.5	82.6	176.2	1.09
	67.2	80.2	178.7	1.12
B31	73.2	88.6	170.8	0.88
	65.3	79.2	140.2	0.78
D3	67.8	75.5	117.6	0.70
	57.0	68.5	118.7	0.82
B32	61.6	76.2	169.7	1.11
	58.9	73.2	134.6	0.89
B28	64.9	78.2	147.0	0.96
	61.9	76.0	164.0	1.05
D2	59.3	67.0	120.3	0.95
	54.2	67.4	118.8	0.93
B33	53.1	70.2	162.8	1.25
	52.1	69.2	172.0	1.28
		HAZ Specimens		
B30	65.1	85.8	203.9	1.20
B29	71.7	78.8	189.5	1.06
B31	71.0	87.6	160.5	0.87
D3	64.7	84.3	173.8	1.10
B32	61.1	84.0	179.3	1.02
B28	68.5	86.2	189.4	1.15
D2	58.7	75.0	116.8	0.78
B33	56.2	74.3	146.5	0.96

*1 ksi = 6.89 MPa

The UTSs of the A516 HAZ specimens varied between 74.3 and 87.6 ksi (512.3 and 604 MPa), with increasing heat inputs and nugget areas associated with decreasing UTSs. The linear correlation coefficients for the HAZ UTS versus heat input and nugget area were −0.710 and −0.640, respectively. As with the yield strengths, the A516 HAZ UTS correlated better with heat input and nugget area than did the A36 HAZ UTS. There was also a higher correlation with heat input than with nugget area for the A516 HAZ UTS.

To indicate the strength and ductility of the weldments, the true fracture stress and strain at fracture were calculated for all specimens tested. There was no significant correlation between heat input or nugget area and these two quantities.

Impact Test Results

Figures 66 through 73 graph for each weldment the dynamic tear impact energy absorbed versus test temperature for the range of nugget areas and heat inputs investigated. Each figure contains the all-weld metal impact results and the associated HAZ impact results. As with the A36 GMAW tests, the impact energy at a given temperature for the HAZ specimens was lower than that for the weld metal specimens, except for the highest heat input and nugget area (72 kJ/in. [2834.7 J/mm] and 0.13 sq in. [83.9 mm^2]). The transition temperatures of the HAZ specimens were all above 20°C. The transition temperatures of the all-weld metal specimens varied between 25 and 40°C – except the 72 kJ/in. (2834.6 J/mm) weldment, which had a transition temperature of −30°C. The HAZ specimens showed higher transition temperatures than the all-weld specimens. Unlike the A36 dynamic tear test results, both HAZ and weld metal transition temperatures appeared to decrease with increasing heat input and nugget area.

Analysis of Mechanical Properties

The mechanical properties of the A516 weldments, when compared with the specification requirements, indicate that the yield strength of the E70S-3 electrode drops below the 60 ksi (413.7 MPa) minimum requirement at heat inputs and nugget areas greater than 50 kJ/in. (1968.5 J/mm) and 0.1 sq in. (64.5 mm^2), respectively (Figures 64 and 65). But none of the HAZ yield strengths dropped below the 38 ksi (262 minimum MPa) yield strength specified for the base plate, or the 40 ksi (275.8 MPa) yield strength presented in Table 4.

The UTS of the weld metal specimens dropped below the 72 ksi (496.4 MPa) minimum requirement of the A516 base plate at heat inputs and nugget areas greater than 50 kJ/in. (1968.5 J/mm) and 0.10 sq in. (64.5 mm^2). respectively. The UTSs of the HAZ specimens were all within the 70 to 90 ksi (482.6 to 620.5 MPa) range for the A516 base plate.

Neither the A516 plate nor the E70S-3 electrodes have specified dynamic tear impact requirements. Figure 2 shows that the A516 base plate used in this investigation has a transition temperature of approximately −5°C. The HAZ and weld metal have significantly higher transition temperatures. Thus, the impact resistance of the HAZ and weld metal may be significantly less than that of the base plate and should be considered in the design and fabrication of the A516 welded components if impact resistance is critical.

As with the A36 plate, sidewall fusion and depth of penetration became increasingly difficult to control at heat inputs and nugget areas less than 20 kJ/in. and 0.045 sq in. (787.4 J/mm and 29.0 mm^2), respectively. This, when coupled with the weld metal yield strength criteria, places the acceptable range for heat input at 20 to 50 kJ/in. (787.4 to 1968.5 J/mm) and the nugget area at 0.045 to 0.10 sq in. (29.0 to 64.5 mm^2) for GMAW using the E70S-3 electrodes and carbon dioxide shield gas on A516 steel.

A514 GMAW Weldments

Tensile Test Results

Table 15 and Figures 74 and 75 present the tensile test results of the E120S-1 weld metal and the A514 HAZ specimens over the range of heat input and nugget areas tested. The weld metal yield strengths were between 86 and 144 ksi (724 and 923 MPa). Figures 74 and 75 show the weld metal yield strength data plotted against heat input and nugget area. Both figures show a linear trend of decreasing weld metal yield strength as heat input and nugget area increase ($r = -0.723$ for yield strength versus heat input, and $r = -0.762$ for yield strength versus nugget area). As with the A36 and the A516 GMAW test series, the difference between nugget area and heat input values is too small to evaluate the relative sensitivity of the two parameters to the physical test results.

The HAZ yield strengths varied between 47 and 137.4 ksi (324 and 947.4 MPa). The HAZ yield strengths correlated significantly with heat input ($r = -0.743$) and nugget area ($r = -0.783$), and tended

to decrease with increasing heat inputs and nugget areas. The extremely low HAZ yield strength (47 ksi [324 MPa]) of the highest heat input and largest nugget area specimen (B34) occurred because the heat of welding changed the microstructure of the base material in the HAZ from a quenched and tempered martensitic structure (high strength) to a structure containing considerable amounts of pearlite (low strength). The linear regression was analyzed, including the tensile test results from this plate; however, if the results were removed from the linear regression analysis, the coefficient r would become −0.313. Physically speaking, the HAZ data for weldment B34 should not be included because of the phase change encountered in the HAZ. The higher correlation coefficient with these data included indicates that the linear relationship between the heat input and strength level for the A514 steel is not of physical significance, although there is some statistical significance.

The UTS of the weld metal specimens varied between 114.3 and 149.4 ksi (788.1 and 1030.1 MPa). The weld metal UTS did not correlate very well with heat input (r = −0.479) or nugget area (r = −0.479), but tended to decrease with increasing heat inputs and nugget areas – similar to the yield strength tendencies.

The UTS of the HAZ specimens varied between 69.5 and 140.5 ksi (479.2 and 968.7 MPa). As with the HAZ yield strength, the HAZ UTS had a more significant correlation with the heat input (r = −0.694) and nugget area (r = −0.736) when the results from the HAZ of weldment B34 were included. When these results were not included, the correlation coefficient for the HAZ UTS versus heat input was −0.148, and for nugget area, −0.151. Like the HAZ yield strength results, these should not be included in the linear regression analysis.

True fracture stress and strain at fracture were calculated to provide information on the strength and ductility of the weldments. There was no significant correlation between either heat input or nugget area with these two quantities.

Table 15
All-Weld and HAZ Tensile Data for A514 GMAW Butt Welds Using E120S-1 Electrodes

Specimen Code	Yield Strength (ksi)*	Ultimate Tensile Strength (ksi)	True Stress at Fracture (ksi)	True Fracture Strain
		All-Weld Metal Specimens		
B39	143.4	144.4	296.2	1.25
	140.0	149.4	312.5	1.16
B38	130.5	136.0	287.0	1.22
	135.3	146.0	259.6	1.01
B36	118.8	125.3	274.2	1.32
	116.3	123.3	251.0	1.25
B35	114.8	120.5	225.8	1.09
	105.3	114.3	137.3	0.32 (defect)
B37	116.5	124.3	234.0	1.12
	118.1	134.5	240.0	1.04
D1	116.0	138.0	201.5	0.92
	123.3	130.5	165.9	0.36
B34	86.1	114.5	140.2	0.35 (defect)
	111.3	130.1	293.3	1.19
		HAZ Specimens		
B39	113.0	120.5	257.1	1.25
B38	137.4	140.5	284.0	1.11
B36	107.8	116.5	237.4	1.22
B35	110.1	118.1	276.3	1.37
B37	103.5	112.3	250.9	1.32
D1	114.8	127.1	179.7	0.53
B34	46.9	69.5	144.7	1.06

*1 ksi = 6.89 MPa

Impact Test Results

Figures 76 through 82 graph the dynamic tear impact energy versus test temperature for each weldment. Each figure contains the all-weld metal impact results and the associated HAZ impact results. In all cases, the impact energy at a given temperature for the HAZ specimens is lower than the all-weld metal specimens. Additionally, it appears that for the range of temperatures tested (−40 to +40°C) the HAZ specimens were all on one shelf or the other, and the all-weld metal specimens were generally on the upper shelf. Thus it was impossible to compare the influence of heat input and nugget area on transition temperatures for HAZ and weld metal specimens.

Analysis of Mechanical Properties

The mechanical properties of the A514 weldments, when compared with the specification requirements, indicate that the yield strength of the E120S-1 weld metal exceeds the 105 to 122 ksi (724 to 841.2 MPa) requirements at the extremes of the heat inputs and nugget areas investigated. Below 16 kJ/in. (629.9 J/mm) and 0.04 sq in. (25.8 mm^2), the yield strength exceeds the maximum; at 50 kJ/in. (1968.5 J/mm) and 0.13 sq in. (83.9 mm^2) the yield strength becomes marginal, with one of the specimens dropping below the 105 ksi (724 MPa) minimum. The HAZ yield strengths dropped below the 100 ksi (689.5 MPa) minimum ASTM A514 base plate requirement at heat inputs and nugget areas greater than 40 kJ/in. (1574.8 J/mm) and 0.12 sq in. (77.4 mm^2). It should be remembered that with heat inputs between 40 and 50 kJ/in. (1514.8 and 1968.5 J/mm) and nugget areas between 0.10 and 0.13 sq in. (64.5 to 83.9 mm^2), a physical change in the HAZ occurs, causing the strength levels of the HAZ to drop sharply from the unaffected A514 base plate. The weld metal UTS did not drop below the 110 ksi (757.9 MPa) minimum required for the entire heat input and nugget area test range, but the HAZ UTS dropped below the 110 ksi (757.9 MPa) minimum base plate requirement at heat inputs and nugget areas greater than 50 kJ/in. (1968.5 J/mm) and 0.12 sq in. (77.4 mm^2).

As with the previous test series, neither the A514 plate nor the E120S-1 electrodes had specified dynamic tear impact requirements. The transition temperature for the A514 steel, as shown in Figure 3, is about −65°C; this, when compared with the impact data, indicates that the HAZ transition temperatures are all significantly higher (above 30°C). Thus, for the most common operating temperatures, the impact resistance of the HAZ is significantly less than that of the base plate and should be considered in the design and fabrication of A514 welded components if impact resistance is critical.

As with the other tests, plate sidewall fusion and depth of penetration became increasingly difficult to control at heat inputs and nugget areas below 20 kJ/in. (787.4 J/mm) and 0.04 sq in. (25.8 mm^2), respectively. This, with the yield strength and UTS restrictions on the weld metal, suggests an acceptable range of heat input at 20 to 50 kJ/in. (787.4 to 1968.5 J/mm) and a nugget area at 0.04 to 0.12 sq in. (25.8 to 77.4 mm^2) for the GMAW using the E120S-1 electrode and argon-2 percent oxygen shield gas on the A514 steel.

Restrained Joints

SMAW Weldments

Visual examination during welding, magnetic particle inspection, radiographic inspection, and macroscopic examination were used to check the weldability of the three steels fabricated under restraint conditions (Table 16). Observations during welding, and in post-weld inspection, indicated that the SMAW welds produced at less than 20 kJ/in. (787.4 J/mm) presented operational problems, poor bead contour, and inadequate fusion during welding. Therefore, extensive grinding of each weld layer was needed to produce a satisfactory weld. Low heat input welds in A36 steel resulted generally in HAZ cracking in some region of the welds. In each case, the cracks began in the HAZ at the midsection of the 3/4-in. (19-mm) plate. Macroscopic examination revealed a very heavy band of inclusions at the center plane of the plate. Only very light inclusions were noted in the A516 and A514 steel macrosections, and no HAZ cracking was observed in these steels at the low heat input level.

Table 17 presents the weld metal and HAZ tensile properties for each of the restrained welds fabricated. One weld specimen for the high heat input weld, T_1, fell below the minimum 60 ksi (413.7 MPa) yield strength for the E7018 electrode. The results of the low heat input weld are comparable to the results from the butt weld tests and fit the curves in Figures 22 and 23 reasonably well. The UTSs of all the weld metal specimens meet the 72 ksi (496.4 MPa) minimum yield strength of AWS A5.1. The UTSs of the HAZ specimens exceed the UTS requirement range for the A36 base plate of 58 to 80 ksi (399.9 to 551.6 MPa). Both the high and low heat input weldments exhibited a UTS greater than 88 ksi (606.7 MPa).

Table 16
Weldability Evaluation – Restrained Joints

	Observations			
	Visual (During Welding)	Magnetic Particle Inspection	Radiographic Inspection	Macroscopic Examination
		SMAW Welds		
Weld T A36 61.6 kJ/in. (2425.2 J/mm)	Good fusion, good bead contour	Acceptable	Acceptable	Clean
Weld M A36 25.8 kJ/in. (1015.8 J/mm)	Slightly cold, acceptable bead contour	Acceptable	Acceptable	Small crack (2-1/8 in. 54 mm]) in HAZ at mid-plate thickness
Weld S A36 19.9 kJ/in. (783.54 J/mm)	Crack along HAZ extending into base metal	----	----	----
Weld R A516 61.6 kJ/in. (2425.2 J/mm)	Good fusion, good bead contour	Acceptable	Acceptable	Light slag – third layer
Weld Q A516 15.5 kJ/in. (610.2 J/mm)	Cold weld, extensive grinding needed each layer	Acceptable	Linear indication 1/4-in. (6.4-mm) long in weld	Clean
Weld P A514 40.9 kJ/in. (1610.2 J/mm)	Good fusion, good bead contour	Acceptable	Acceptable	Light slag and porosity
Weld O A514 15.8 kJ/in. (622.1 J/mm)	Cold weld, extensive grinding needed each layer	Acceptable	Acceptable	Clean
		GMAW Welds		
Weld K A36 49.5 kJ/in. (1948.8 J/mm) CO_2	Good fusion, good bead contour	Acceptable	Acceptable	Clean
Weld L A36 25.0 kJ/in. (984.3 J/mm) CO_2	Slightly cold, high bead crowns	Acceptable	Acceptable	Minor cold shuts
Weld I A516 49.6 kJ/in. (1952.8 J/mm) CO_2	Good fusion, good bead contour	Acceptable	Not radiographed	Clean

Table 16 (cont'd)

	Observations			
	Visual (During Welding)	Magnetic Particle Inspection	Radiographic Inspection	Macroscopic Examination
Weld W A516 24.2 kJ/in. (952.8 J/mm) CO_2	Good fusion, slightly cold beads	Acceptable	Acceptable	Very small cold shuts or elongated pores
Weld V A514 54.8 kJ/in. (2157.5 J/mm) Ar-2% O_2	Good fusion, good bead contour	Acceptable	Acceptable	Clean
Weld U A514 15.9 kJ/in. (626.0 J/mm) Ar-2% O_2	Cold weld, extensive grinding done	Acceptable	Heavy porosity, transverse crack in weld metal	- - -
Weld J A514 24.9 kJ/in. (980.3 J/mm) Ar-2% O_2	Good fusion good bead contour	Acceptable	Heavy porosity	Scattered porosity

The results of the A516 tensile tests shown in Table 17 fit the butt weld tensile data reasonably well, with a high yield strength at the low heat input and a low yield strength at the high heat input. The HAZ yield strength in each weldment substantially exceeded the 38 ksi (262 MPa) minimum required for the A516 steel plate. The UTS for the weld metal of each weldment produced exceeded the 72 ksi (496.4 MPa) minimum required by AWS A5.1. The UTS of the HAZ, in one case the high heat input weld, met the UTS specification requirement of 70 to 90 ksi (482.6 to 620.5 MPa) for the A516 plate. The low heat input weld exceeded the requirement by 5 ksi (34.5 MPa).

The E11018 SMAW weld metal yield strength exceeded the 97 ksi (668.8 MPa) minimum requirement for both the high heat input and the low heat input weldments. As with the other restraint welds, the high heat input weldment had the lower yield strength. The yield strengths of all HAZ specimens met the 100 ksi (689.5 MPa) minimum requirement for the A514 plate. The HAZ specimens also showed the same trend as the weld metal yield strength specimens. The UTS of the weld metal met the specification requirement of 110 ksi (758.4 MPa) minimum in all but one specimen. As with the other weldments, the high heat input weldment produced the lowest UTS, while the low heat input produced the highest. The UTS of the HAZ specimens was at the high end of, or exceeded, the 110 to 130 ksi (758.4 to 896.3 MPa) range for the A514 base plate. The tensile results for the A514 weldments fit the butt weld data reasonably well at the two heat inputs tested for the restraint conditions.

Figures 83 through 88 show the dynamic tear energy versus test temperature for the all-weld metal and HAZ specimens for each of the SMAW restraint weldments. As with the butt welds, the HAZ energy at a given temperature is generally lower than the all-weld metal dynamic tear energy. This suggests that the transition temperature for the HAZ is generally higher than that for the weld metal. The HAZ transition temperature for the A36 and the A516 weldments produced at the high heat input is lower than that for the weldments produced at the low heat input. Comparison of these results with information from previous tests of butt welds indicates that there is no trend in the relationship between HAZ transition temperature and either heat input or nugget area.

GMAW Weldments

Visual examination during welding, magnetic particle inspection, radiographic inspection, and macro-

Table 17
Tensile Properties of the SMAW Restrained Welds

Specimen	Plate Type	Yield Strength (ksi)*	UTS (ksi)	Elongation (Percent)	Reduction in Area (Percent)
		All-Weld Metal Specimens			
T	A36	64.4	81.2	27.5	74.1
		57.9	79.4	30.0	72.8
M	A36	78.7	90.5	26.0	72.4
		71.8	87.8	29.3	73.1
R	A516	65.5	80.0	30.2	73.4
		65.3	80.9	23.6	74.0
Q	A516	83.0	99.0	19.8	54.0
		81.0	94.0	28.1	70.0
P	A514	100.2	109.6	22.5	68.5
		100.2	112.8	22.0	64.8
O	A514	116.0	119.7	19.9	64.4
		113.3	119.3	21.6	63.3
		HAZ Specimens			
T	A36	66.4	88.0	27.5	59.2
M	A36	72.8	91.6	26.7	67.4
R	A516	67.8	86.0	30.0	58.7
Q	A516	83.0	95.0	26.0	69.0
P	A514	117.6	127.1	18.0	59.1
O	A514	126.8	131.1	17.9	54.6

*1 ksi = 6.89 MPa

scopic examination were used to check the weldability of the three steels fabricated under restraint conditions with the GMAW process (Table 16). Observations made during welding and in post-weld inspection revealed that the GMAW welds produced at less than 20 kJ/in. (787.4 J/mm) presented operational problems with poor bead contour and inadequate fusion during welding. Therefore, extensive grinding of each weld layer was needed to produce a satisfactory weld. Low heat input welds in A36 steel resulted generally in HAZ cracking in some regions of the welds. In each case, the cracks began in the HAZ at the midsection of the 3/4-in. (19-mm) plate. These weldments were cut from the same base plate as the SMAW restraint weldment. No HAZ cracking was observed in the A516 or A514 steels. Transverse weld, hydrogen-induced cracking occurred in one A514 GMAW weld (U) made at 16 kJ/in. (629.9 J/mm). This is the only case of weld metal cracking found. A review of the GMAW radiographs suggests that the quality of the carbon dioxide shielded welds was generally better than that of the argon-2 percent oxygen welds, which exhibited varying degrees of porosity. This may be an effect of the deeper bead spike or papillary resulting with argon-2 percent oxygen shielding gas.

The weld metal and HAZ tensile properties are reported in Table 18. The high heat input A36 weldment did not meet the minimum 60 ksi (414 MPa) yield strength requirement for the E70S-3 electrode. It did, however, conform to the 72 ksi (496.4 MPa) minimum UTS requirement. The low heat input weldment exceeded the minimum requirements substantially for the all-weld metal specimens. The HAZ specimens from both welds were very high, and the UTS results were outside the range specified for the A36 plate. The tensile results for the A516 all-weld specimens met the E70S-3 requirements shown in Table 5. As with the A36 weldments, the high heat input A516 weld had lower tensile properties than the low heat input welds, and these properties fit the curves generated from the butt welding portion of this investigation. The all-weld

metal specimen of the high heat input A516 weldment met the yield strength and UTS requirements for the E120S-1 electrode. The low heat input weldment exceeded the specified yield strength range of 105 to 122 ksi (724 to 841.2 MPa). The HAZ results for the A514 weldments showed that the high heat input weldment had high yield strength, with the UTS exceeding the range of 110 to 130 ksi (758.4 to 896.2 MPa) of the A514 specification. The low heat input weld HAZ specimen showed hydrogen damage with extremely low elongation and no determinable yield strength.

Figures 89 through 94 present the dynamic tear energy versus test temperature for the all-weld metal and the HAZ specimens for each restraint weldment. Except for weldment J (A514 steel), the HAZ dynamic tear energy levels at a given temperature are lower than those for the all-weld metal specimens. Consequently, the transition temperature for the HAZ is higher than that for the weld metal. In addition, the HAZ transition temperature of the two A36 weldments is substantially higher than that of the unaffected base plate shown in Figure 1 (30°C versus −5°C). The HAZ transition temperature for the A516 weldments is almost equivalent to the transition temperature for the A516 steel shown in Figure 2. The HAZ transition temperature for weldment V of the A514 steel is substantially higher than that of the unaffected base plate in Figure 3 (−25°C versus −65°C). Weldment J of the A514 steel does not show a transition zone on the HAZ specimens, and only the beginnings of one for the all-weld metal specimens at the lowest test temperature. Therefore, no conclusions can be drawn about the transition for the A514 weldment J.

Restraint Welding Analysis

The results of the restraint welding portion of this investigation indicate that the minimum heat input for each steel and electrode used should be limited to 25 kJ/in. (984.3 J/mm) because of the difficulties in maintaining sidewall fusion, bead contour, and operability

Table 18
Tensile Properties of the GMAW Restrained Welds

Specimen	Plate Type	Yield Strength (ksi)*	UTS (ksi)	Elongation (Percent)	Reduction in Area (Percent)
		All-Weld Metal Specimens			
K	A36	58.9	72.7	30.3	69.4
		58.1	72.7	32.1	72.4
L	A36	71.1	86.7	22.9	54.8
		72.0	80.2	25.5	68.5
I	A516	64.1	78.4	30.2	70.3
		60.4	76.4	28.4	70.5
W	A516	75.0	89.0	26.9	62.0
		69.0	85.0	28.1	70.0
V	A514	110.7	120.6	12.7	70.7
		109.9	135.1	11.2	65.7
J	A514	136.0	145.7	5.6	20.1
		123.0	142.1	4.4	16.3
		HAZ Specimens			
K	A36	71.4	93.8	24.4	49.6
L	A36	75.2	98.2	19.5	40.1
I	A516	63.9	80.8	27.5	67.7
W	A516	81.0	99.0	23.0	53.0
V	A514	121.8	140.1	8.8	62.1
J	A514	--	119.5	0.2	10.1

*1 ksi = 6.89 MPa

of the electrodes. The low heat input also increased the risk of cracking in the weld metal and the HAZ. At the high end of the heat input range, there was no difficulty with the operability and usability of the electrodes, or with cracking because of high restraint on the weld joint.

Under restraint conditions, the A514 steel weldments presented a problem that was not seen with the butt welds. The A514 weld metal suffered hydrogen damage that noticeably reduced the elongation and ductility of the material and created problems in attaining the yield strength levels required of the weld metal. The increased effect of the shrinkage stresses on the weld metal and the hydrogen content of the metal are responsible for these problems. Therefore, it is reasonable to require an increased preheat of the weld joint before fabrication. The structural welding code, AWS D1.1, now requires a minimum preheat of 10°C for A514 plate up to 3/4-in. (19-mm) thickness. This means that at room temperature, no preheat is required for the plate thickness used in this investigation. An increase to 93.3°C of preheat would help reduce the hydrogen damage. Another alternative would be to post-weld soak the joint at 121°C for 1 hour after the completion of the weld.

The conclusions about high heat input from the restraint weldment investigation did not alter the butt weld investigation's results concerning the limits on heat input and nugget area for the A36 and A516 steels. However, the conclusions about the high heat input limit for the A514 steel were affected. The heat input for weldment V was 51.8 kJ/in. (2039.4 J/mm); this was more than the highest butt weld heat input, but weldment V did not show the degradation of the HAZ tensile results that butt weld B34 did.

Observations

Generally, the low heat input (below 20 kJ/in. [787.4 J/mm]) weldments cause problems with operability and usability. The weld beads look ropy, and sidewall fusion and penetration become minimal. In the case of the GMAW weldments, the strength requirements also are a problem at heat inputs below 20 kJ/in. (787.4 J/mm). The deposited weld metal responds much more to both heat input and nugget area with this system than with SMAW. Therefore, the weld metal attains a very high strength level at low heat inputs and falls off rather rapidly as the heat input is increased. The SMAW system, on the other hand, shows much less response to the heat input and nugget area.

The high heat impact limits were based on strength requirements for the weld metal and HAZ base plate. Again, because of the GMAW process' drop in strength, the high end of the range is much better defined than in the SMAW process. The A36 and A516 SMAW weld metal yield strengths from the highest heat input welds were at marginal levels (at or near 60 ksi [413.7 MPa]); consequently, a conservative limit was assumed. The high heat input limit for A514 steel was determined by the usability of the E11018 electrode. In the one weldment made above 50 kJ/in. (1968.5 J/mm), the A514 GMAW system showed degradation of the HAZ properties because of a phase change. The SMAW process did not cause this degradation in the A514 plate – possibly because the heat source of this process is more diffuse. The cooling time between passes is another possible explanation for this peculiar performance. No maximum preheat temperature is required for the A514 steel; consequently, an individual could place bead after bead in the joint, building the temperature to a point where the phase change would probably occur.

No conclusive evidence was found that the impact energy responded to heat input or nugget area. Some of the high heat input welds showed reasonably good toughness with a low transition temperature.

The transient weldments confirmed the lower limit and indicated the possibility of hydrogen problems in the A514 GMAW weldment system.

Table 19 presents the results of this investigation on the limits of heat input and nugget area for the three plate steels and four electrodes used.

4 CONCLUSION

This study has determined voltage, current, and travel speed limits necessary to ensure proper weld strength levels for construction steels. Table 9 lists specific voltage limits for SMAW electrodes. The welding current limits as defined by AWS A5.1 for SMAW electrodes were found to be satisfactory for the electrodes used in this investigation. Travel speed limits are shown in Figures 8 through 14 for each SMAW electrode used. Limits on heat input and nugget area are given in Table 19; these limits should be applied to Corps of Engineers construction using the three steels and four electrodes discussed in this report.

Table 19
Heat Input and Nugget Area Limits for A36, A516, and A514 Steel

Steel	Electrode	Heat Input Limits, kJ/in. (J/mm)	Nugget Area Limits, sq in. (mm^2)
A36	E7018	20 to 55 (787.4 to 2165.4)	0.03 to 0.08 (19.4 to 51.6)
	E70S-3	20 to 50 (787.4 to 1968.5)	0.045 to 0.10 (29.0 to 64.5)
A516	E7018	20 to 50 (787.4 to 1968.5)	0.03 to 0.07 (19.4 to 45.2)
	E70S-3	20 to 50 (787.4 to 1968.5)	0.045 to 0.10 (29.0 to 64.5)
A514	E11018	20 to 55 (787.4 to 2165.4)	0.03 to 0.08 (19.4 to 51.6)
	E120S-1	25 to 50 (984.3 to 1968.5)	0.06 to 0.12 (38.7 to 77.4)

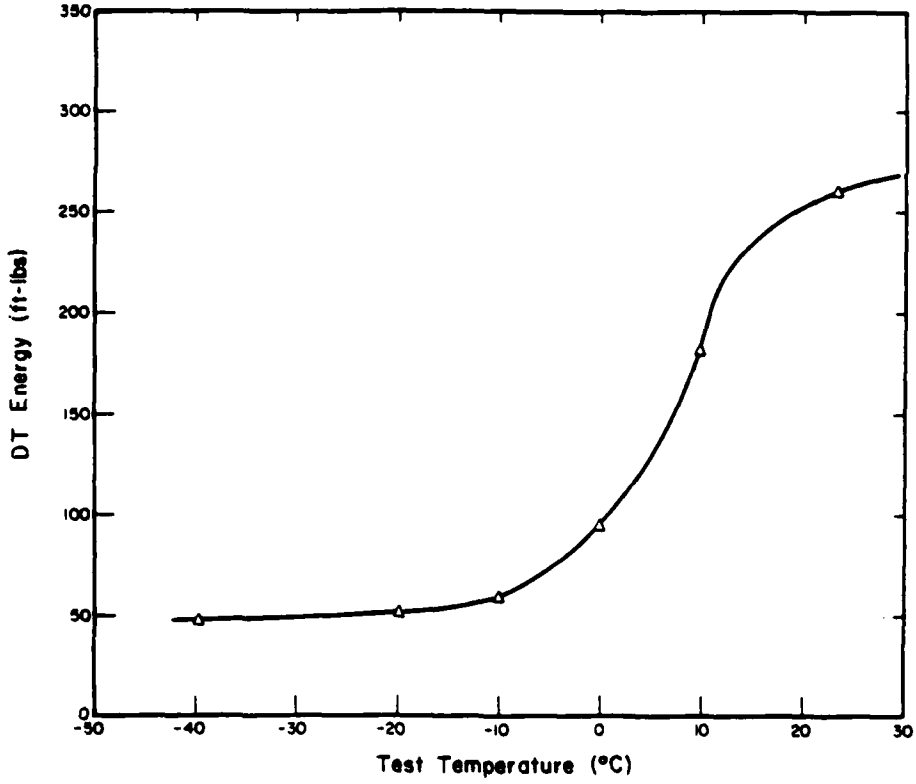

Figure 1. Dynamic tear test energy versus test temperature for A36 steel plate.

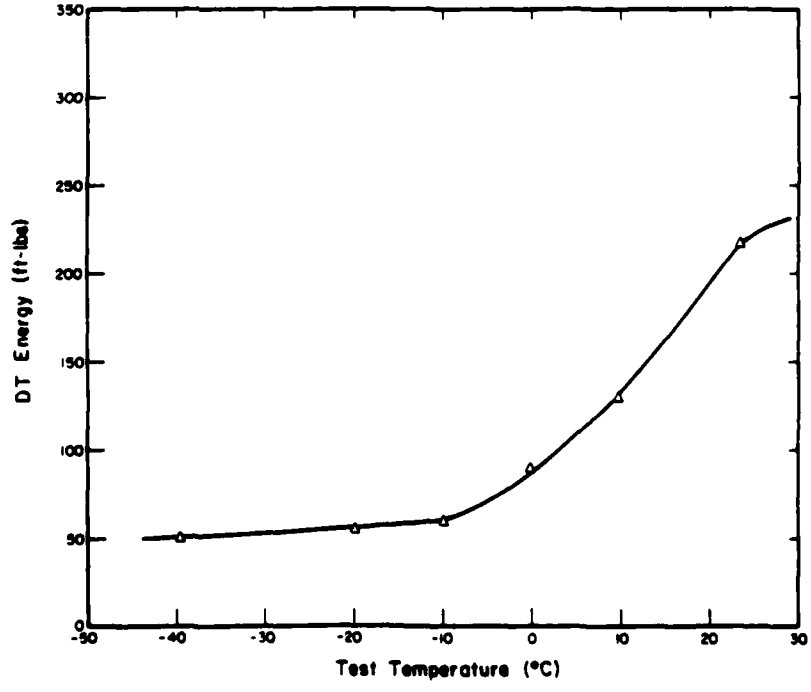

Figure 2. Dynamic tear test energy versus test temperature for A516 steel plate.

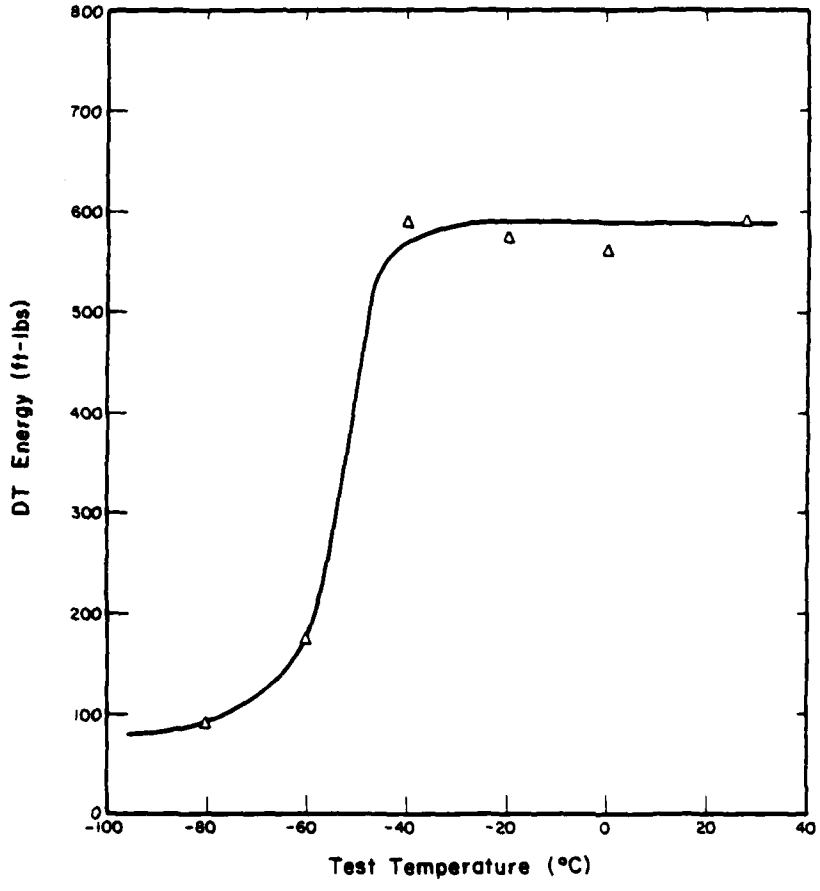

Figure 3. Dynamic tear test energy versus test temperature for A514 steel plate.

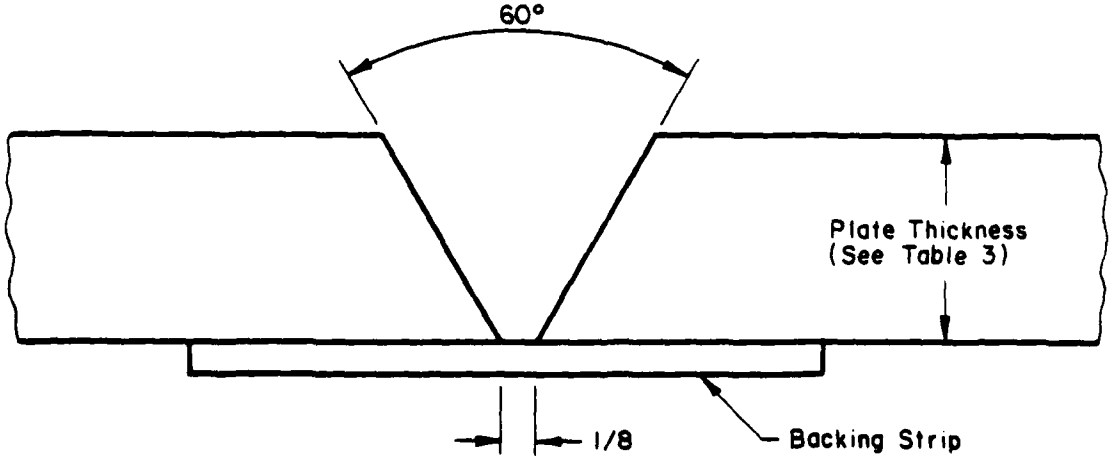

Figure 4. Joint design used for the A36, A514, and A516 steel weldments.

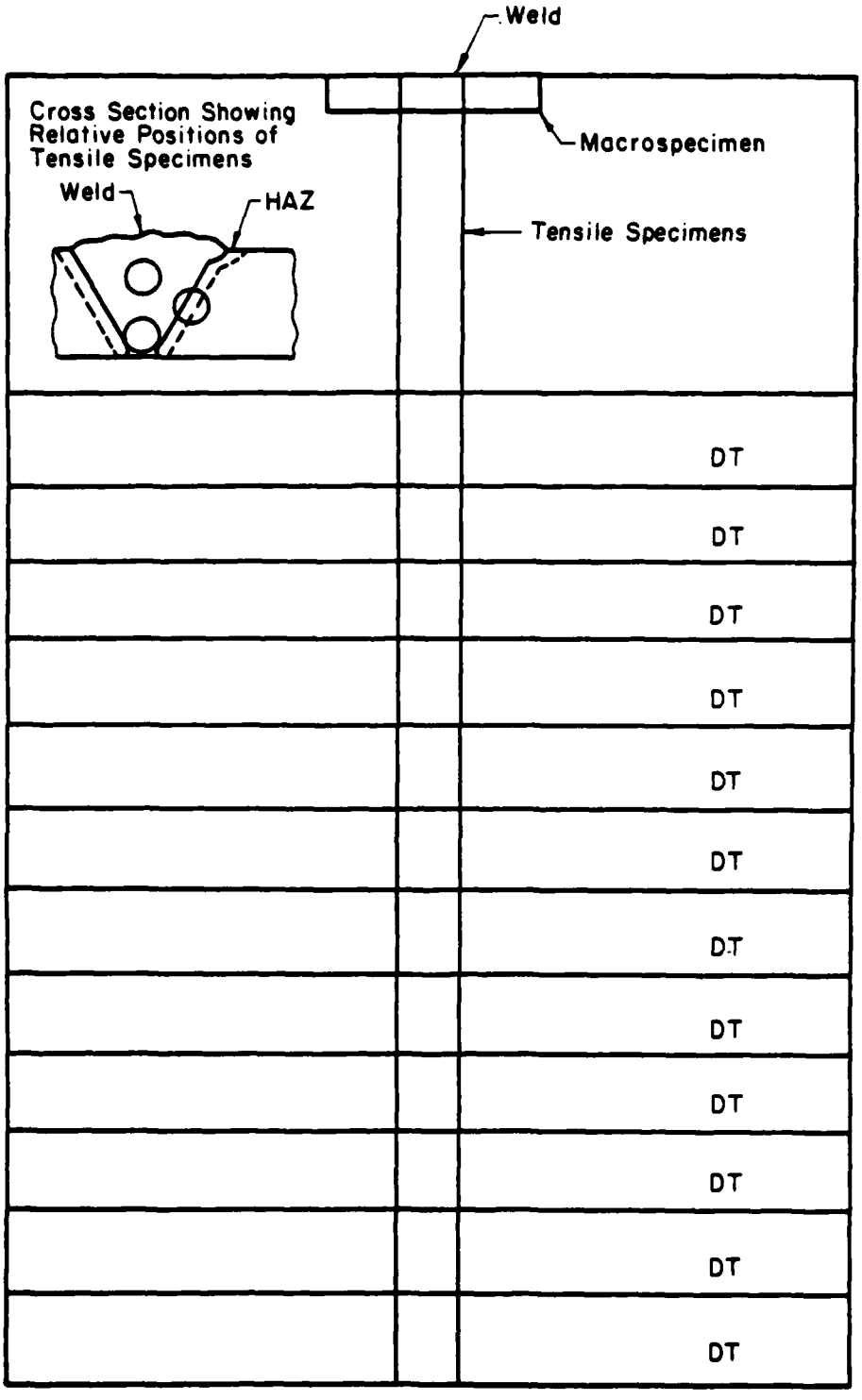

Note: Half of DTs Notched in Weld Metal, and Half of DTs Notched in HAZ.

Figure 5. Schematic showing specimen location as machined from weldment.

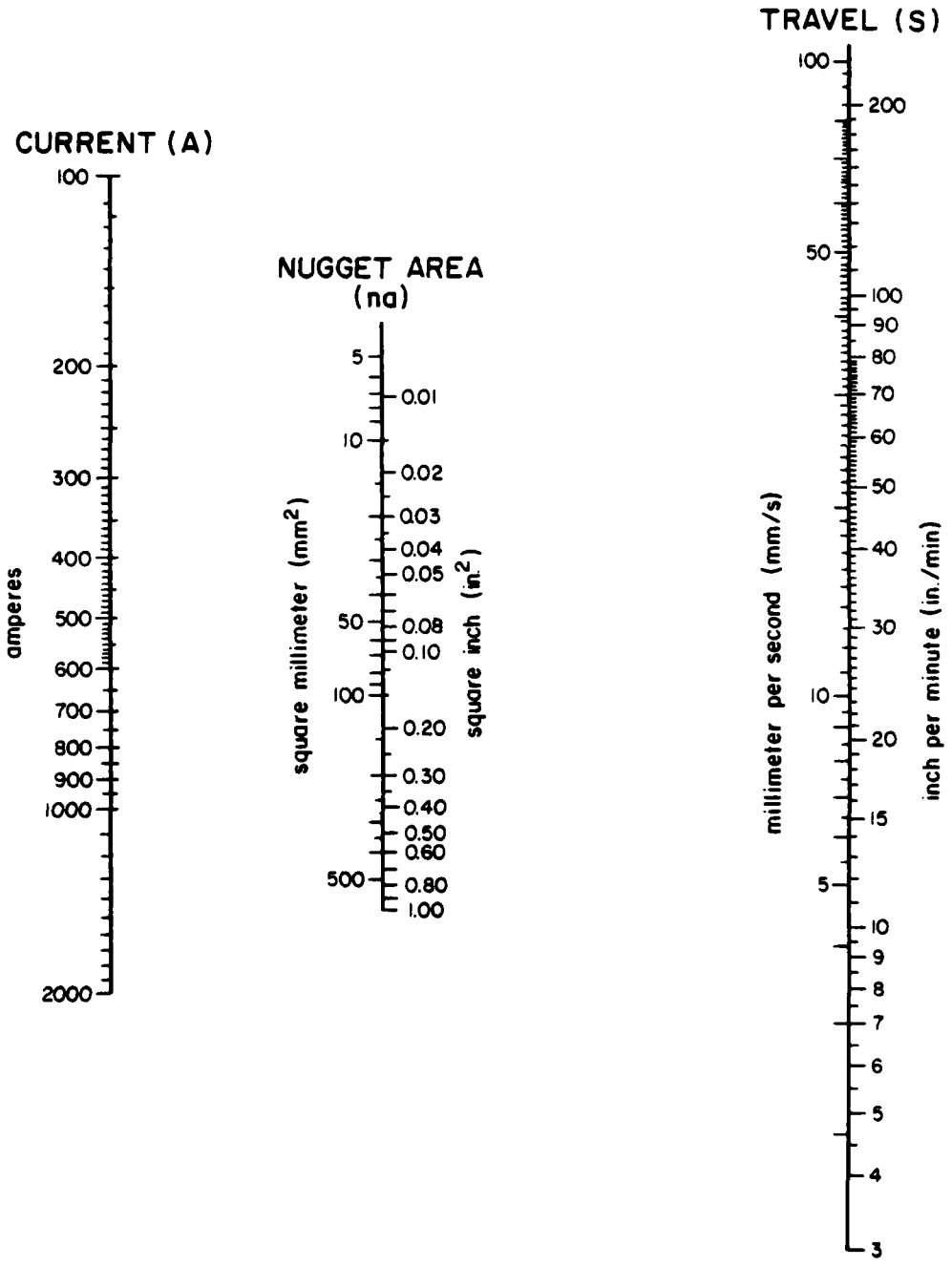

Figure 6. Nomograph for determining nugget area (from B. L. Schultz and C. E. Jackson, "Influence of Weld Bead Area on Weld Mechanical Properties," *Welding Journal*, Vol. 52 [January 1973], Research Supplement, p. 36s).

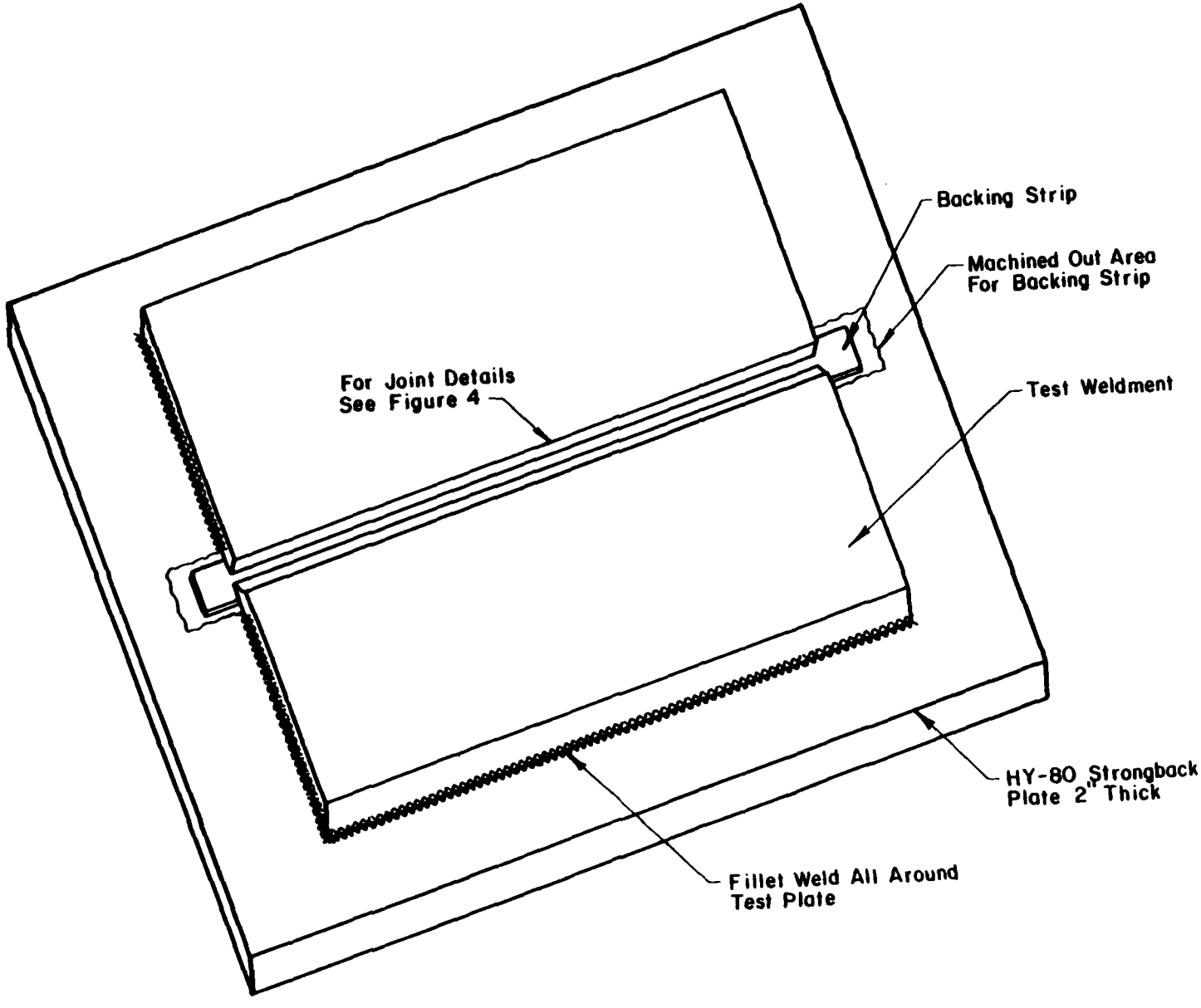

Figure 7. Schematic diagram of highly restrained weld layout.

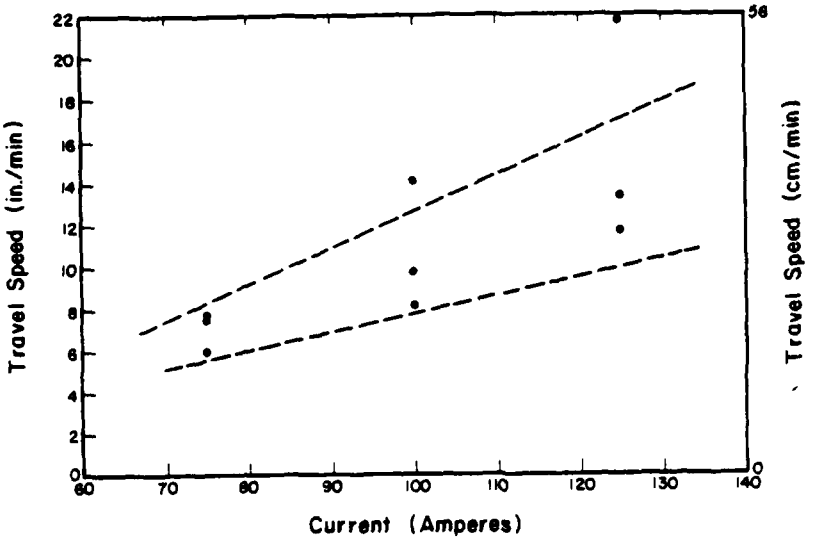

Figure 8. Graph showing travel speed limits for current levels used for 1/8-in. (3.2-mm) diameter E6010 SMAW electrode. Dashed lines show travel speed limits as determined by amount of undercut and bead shape.

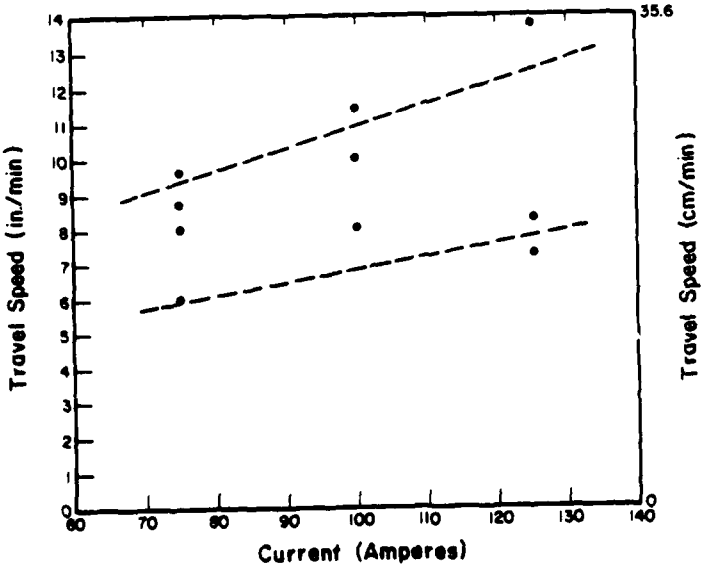

Figure 9. Graph showing travel speed limits for current levels used for 1/8-in. (3.2-mm) diameter E6011 SMAW electrode. Dashed lines show travel speed limits as determined by amount of undercut and bead shape.

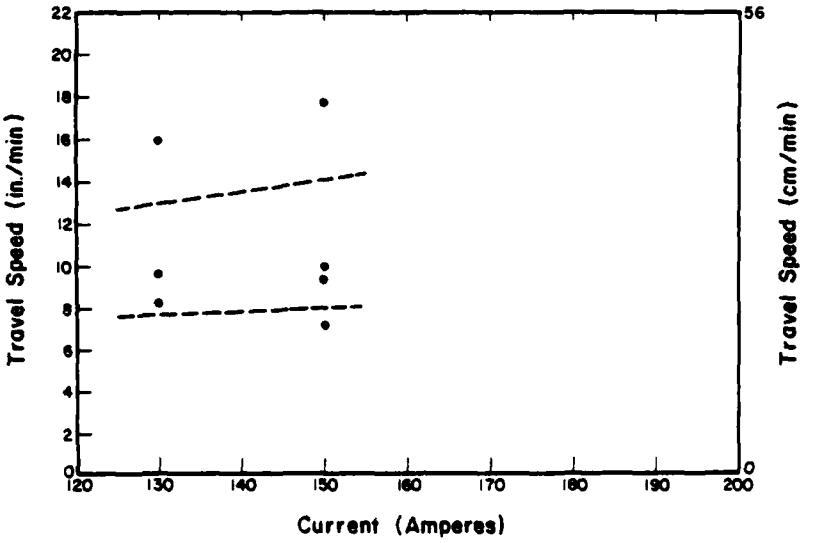

Figure 10. Graph showing travel speed limits for current levels used for 1/8-in. (3.2-mm) diameter E6013 SMAW electrode. Dashed lines show travel speed limits as determined by amount of undercut and bead shape.

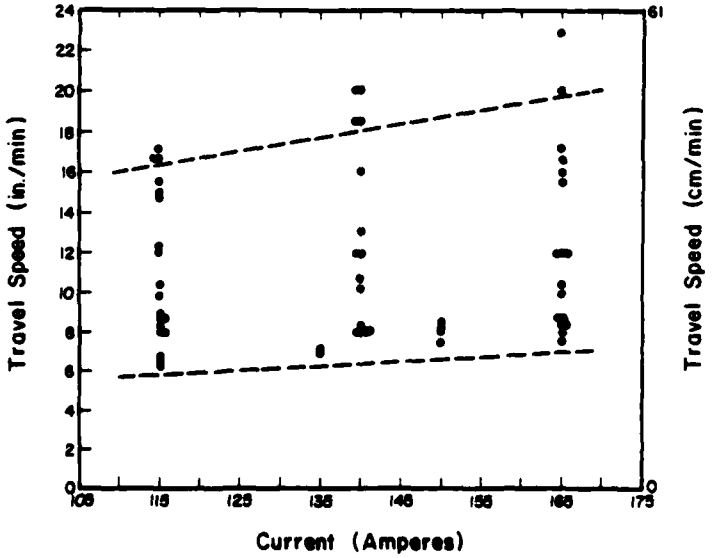

Figure 11. Graph showing travel speed limits for current levels used for 1/8-in. (3.2-mm) diameter E7018 SMAW electrode. Dashed lines show travel speed limits as determined by amount of undercut and bead shape.

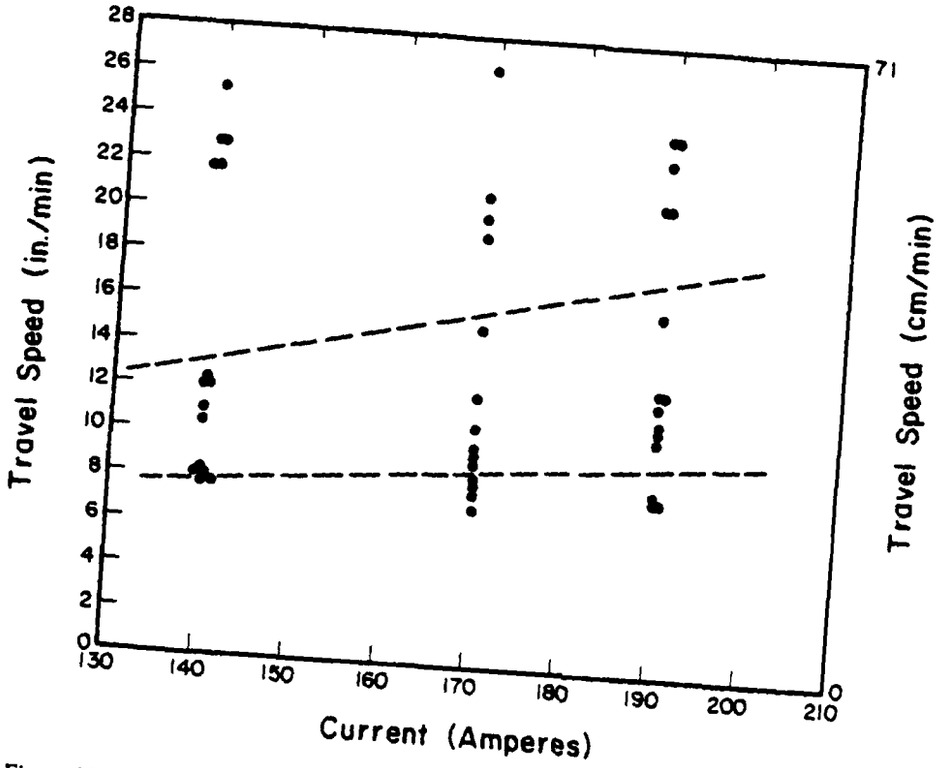

Figure 12. Graph showing travel speed limits for current levels used for 1/8-in. (3.2-mm) diameter E7024 SMAW electrode. Dashed lines show travel speed limits as determined by amount of undercut and bead shape.

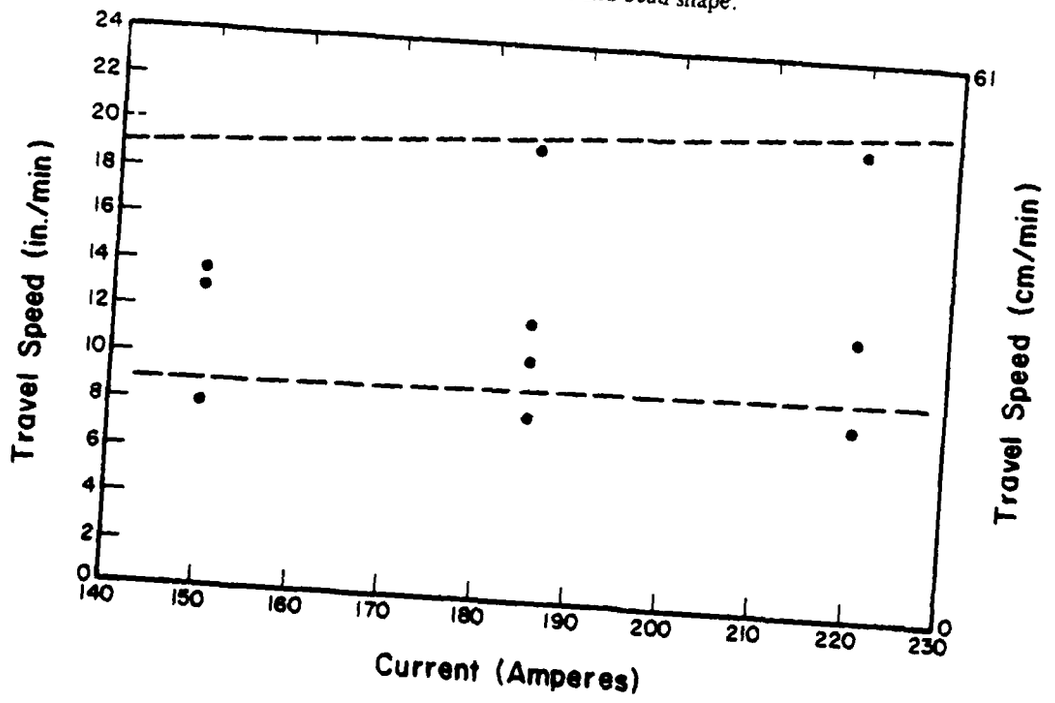

Figure 13. Graph showing travel speed limits for current levels used for 5/32-in. (4.0-mm) diameter E8018 SMAW electrode. Dashed lines show travel speed limits as determined by amount of undercut and bead shape.

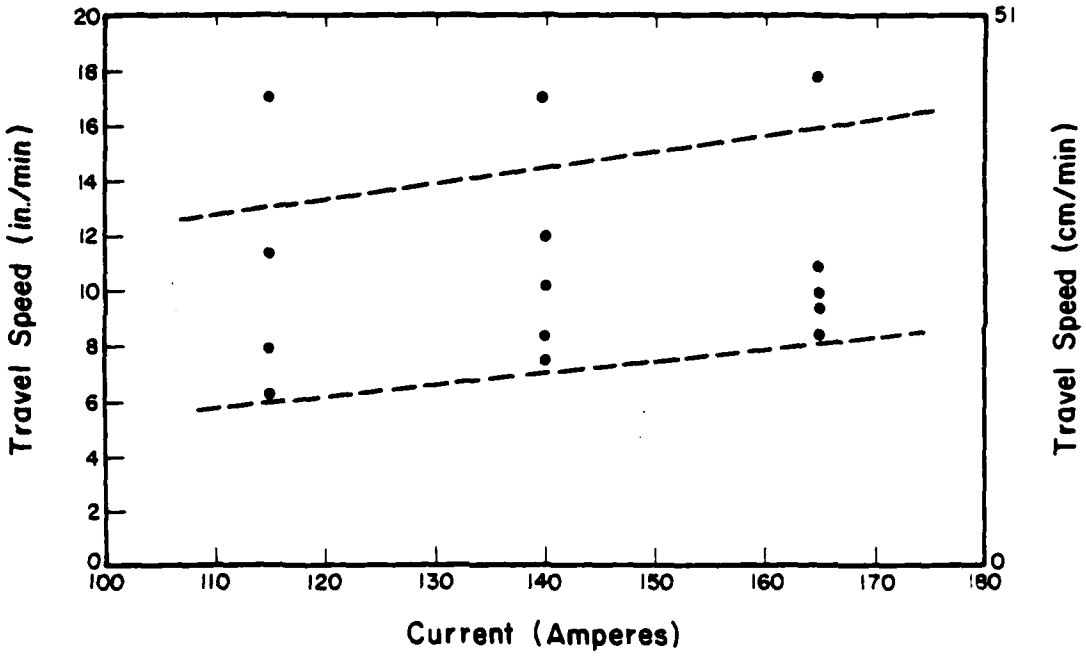

Figure 14. Graph showing travel speed limits for current levels used for 1/8-in. (3.2-mm) diameter E11018 SMAW electrode. Dashed lines show travel speed limits as determined by amount of undercut and bead shape.

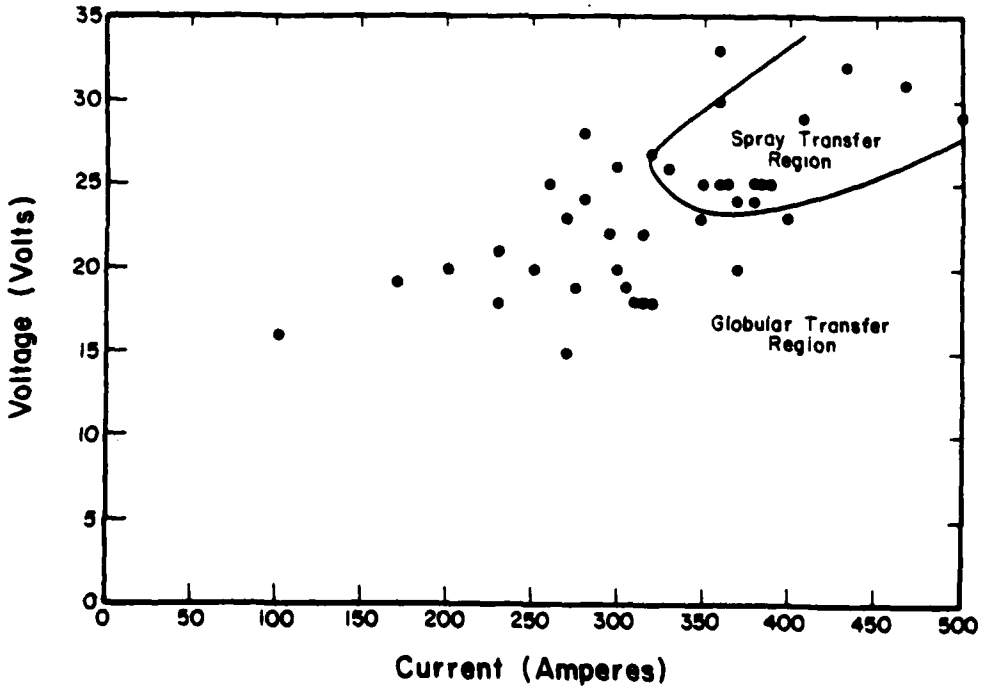

Figure 15. Graph of voltage versus current for E70S-2 electrode and shield gas of argon with 2 percent oxygen addition.

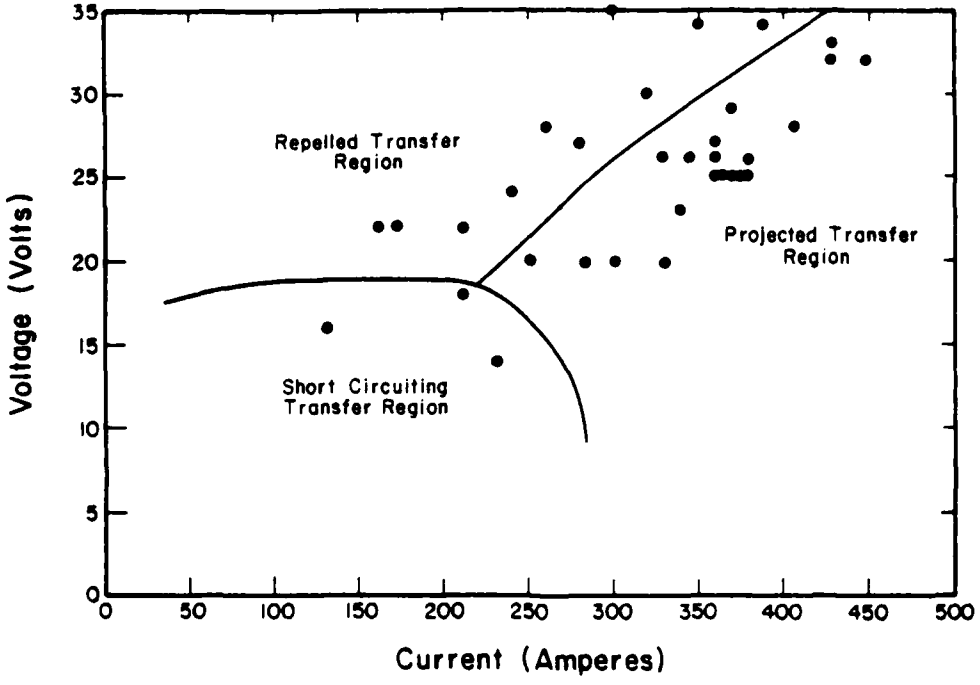

Figure 16. Graph of voltage versus current for E70S-2 electrode and carbon dioxide shield gas.

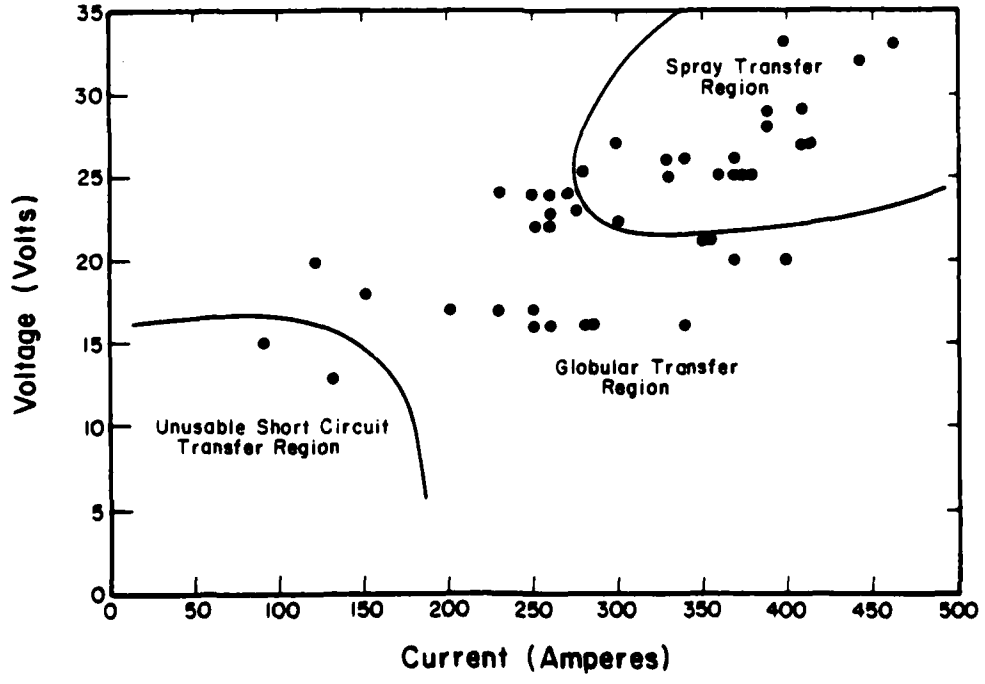

Figure 17. Graph of voltage versus current for E70S-3 electrode and shield gas of argon with 2 percent oxygen addition.

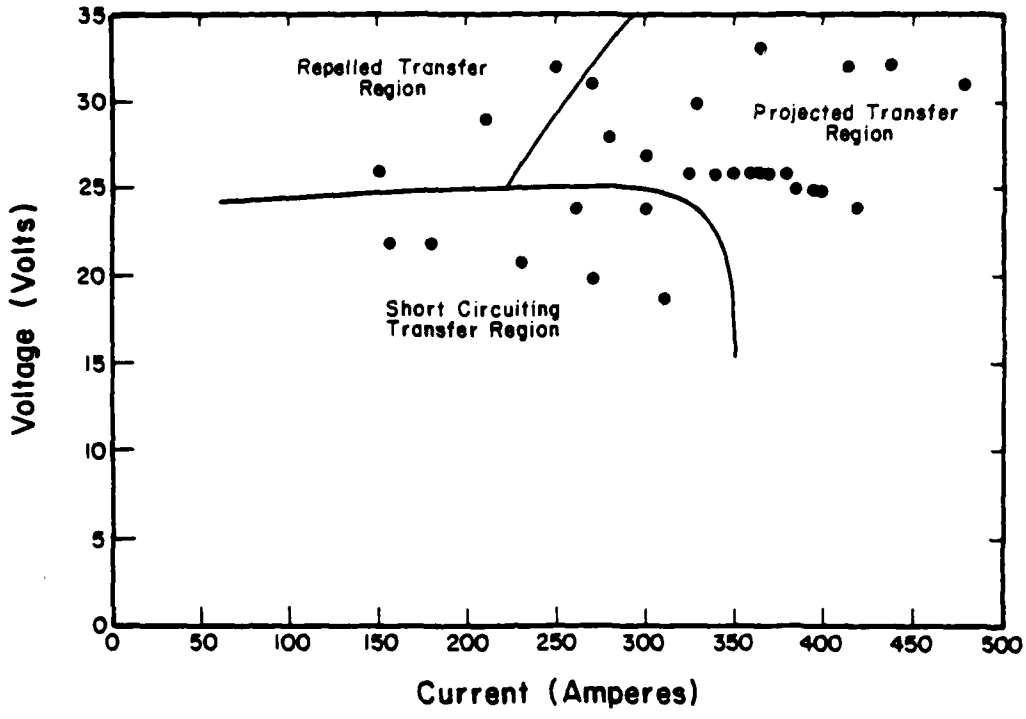

Figure 18. Graph of voltage versus current for E70S-3 electrode and carbon dioxide shield gas.

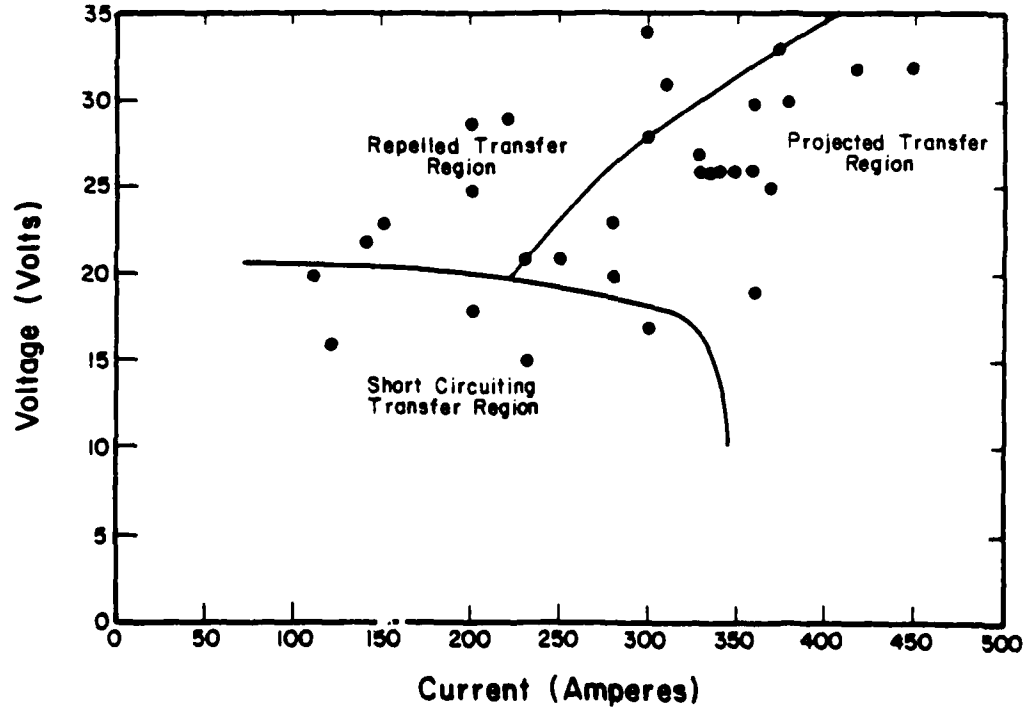

Figure 19. Graph of voltage versus current for E70S-4 electrode and carbon dioxide shield gas.

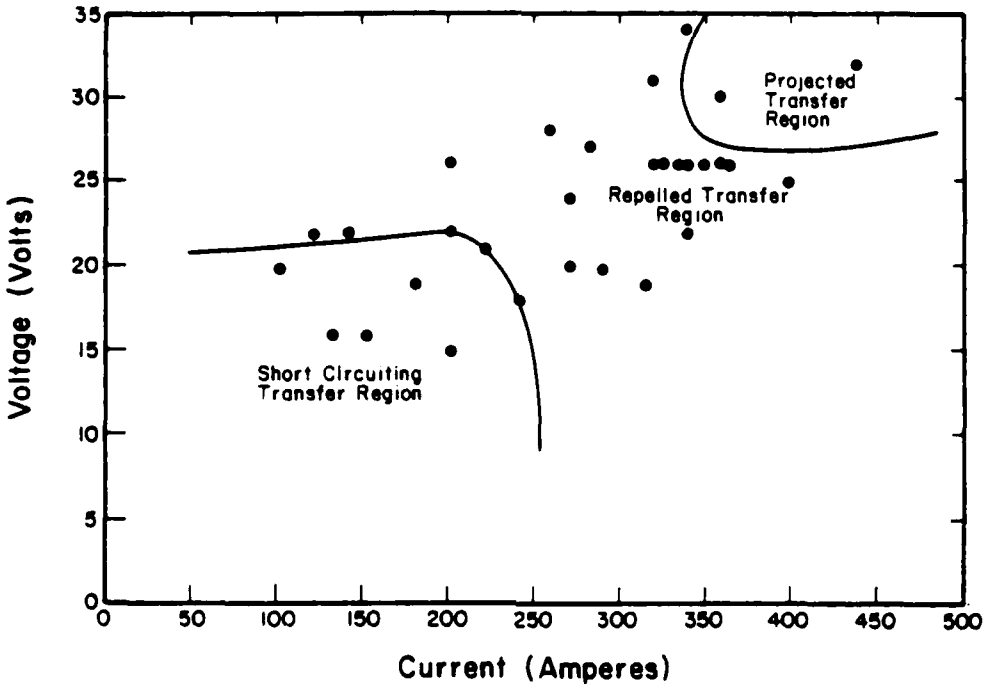

Figure 20. Graph of voltage versus current for E70S-6 electrode and carbon dioxide shield gas.

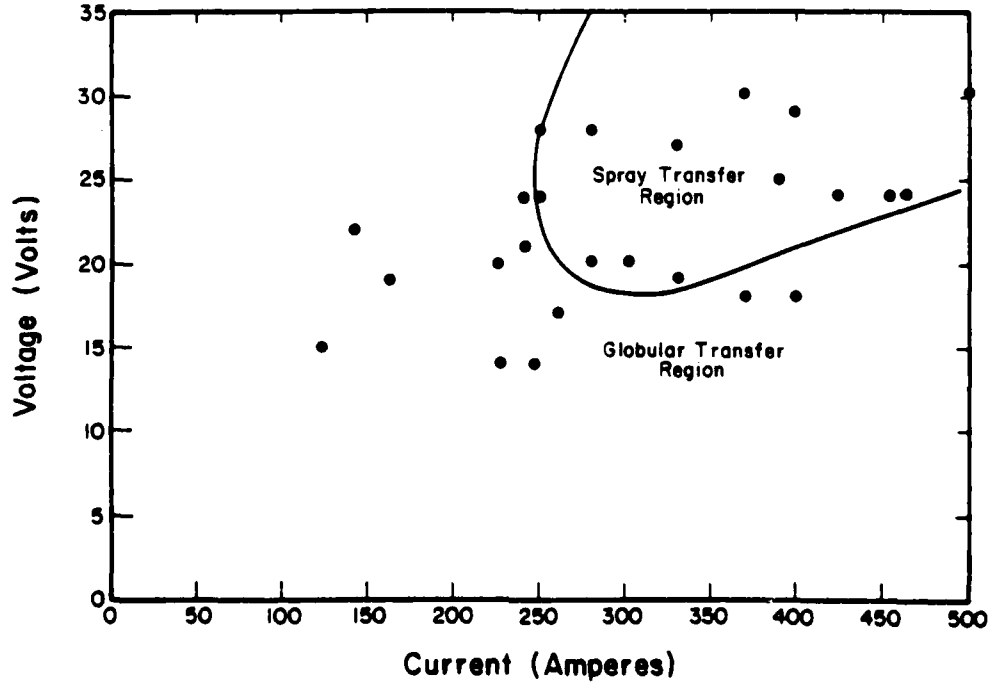

Figure 21. Graph of voltage versus current for E110S electrode and shield gas of argon with 2 percent oxygen addition.

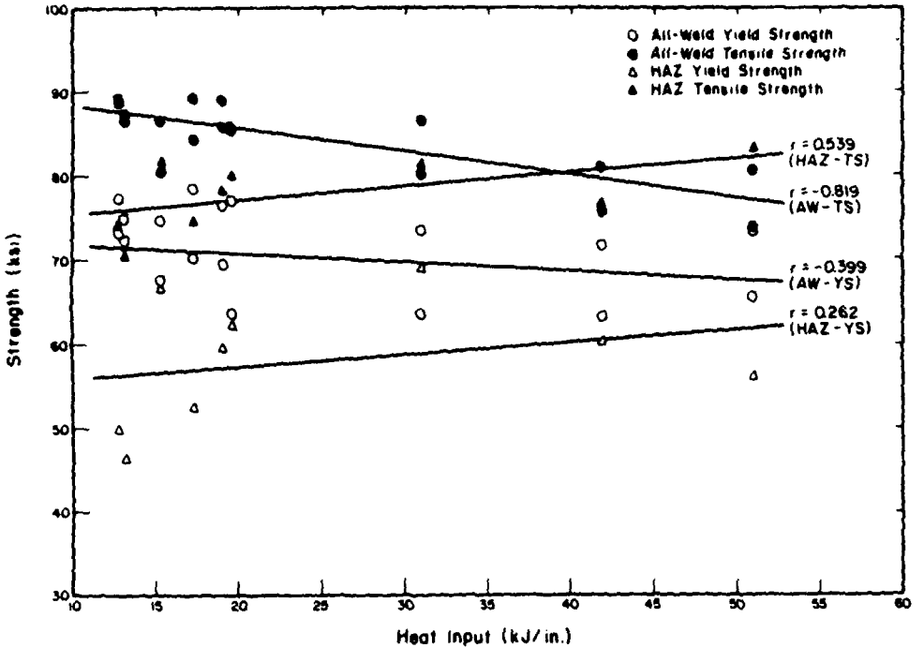

Figure 22. *Weld metal and HAZ tensile and yield strength versus heat input for A36 SMA weldment.*

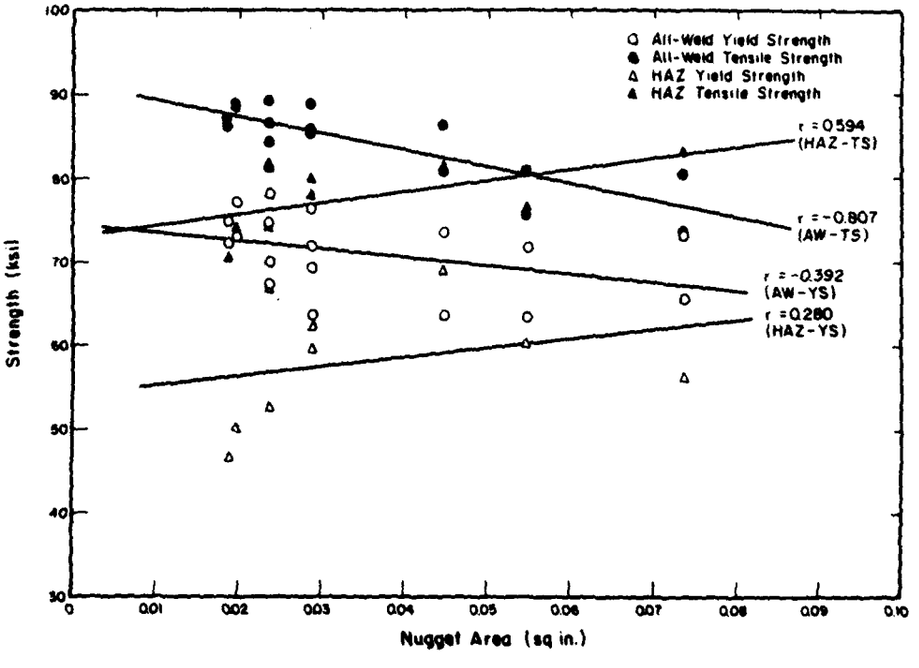

Figure 23. Weld metal and HAZ tensile and yield strength versus nugget area for A36 SMA weldment.

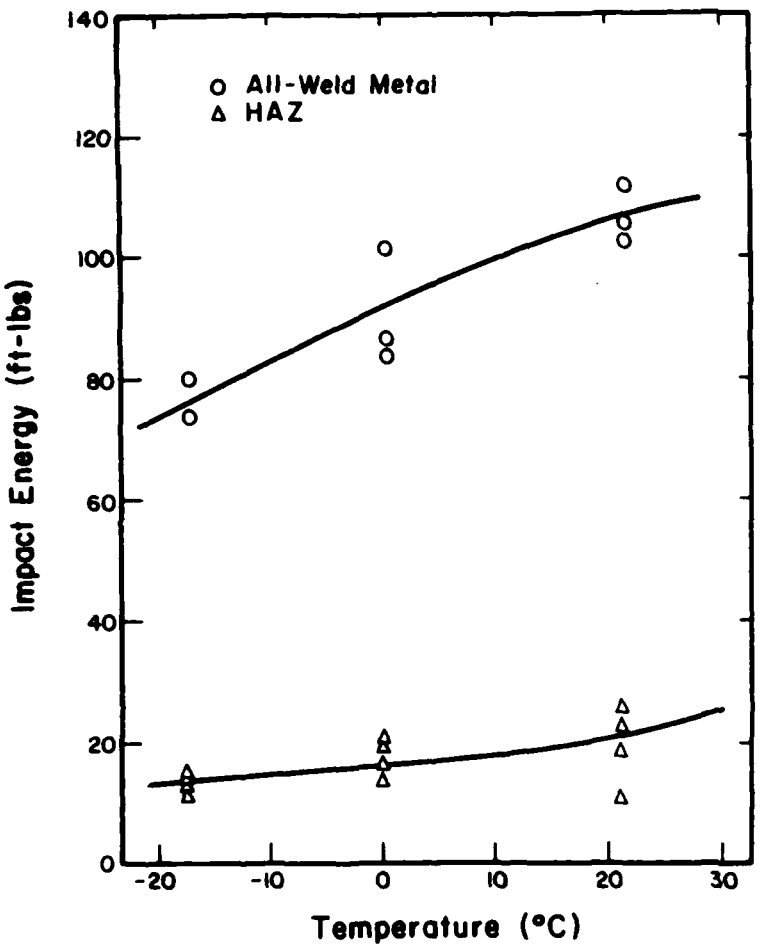

Figure 24. Charpy V-notch impact energy versus test temperature for A36 SMA weldment B4.

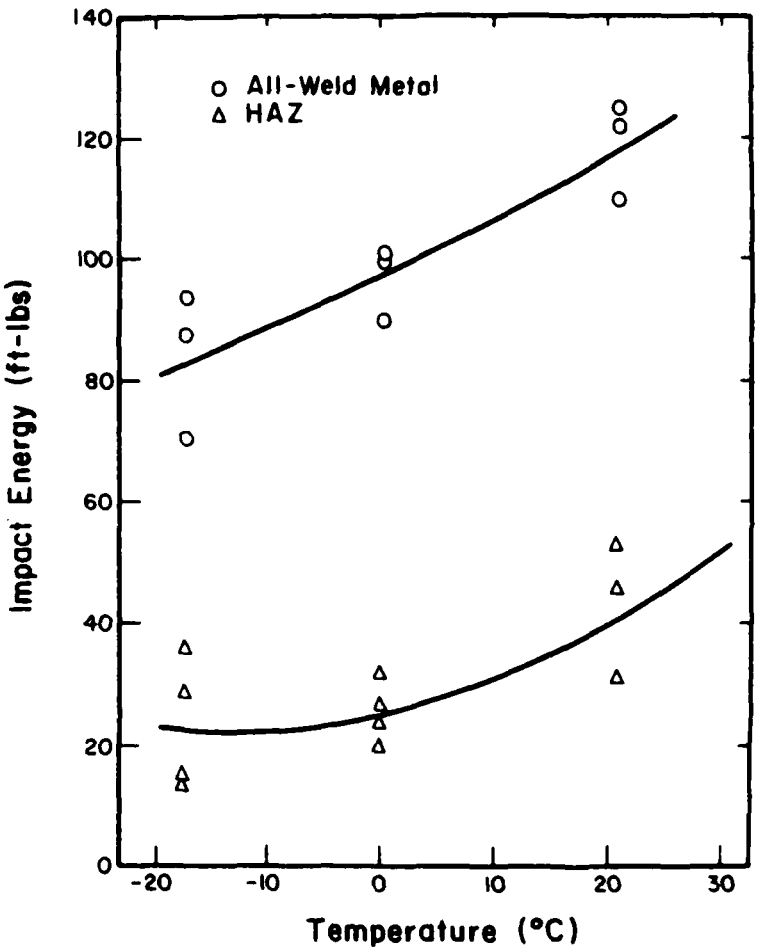

Figure 25. Charpy V-notch impact energy versus test temperature for A36 SMA weldment B7.

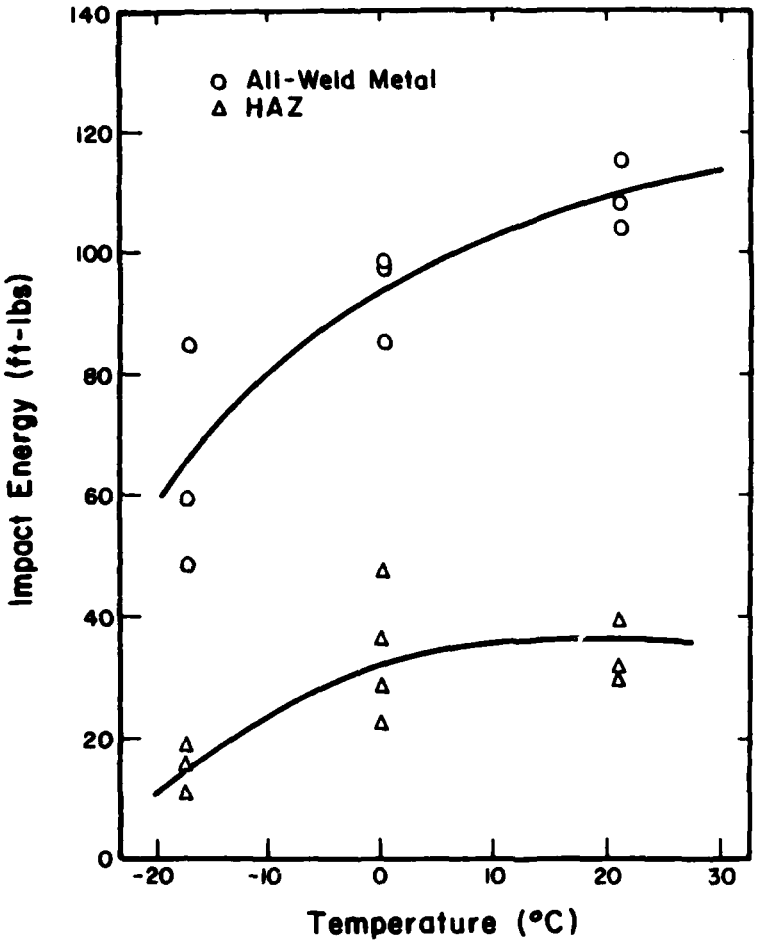

Figure 26. *Charpy V-notch impact energy versus test temperature for A36 SMA weldment B8.*

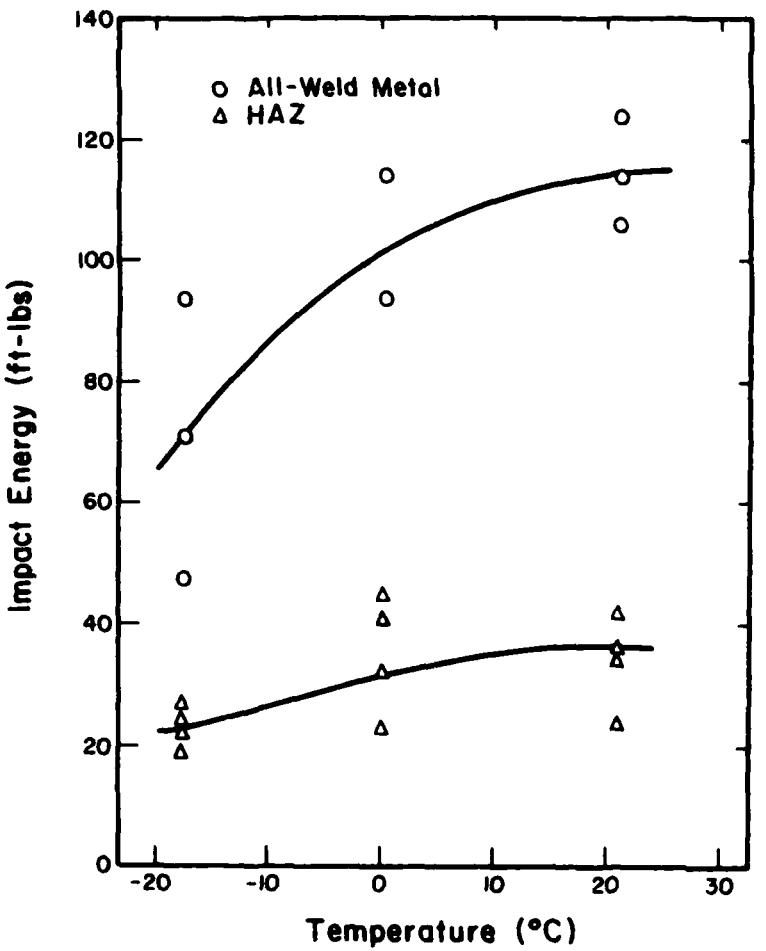

Figure 27. *Charpy V-notch impact energy versus test temperature for A36 SMA weldment B9.*

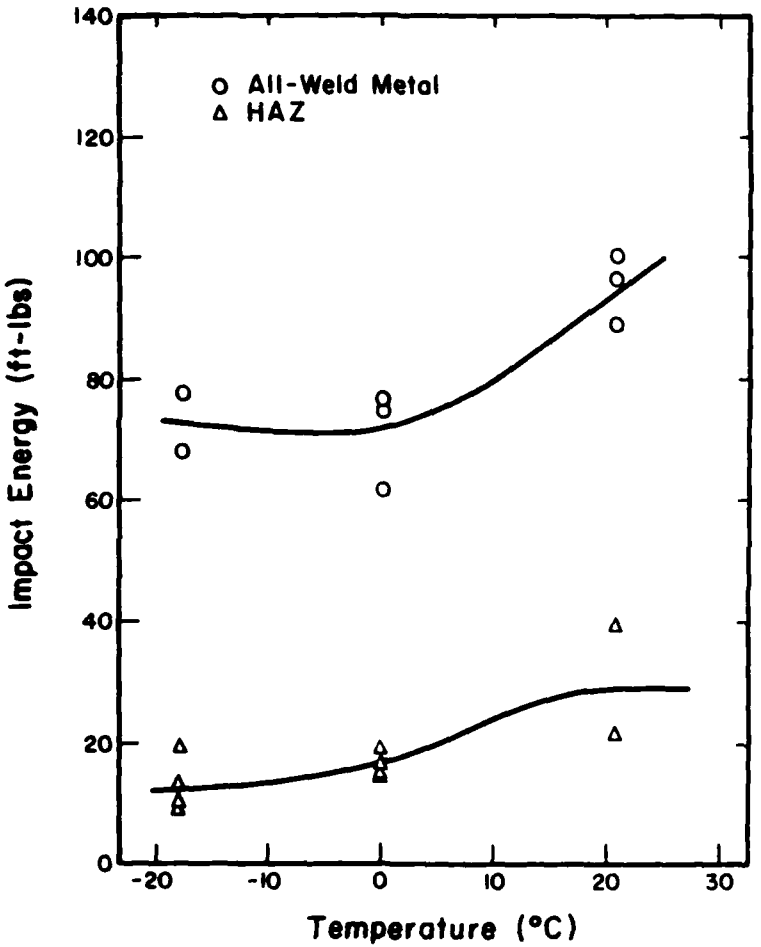

Figure 28. Charpy V-notch impact energy versus test temperature for A36 SMA weldment B6.

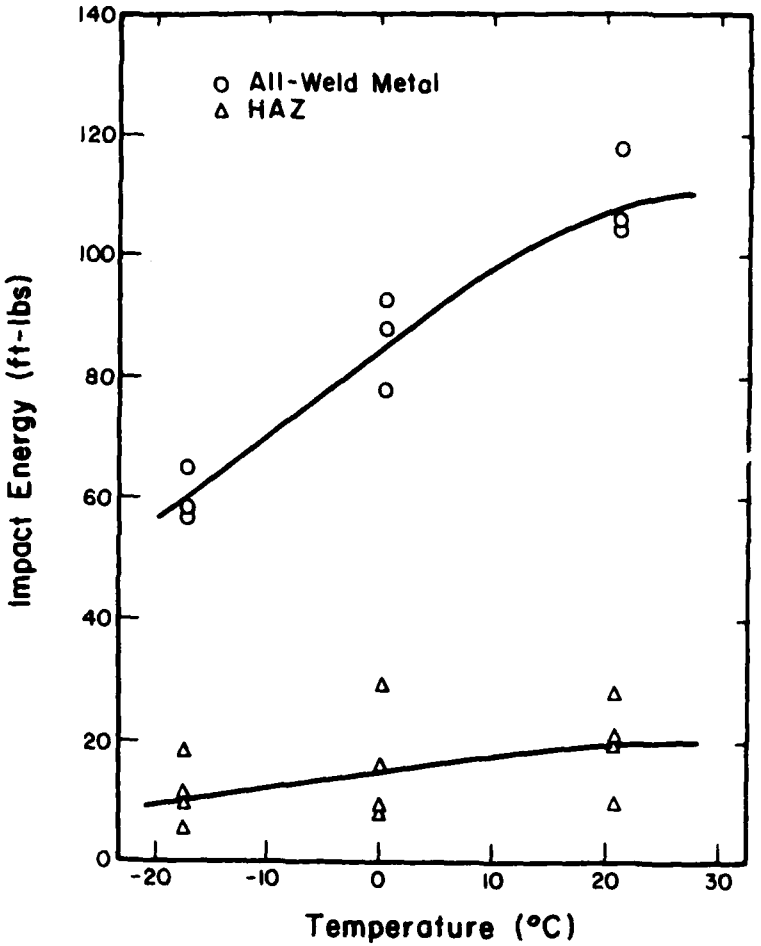

Figure 29. Charpy V-notch impact energy versus test temperature for A36 SMA weldment B3.

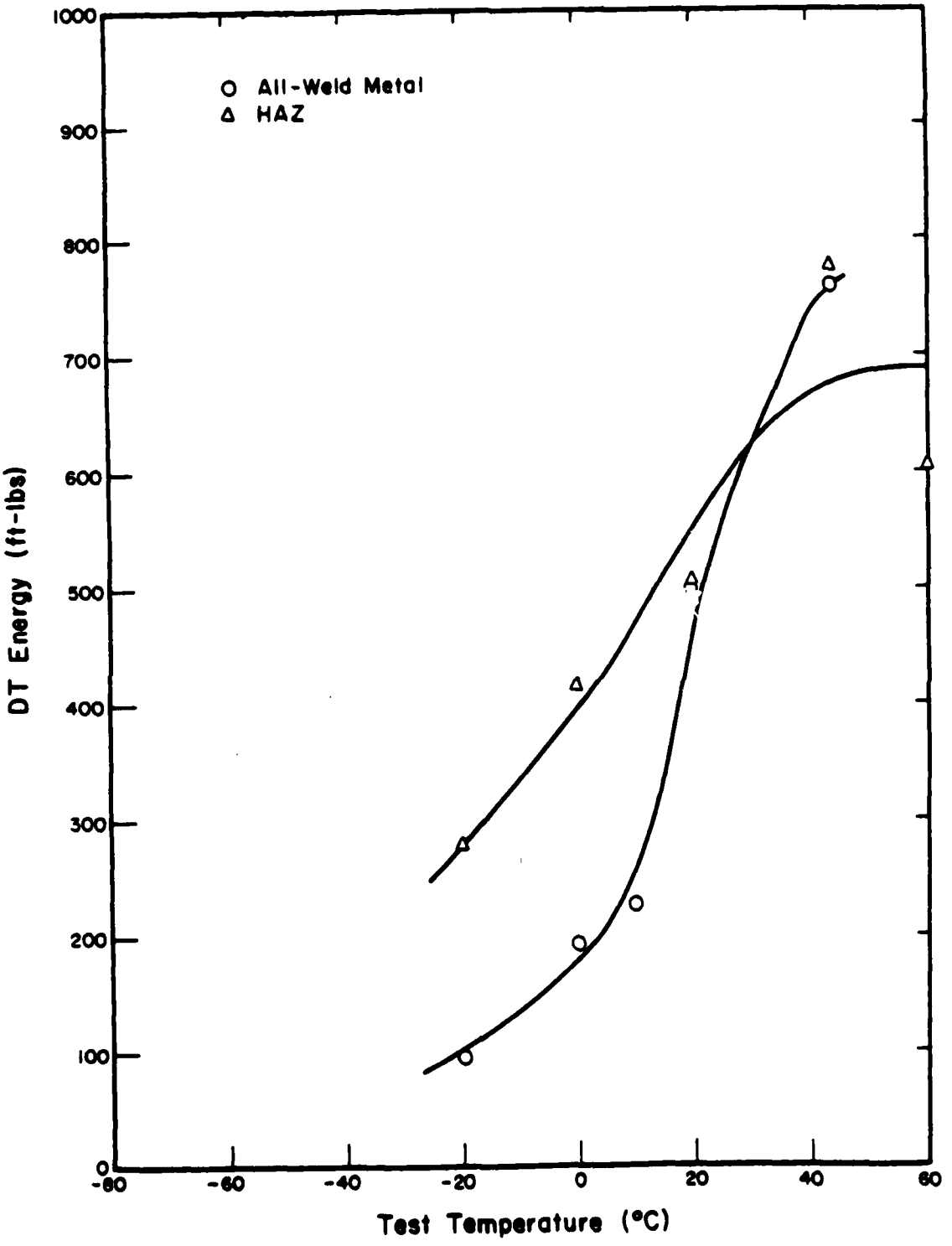

Figure 30. Dynamic tear impact energy versus test temperature for A36 SMA weldment C2.

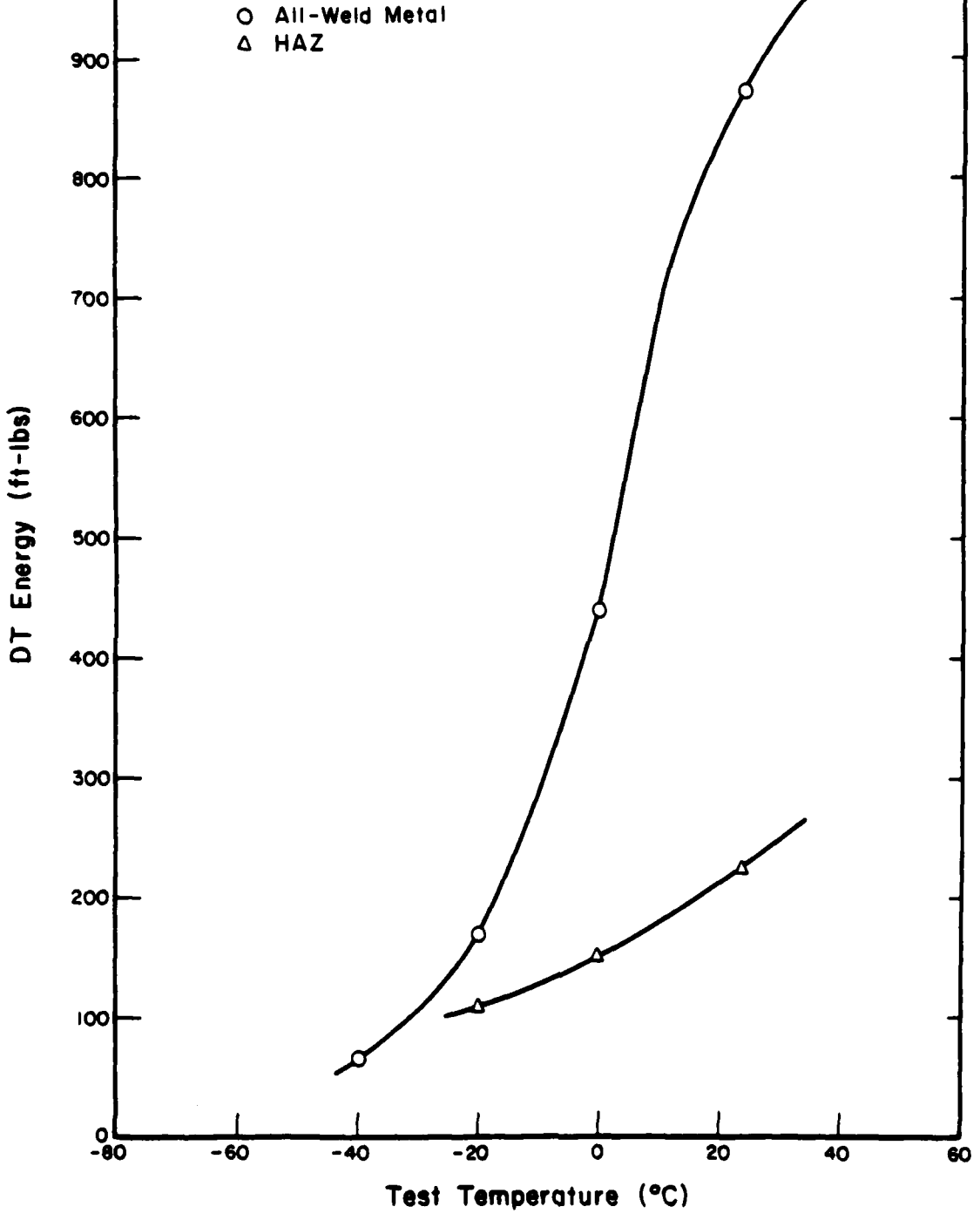

Figure 31. Dynamic tear impact energy versus test temperature for A36 SMA weldment C1.

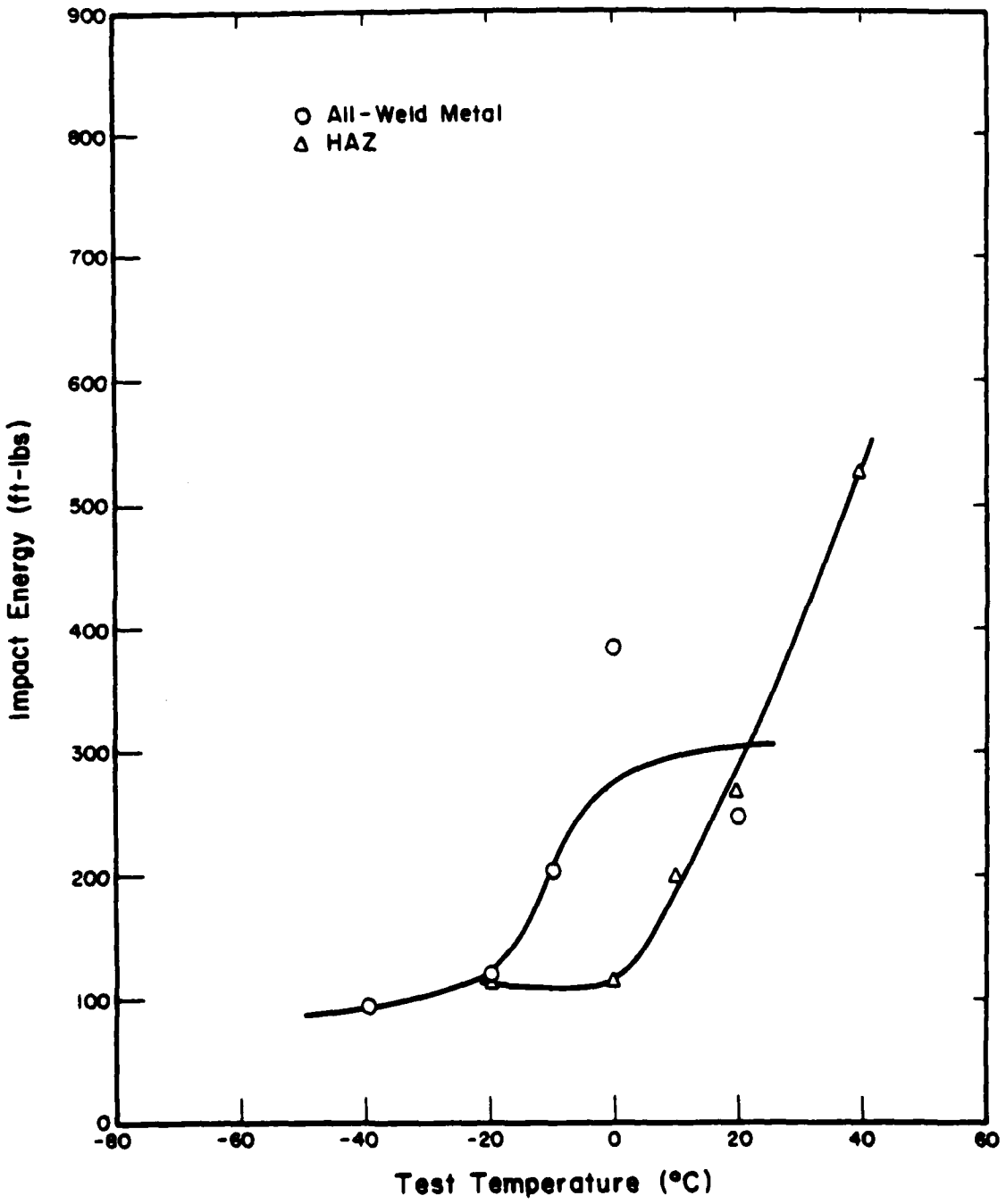

Figure 32. Dynamic tear impact energy versus test temperature for A36 SMA weldment D6.

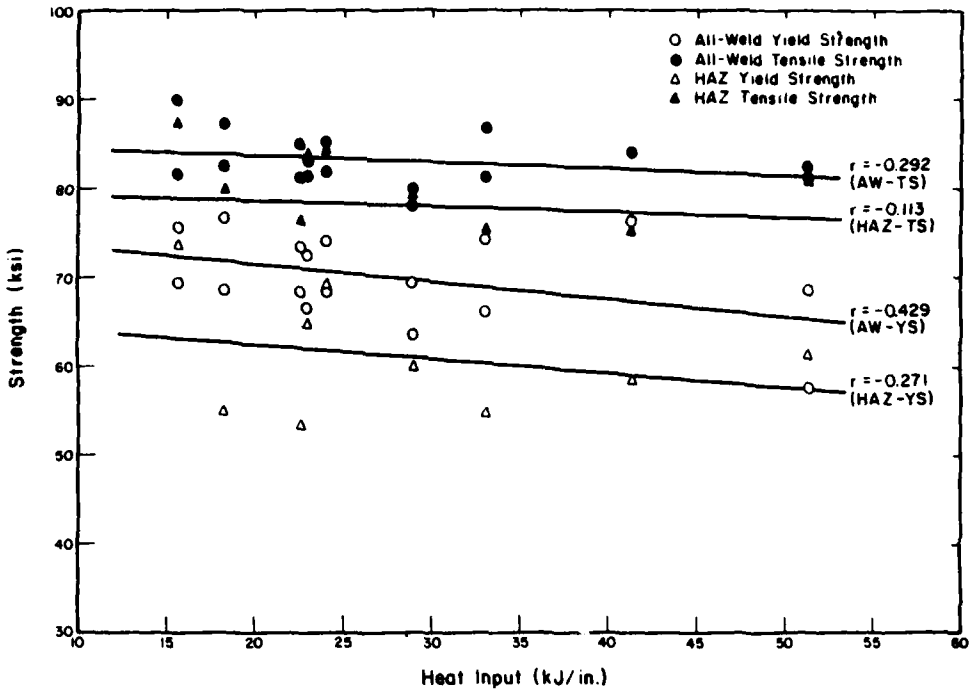

Figure 33. Weld metal and HAZ tensile and yield strength versus heat impact for A516 SMA weldments.

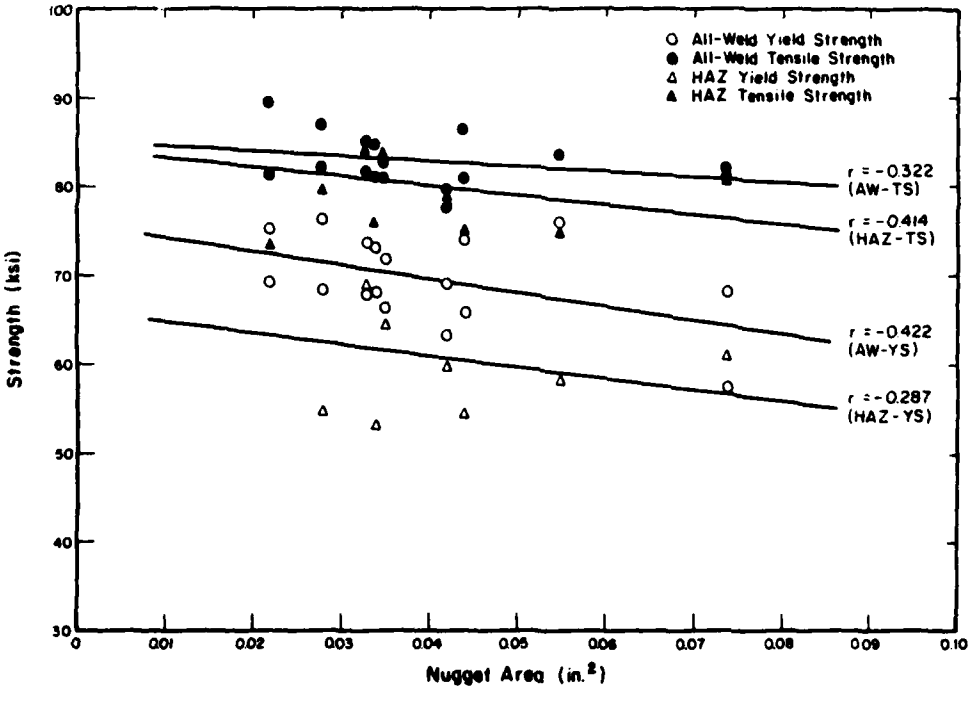

Figure 34. Weld metal and HAZ tensile and yield strength versus nugget area for A516 SMA weldments.

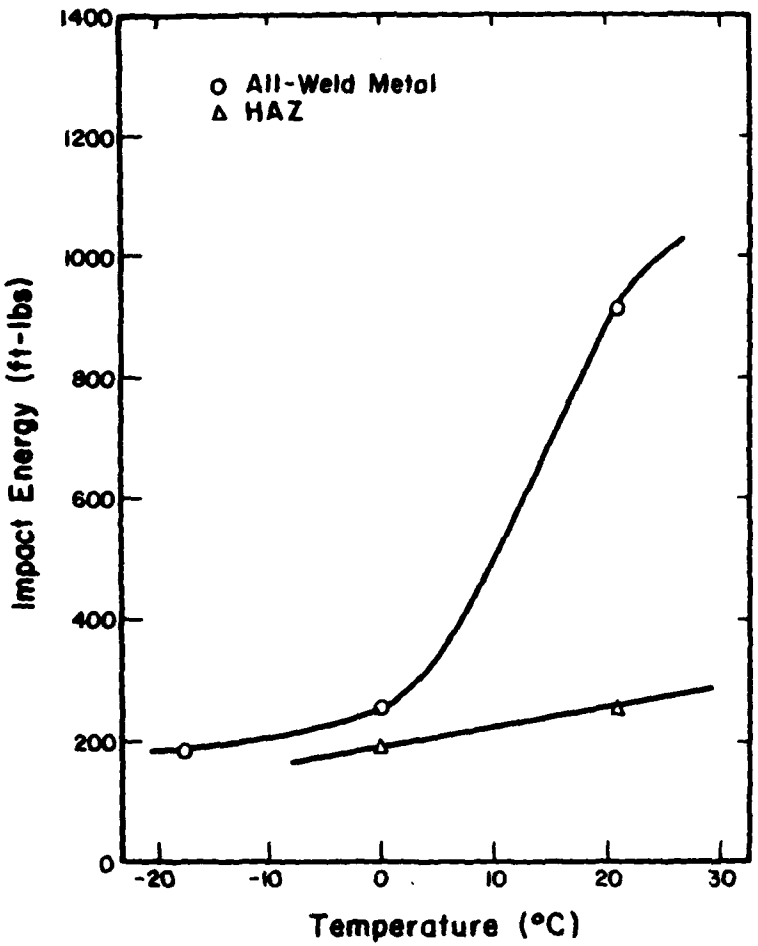

Figure 35. Dynamic tear impact energy versus temperature for A516 SMA weldment B10.

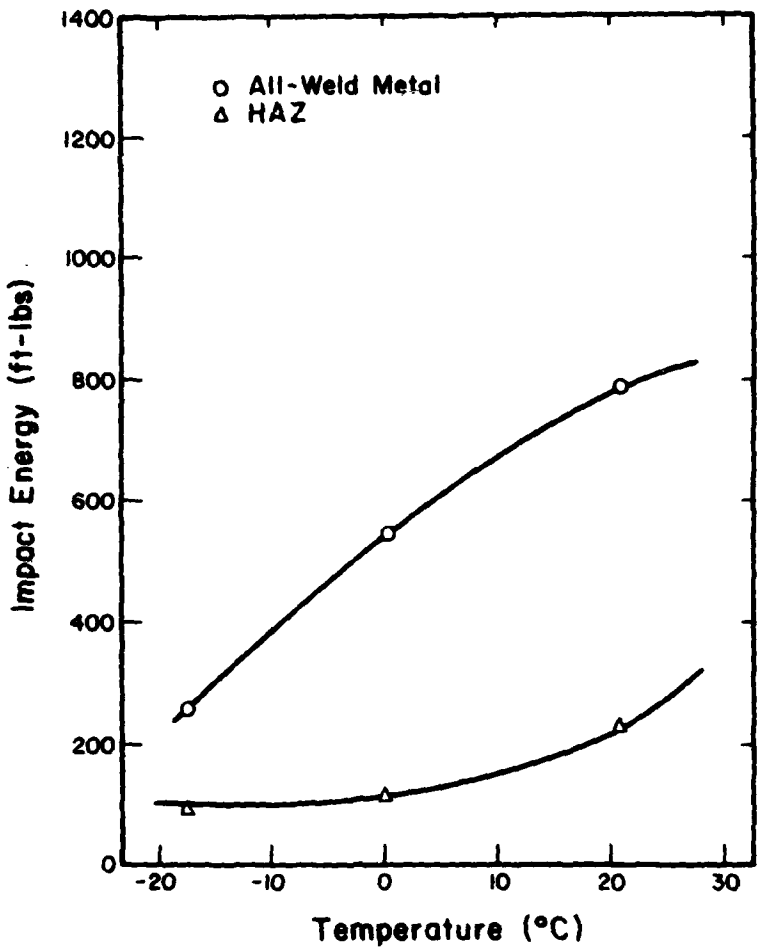

Figure 36. Dynamic tear impact energy versus temperature for A516 SMA weldment B11.

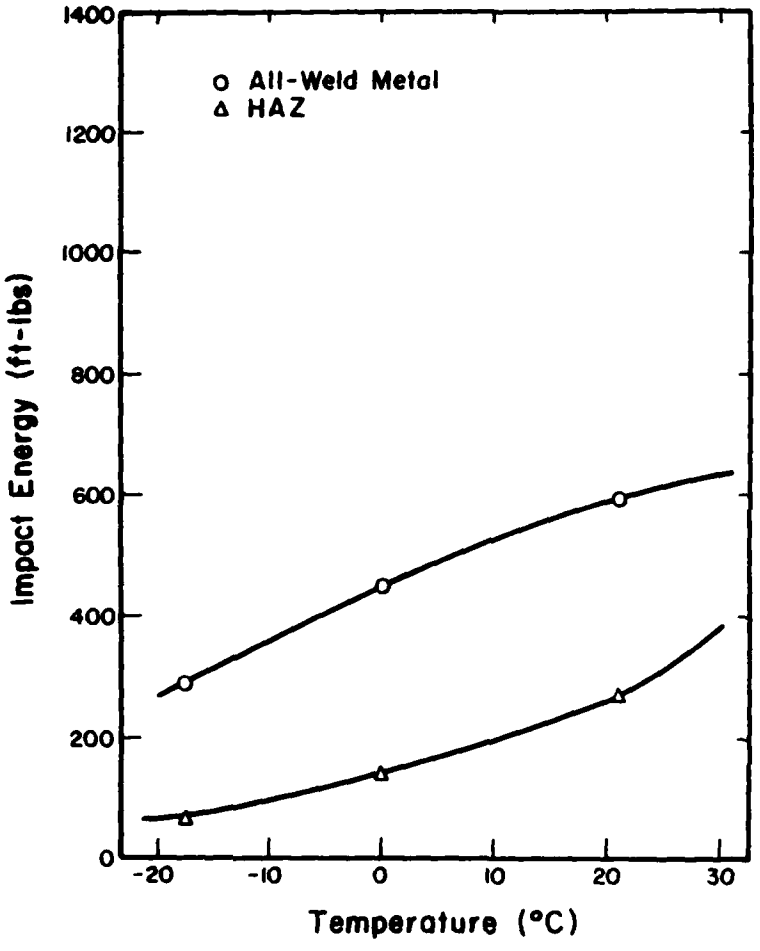

Figure 37. Dynamic tear impact energy versus temperature for A516 SMA weldment B12.

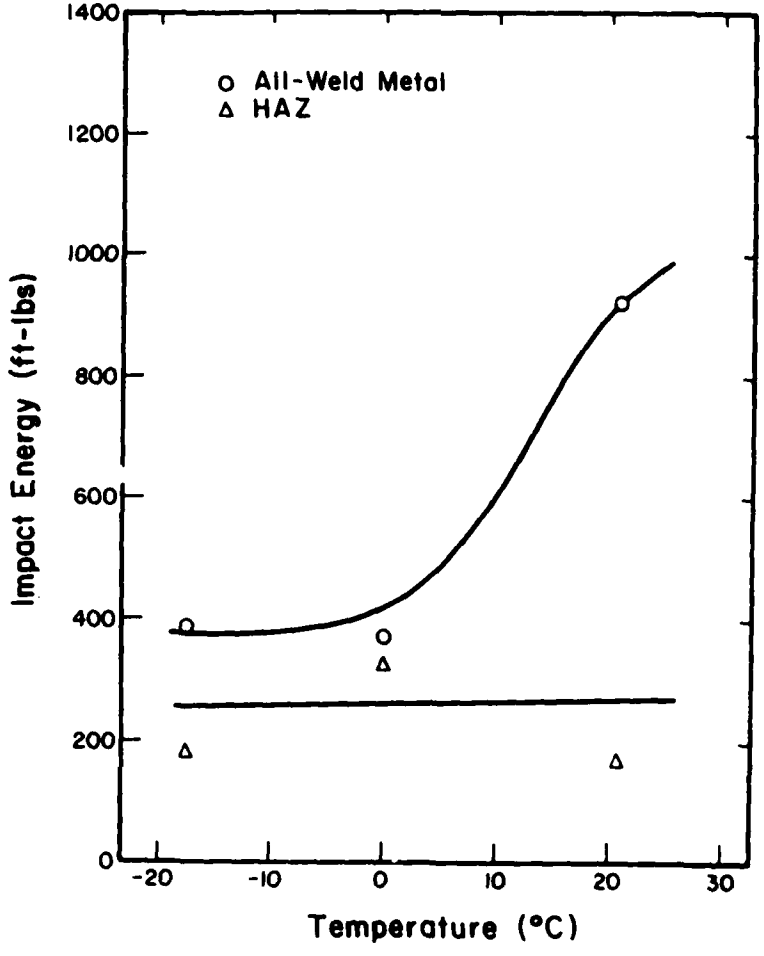

Figure 38. Dynamic tear impact energy versus temperature for A516 SMA weldment B14.

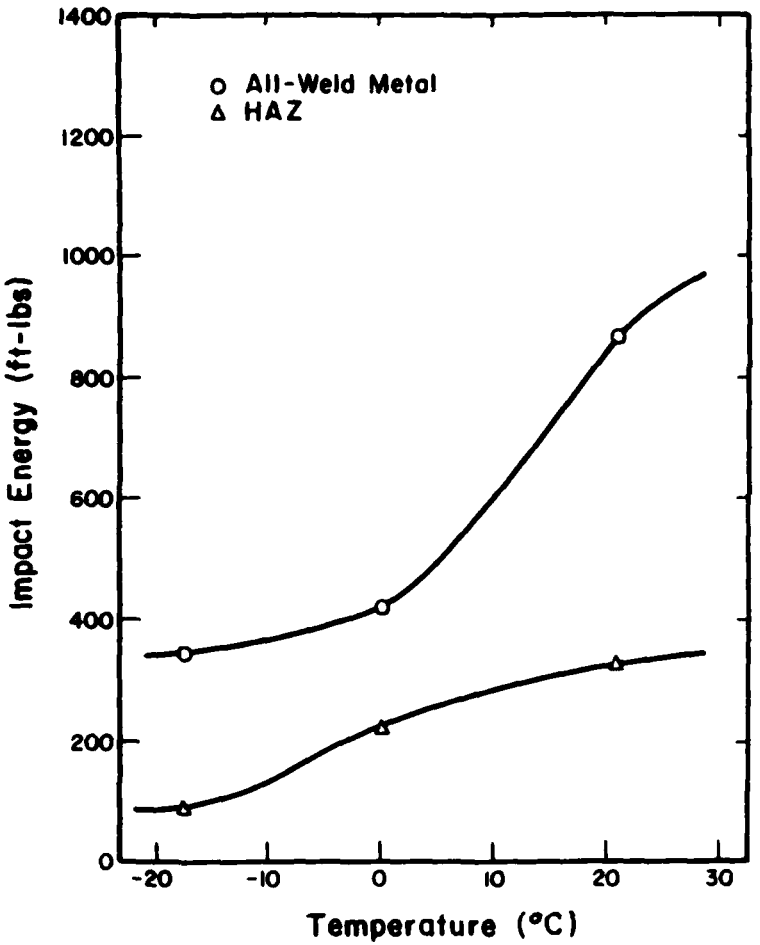

Figure 39. Dynamic tear impact energy versus temperature for A516 SMA weldment B13.

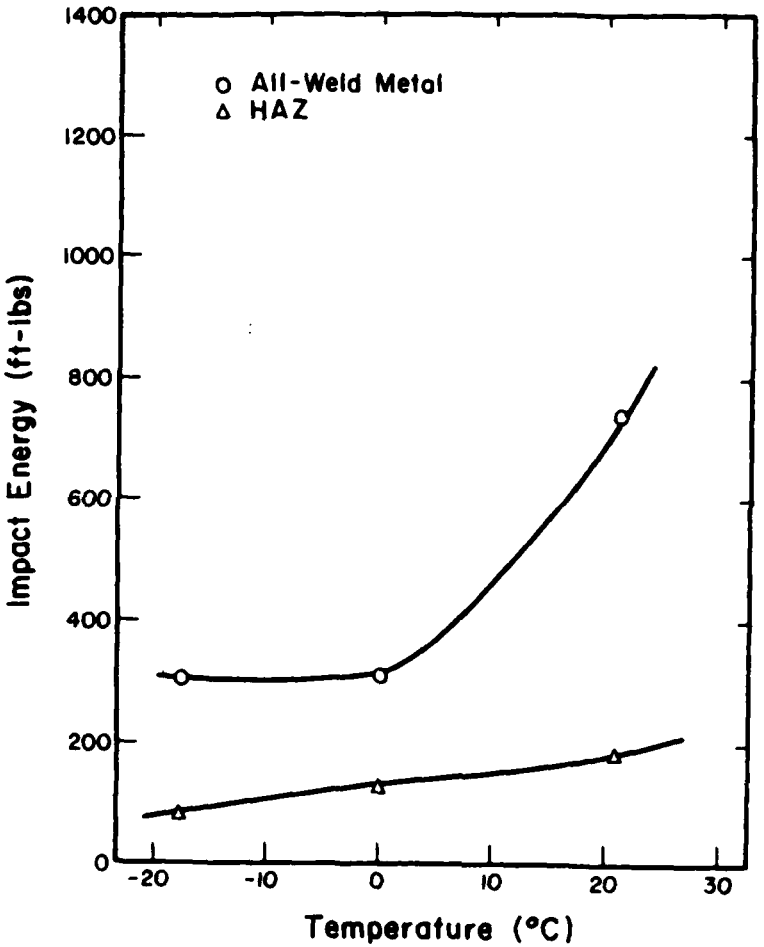

Figure 40. Dynamic tear impact energy versus temperature for A516 SMA weldment B15.

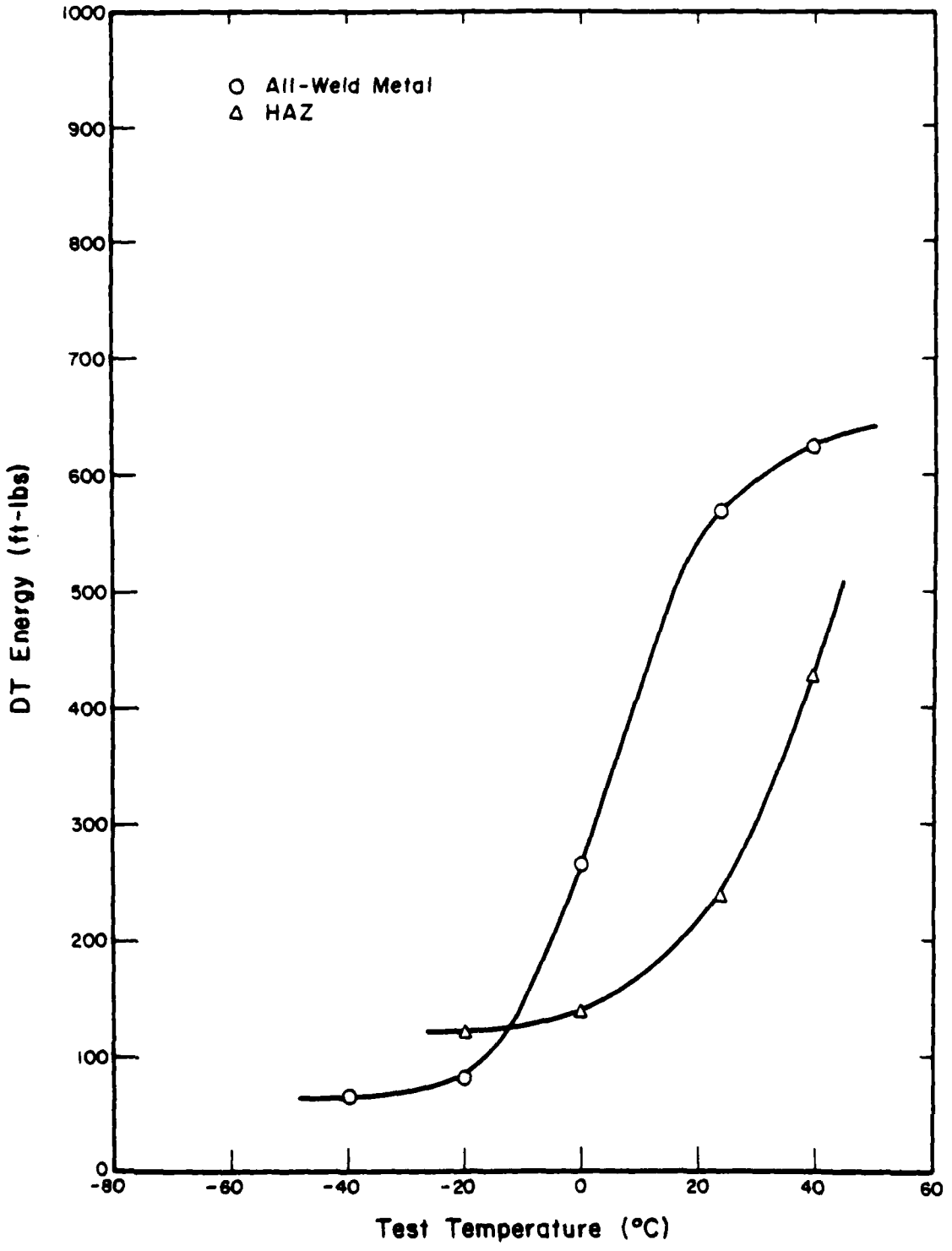

Figure 41. Dynamic tear impact energy versus test temperature for A516 SMA weldment C3.

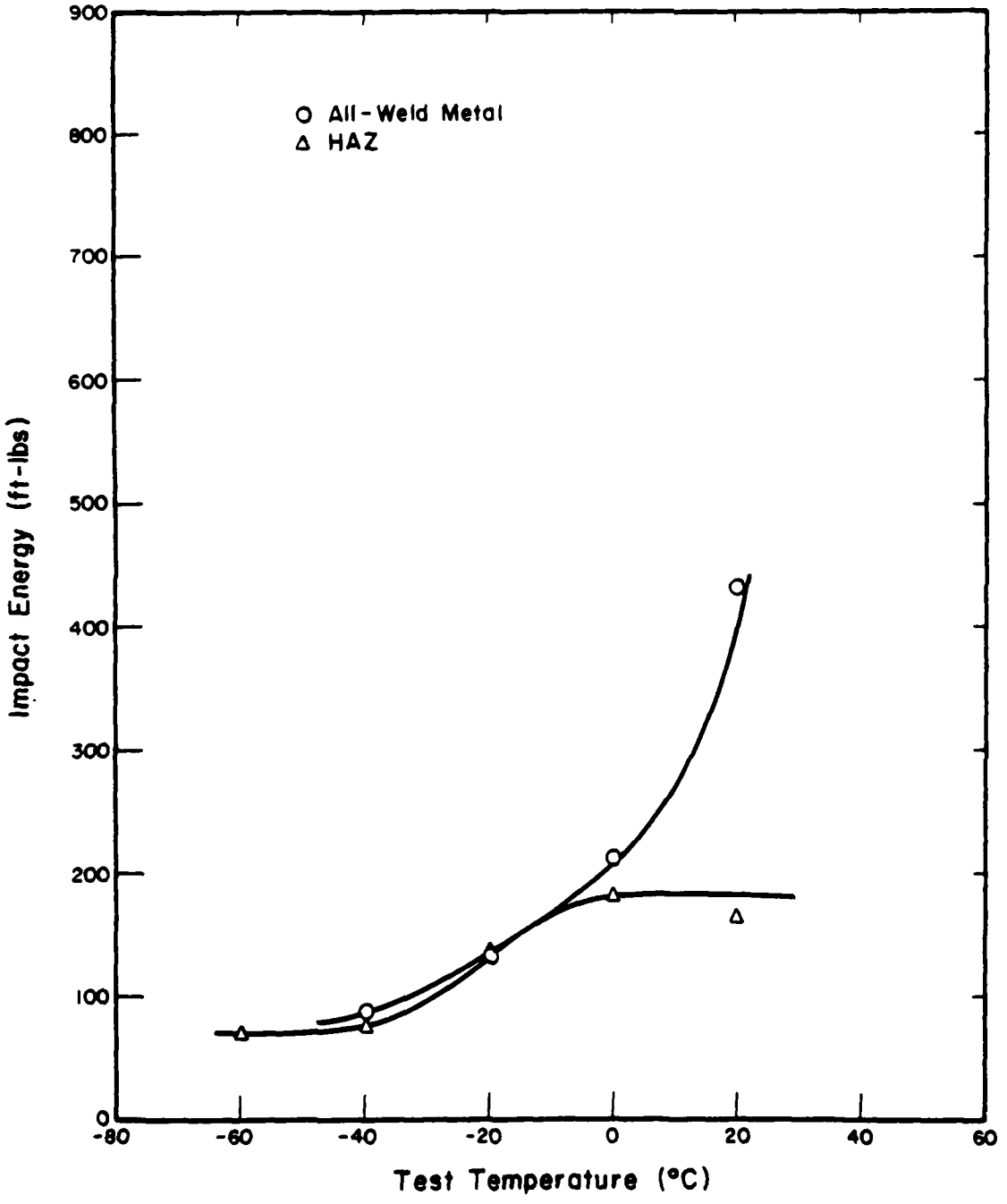

Figure 42. Dynamic tear impact energy versus test temperature for A516 SMA weldment D5.

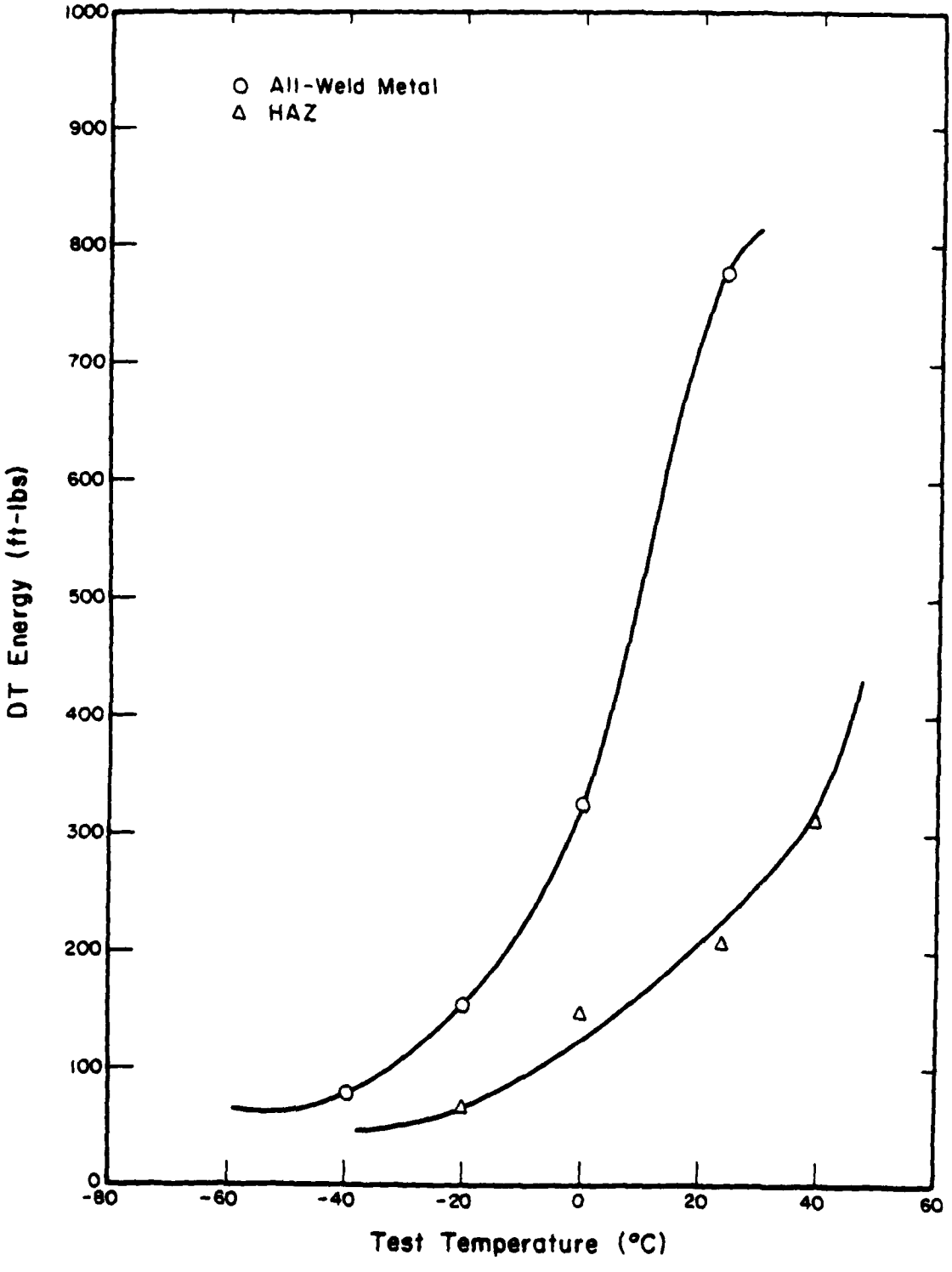

Figure 43. Dynamic tear impact energy versus test temperature for A516 SMA weldment C4.

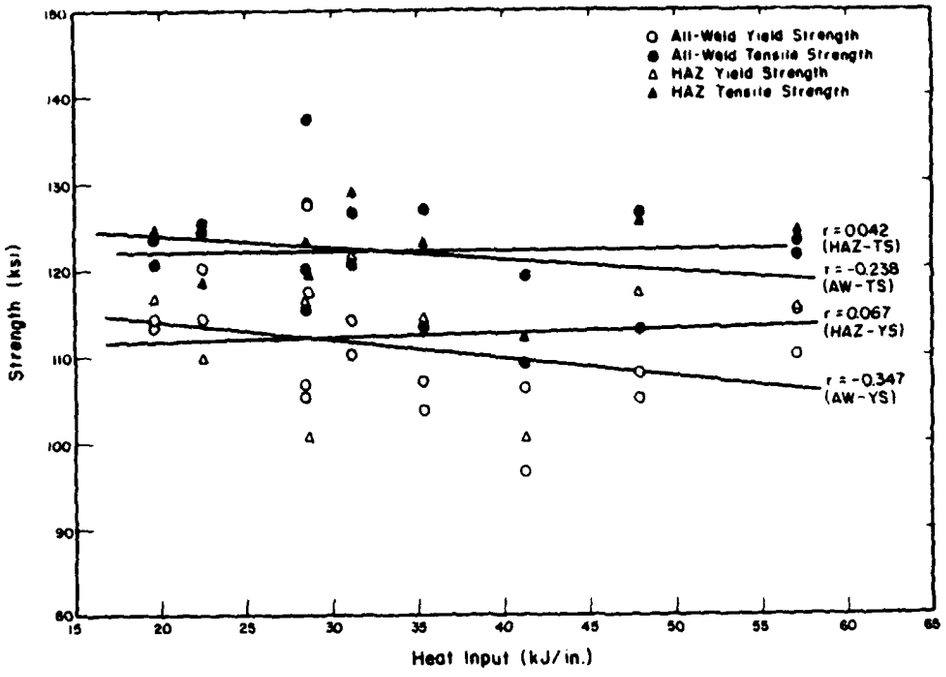

Figure 44. Weld metal and HAZ tensile and yield strength versus heat input for A514 SMA weldments.

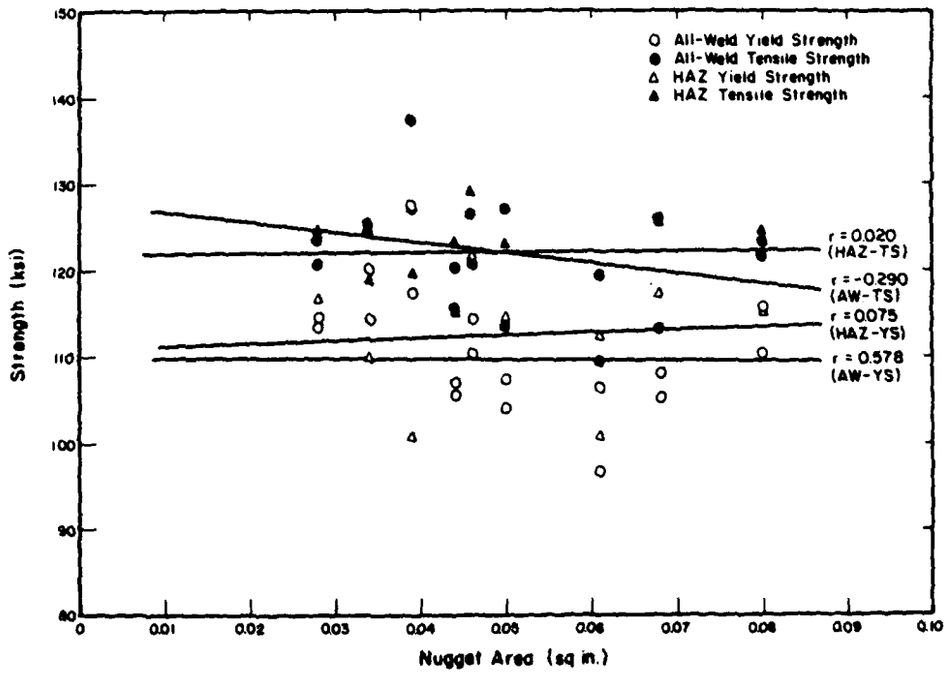

Figure 45. *Weld metal and HAZ tensile and yield strength versus nugget area for A514 SMA weldments.*

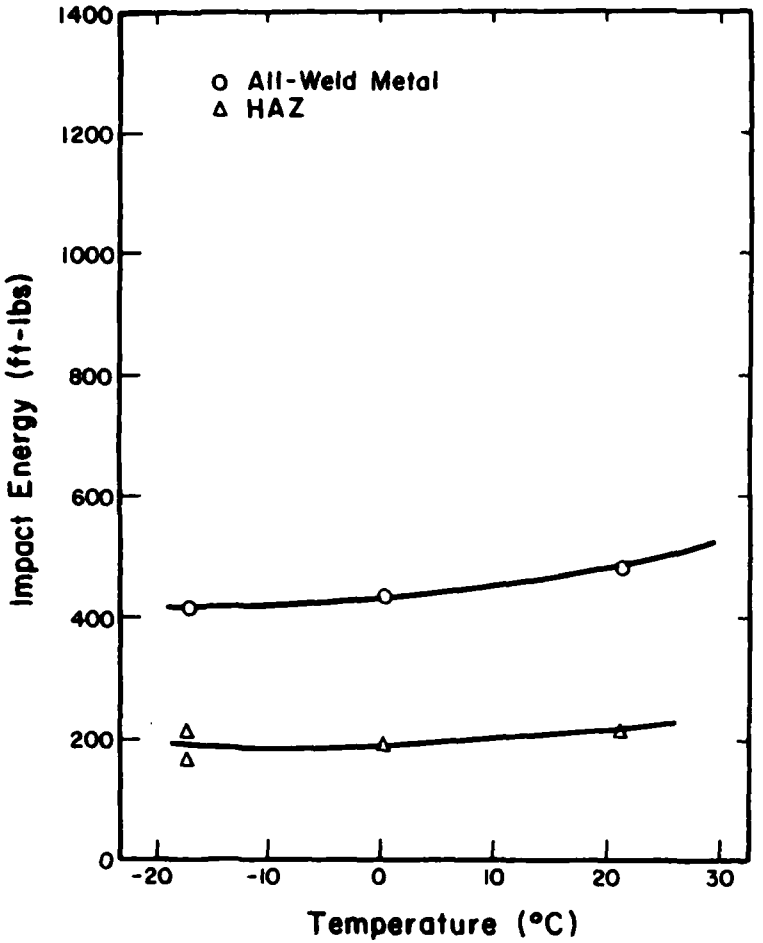

Figure 46. Dynamic tear impact energy versus temperature for A514 SMA weldment B16.

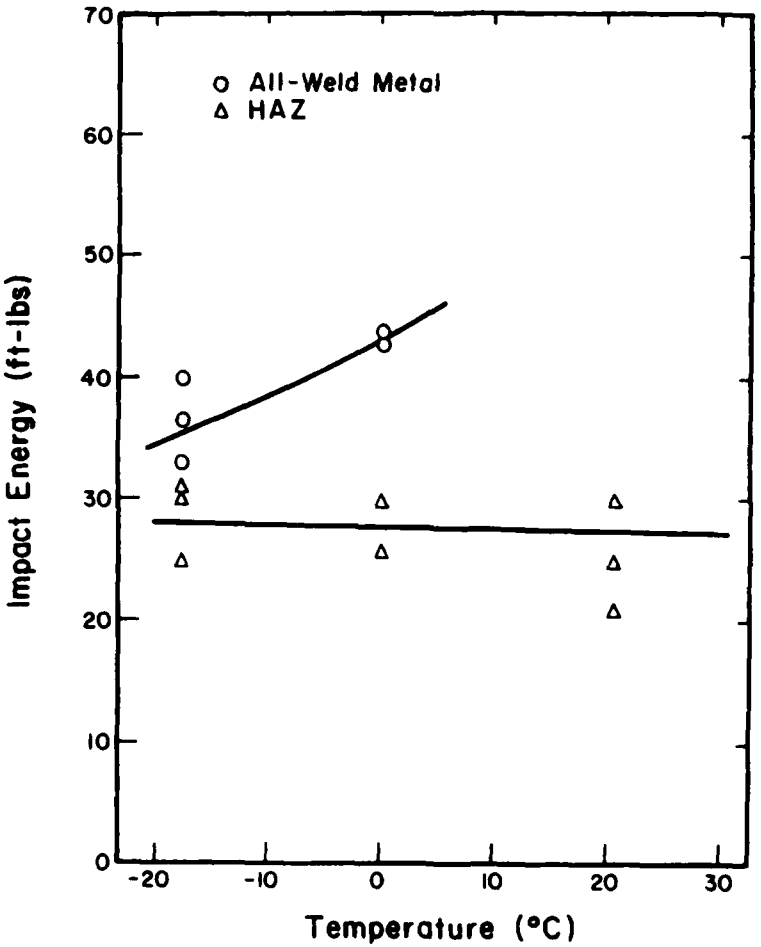

Figure 47. Charpy V-notch impact energy versus temperature for A514 SMA weldment B17.

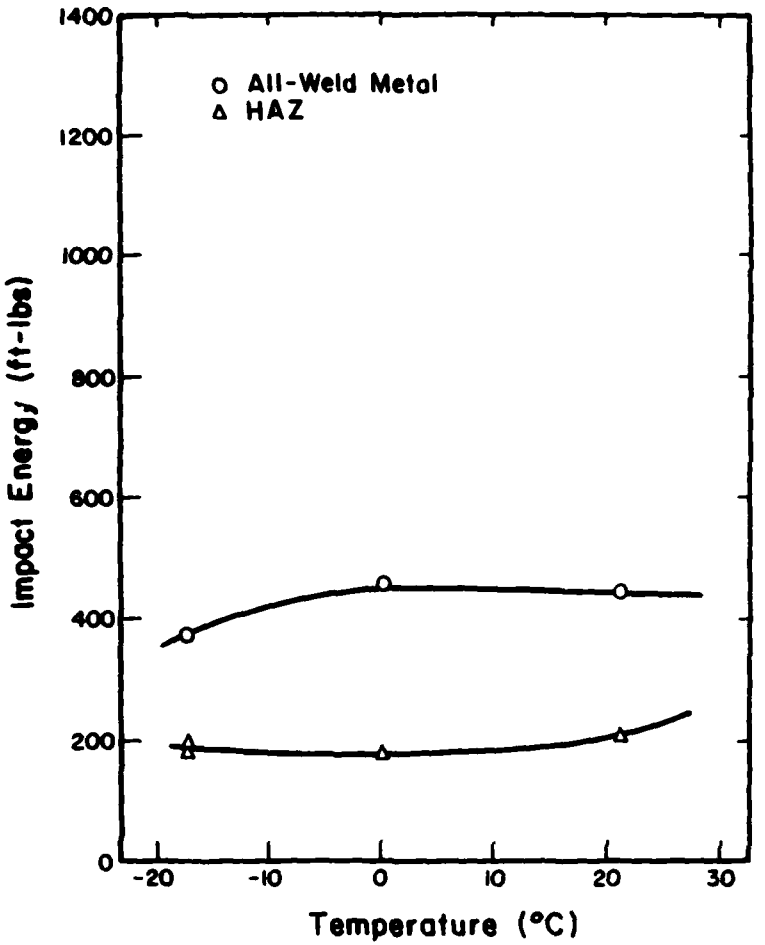

Figure 48. *Dynamic tear impact energy versus temperature for A514 SMA weldment B18.*

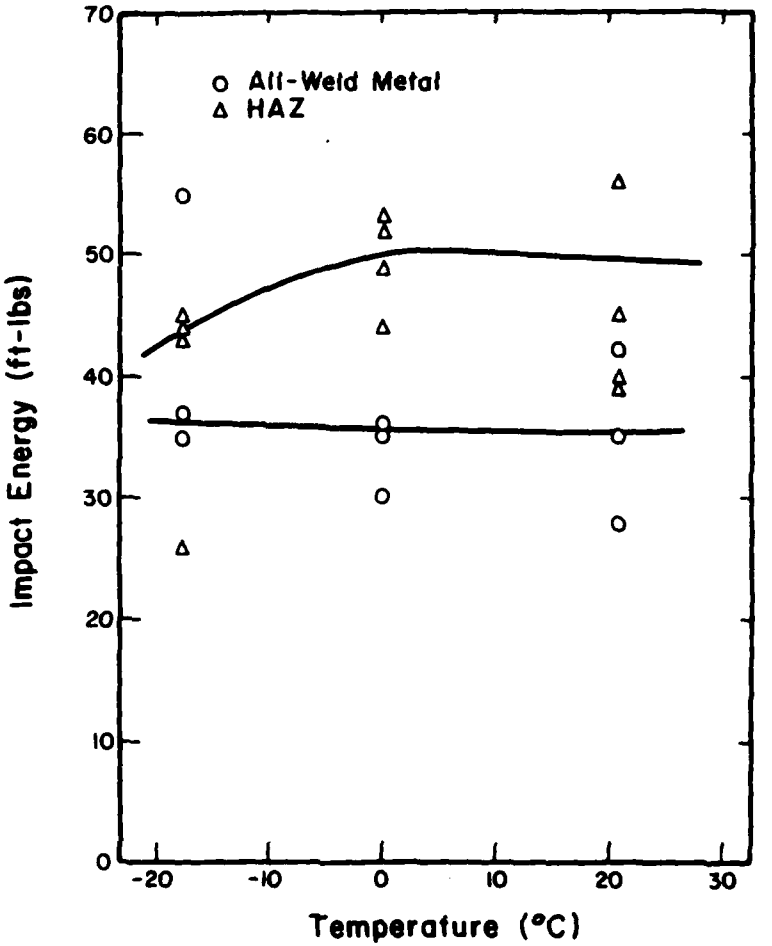

Figure 49. Charpy V-notch impact energy versus temperature for A514 SMA weldment B19.

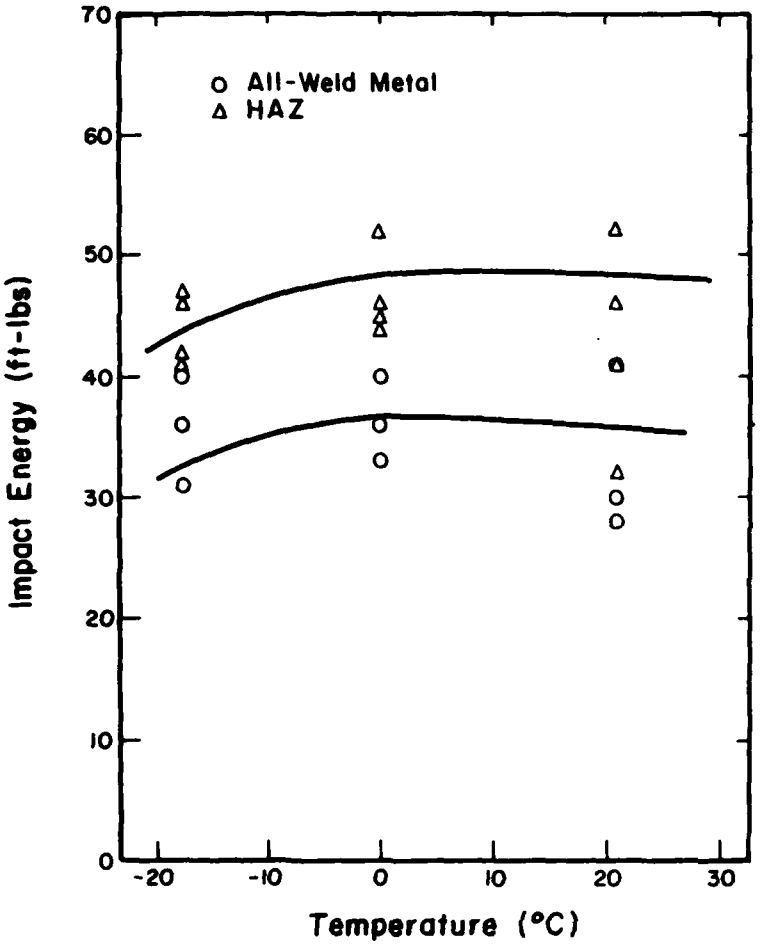

Figure 50. Charpy V-notch impact energy versus temperature for A514 SMA weldment B20.

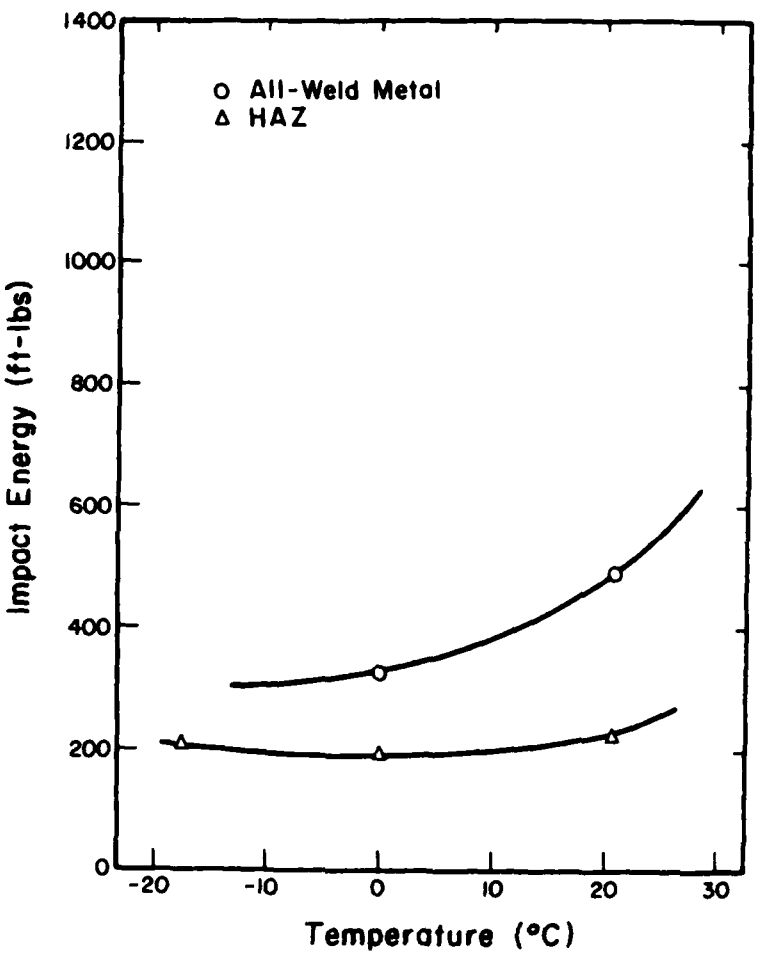

Figure 51. Dynamic tear impact energy versus temperature for A514 SMA weldment B21.

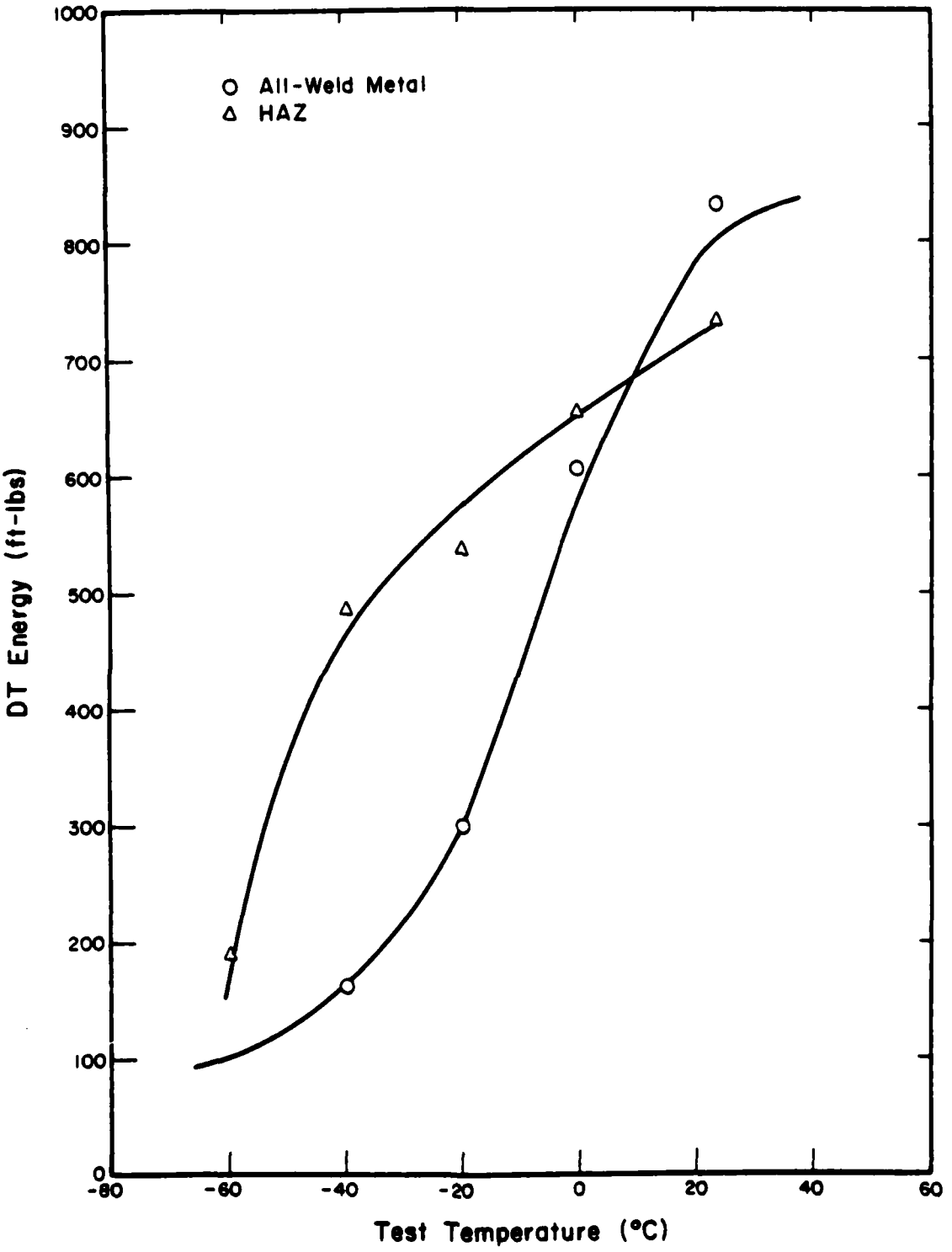

Figure 52. Dynamic tear impact energy versus test temperature for A514 SMA weldment C5.

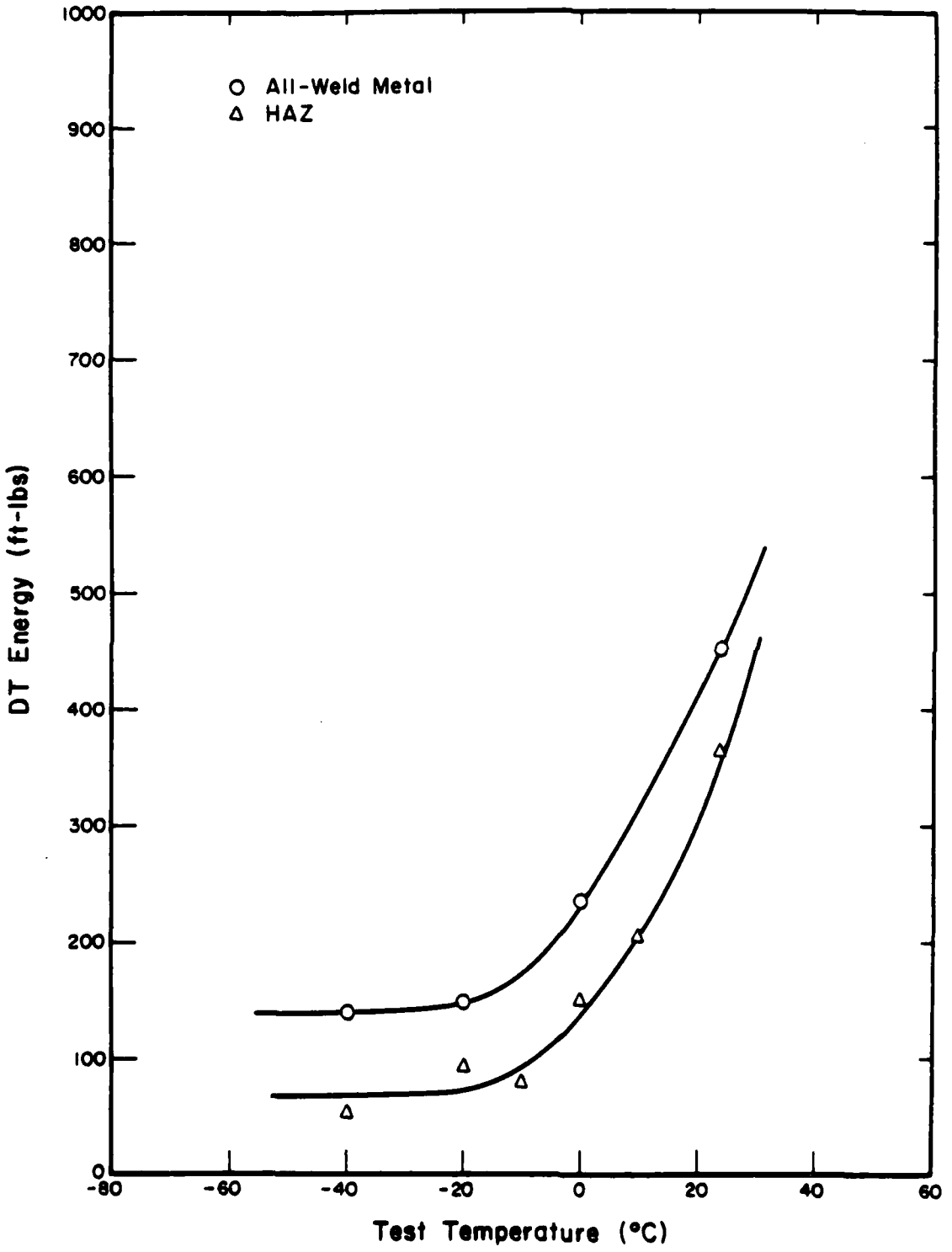

Figure 53. Dynamic tear impact energy versus test temperature for A514 SMA weldment C6.

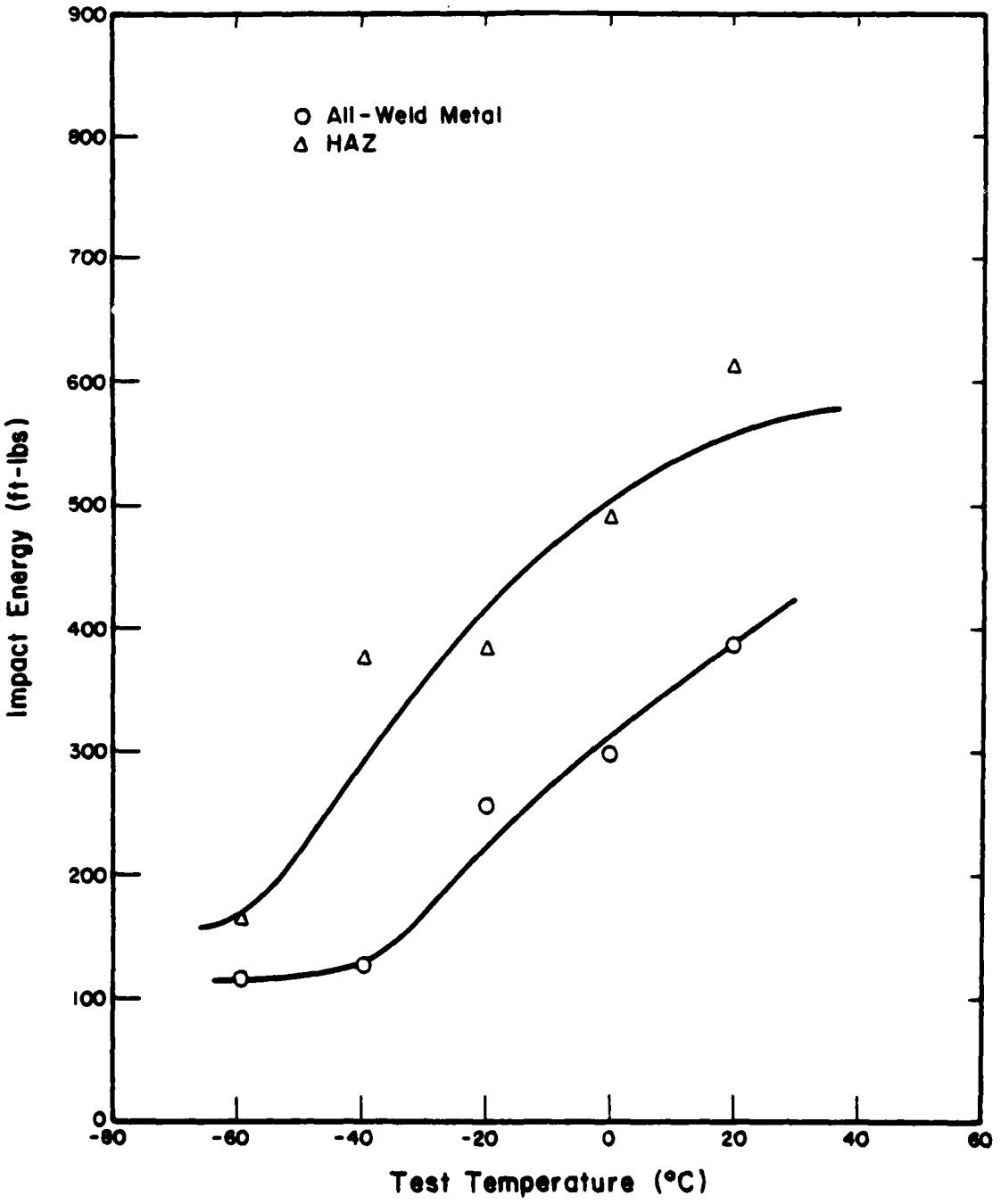

Figure 54. Dynamic tear impact energy versus test temperature for A514 SMA weldment D7.

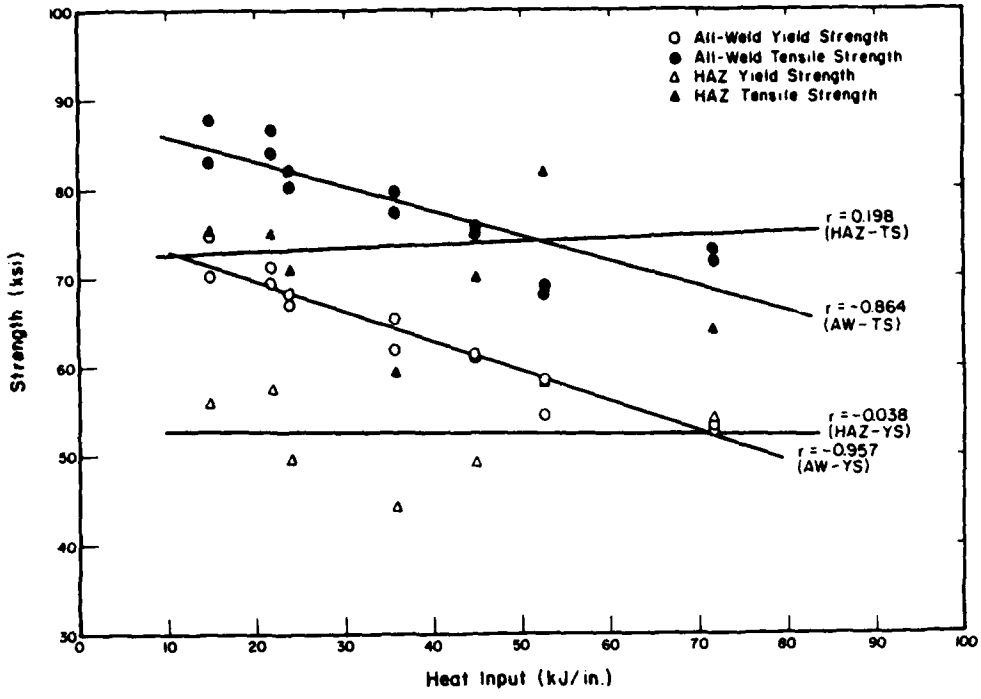

Figure 55. Weld metal and HAZ tensile and yield strength versus heat input for A36 GMA weldments.

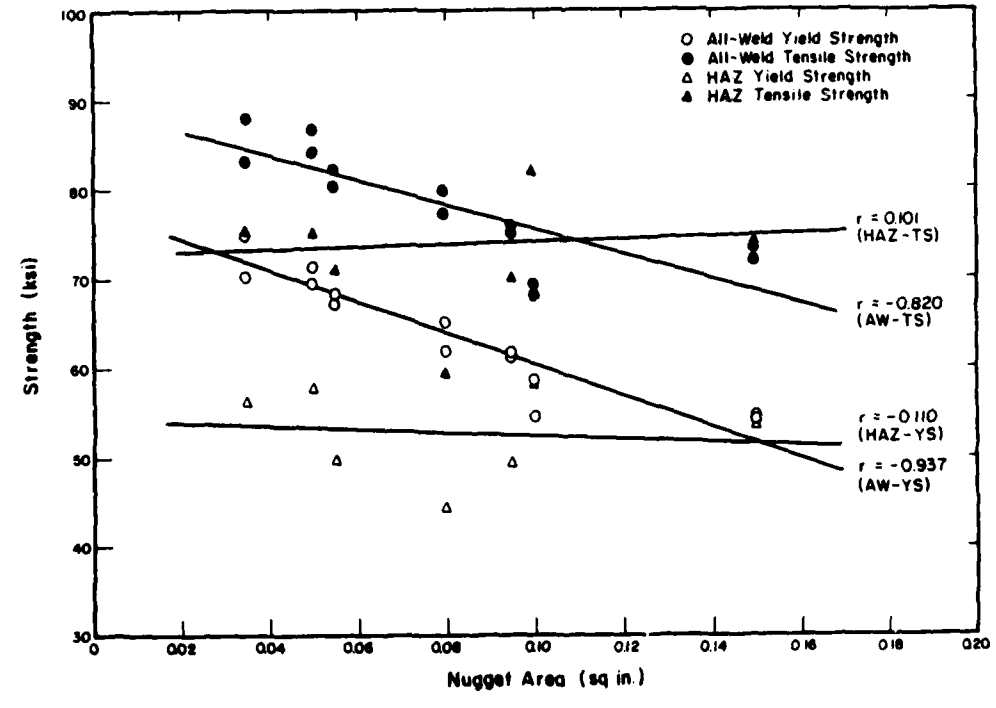

Figure 56. Weld metal and HAZ tensile and yield strength versus nugget area for A36 GMA weldments.

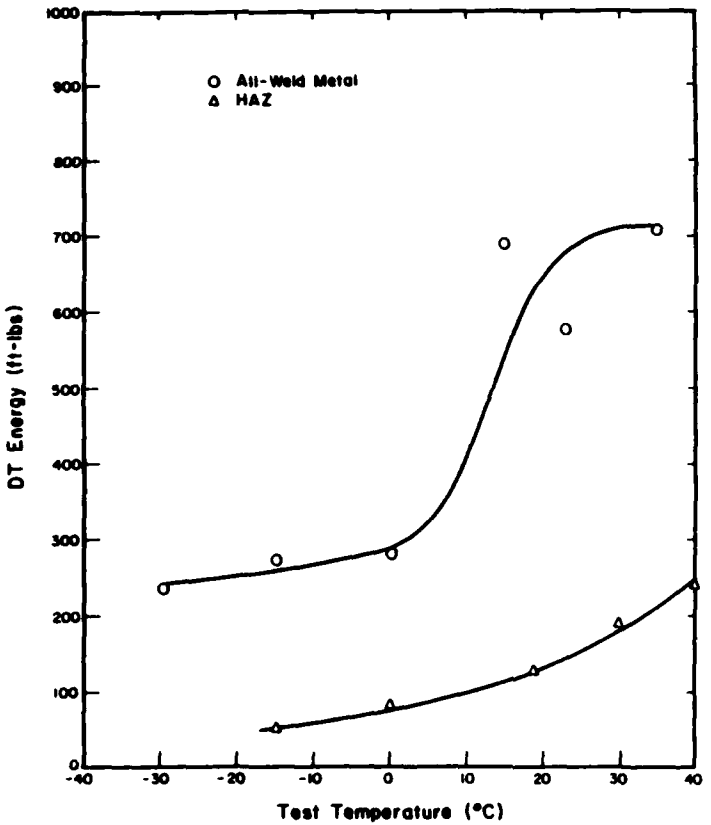

Figure 57. Dynamic tear impact energy versus test temperature for A36 GMA weldment B25.

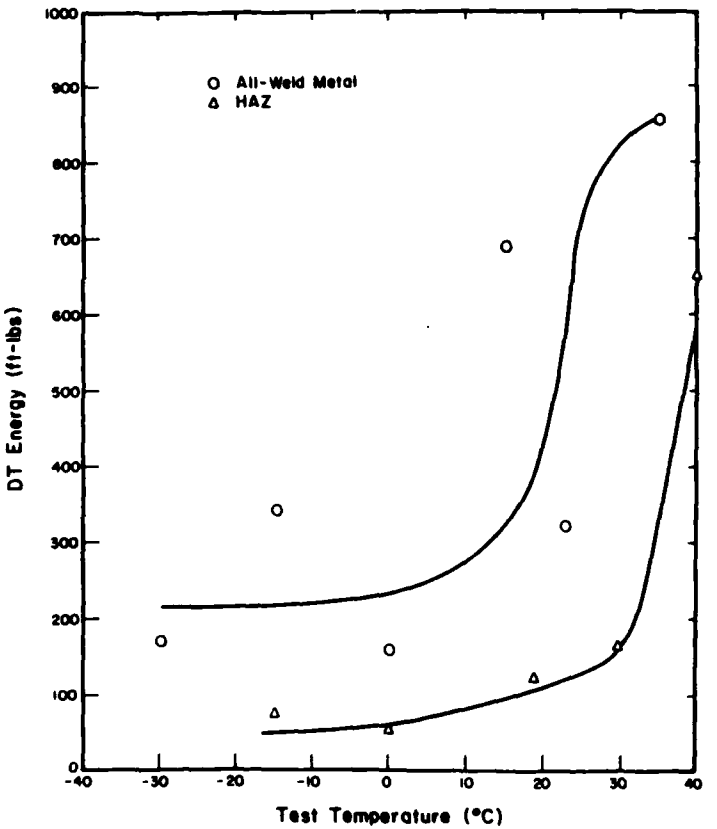

Figure 58. Dynamic tear impact energy versus test temperature for A36 GMA weldment B26.

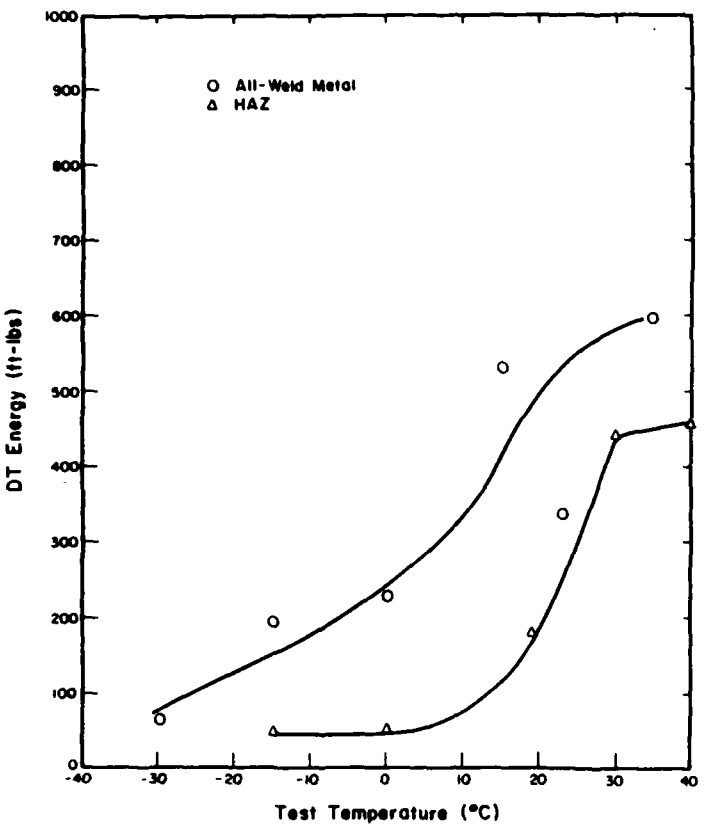

Figure 59. Dynamic tear impact energy versus test temperature for A36 GMA weldment B24.

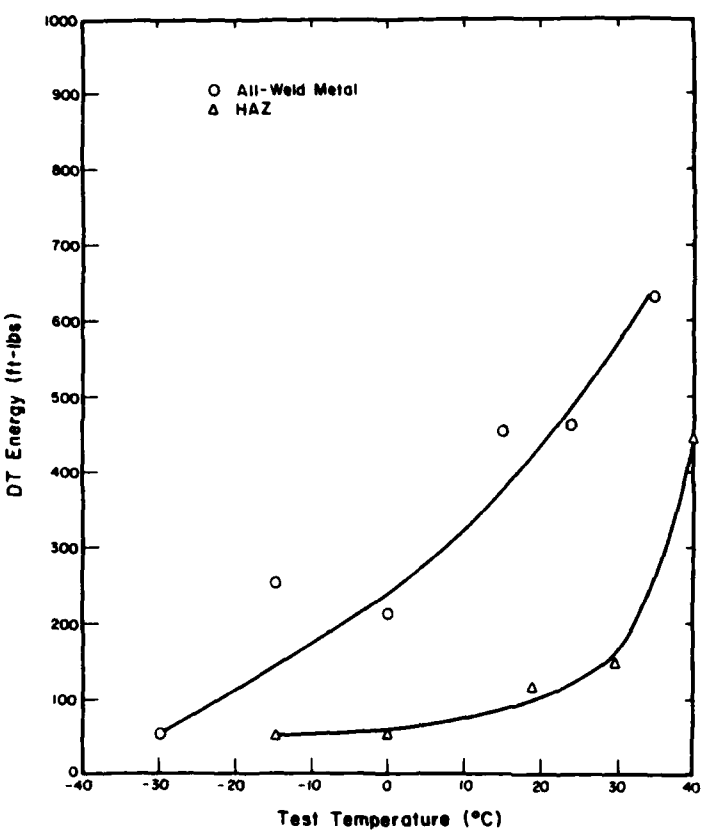

Figure 60. Dynamic tear impact energy versus test temperature for A36 GMA weldment B23.

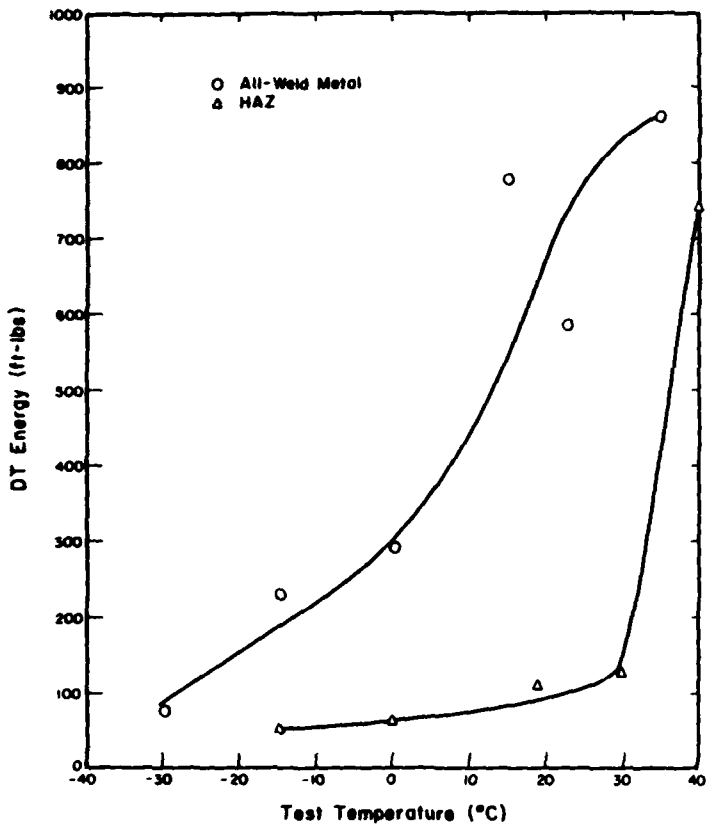

Figure 61. Dynamic tear impact energy versus test temperature for A36 GMA weldment B27.

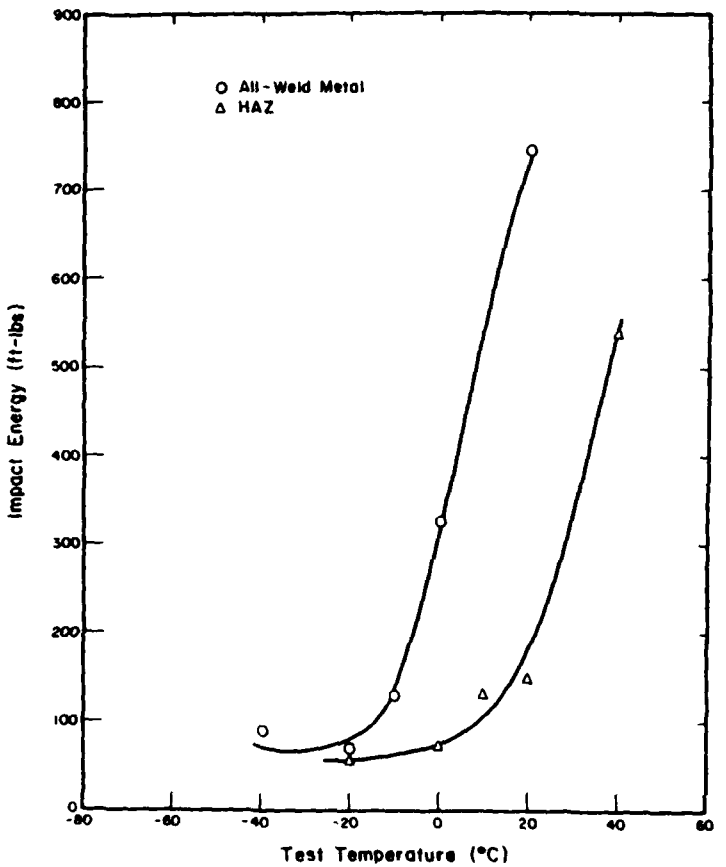

Figure 62. Dynamic tear impact energy versus test temperature for A36 GMA weldment D4.

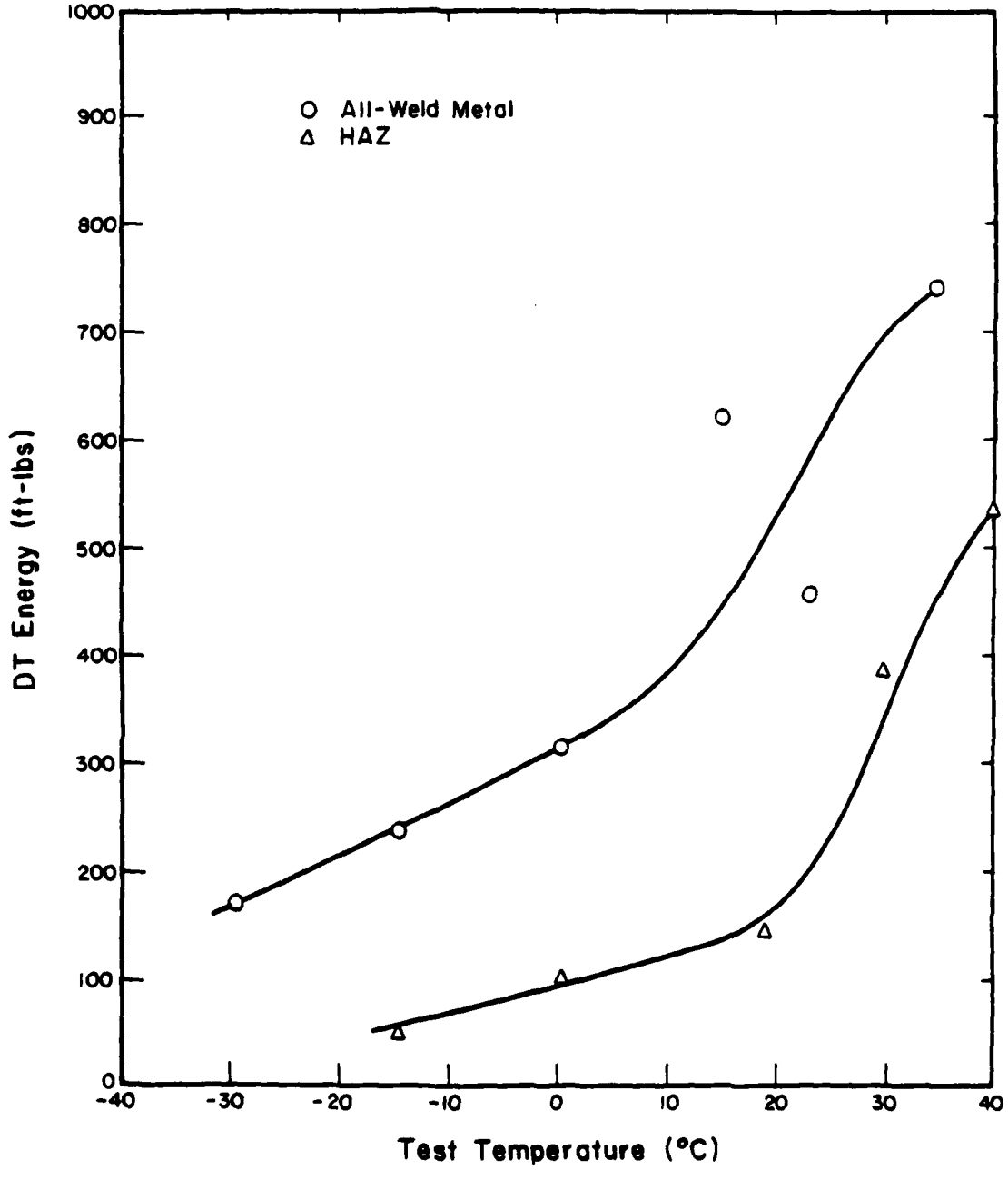

Figure 63. Dynamic tear impact energy versus test temperature for A36 GMA weldment B22.

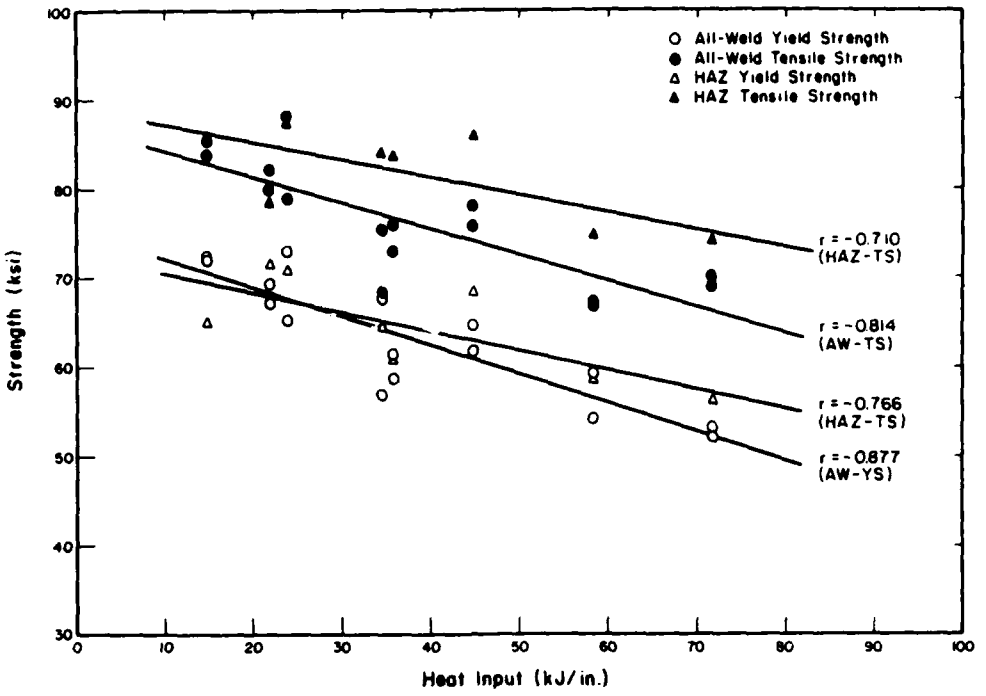

Figure 64. Weld and HAZ tensile and yield strength versus heat input for A516 GMA weldments.

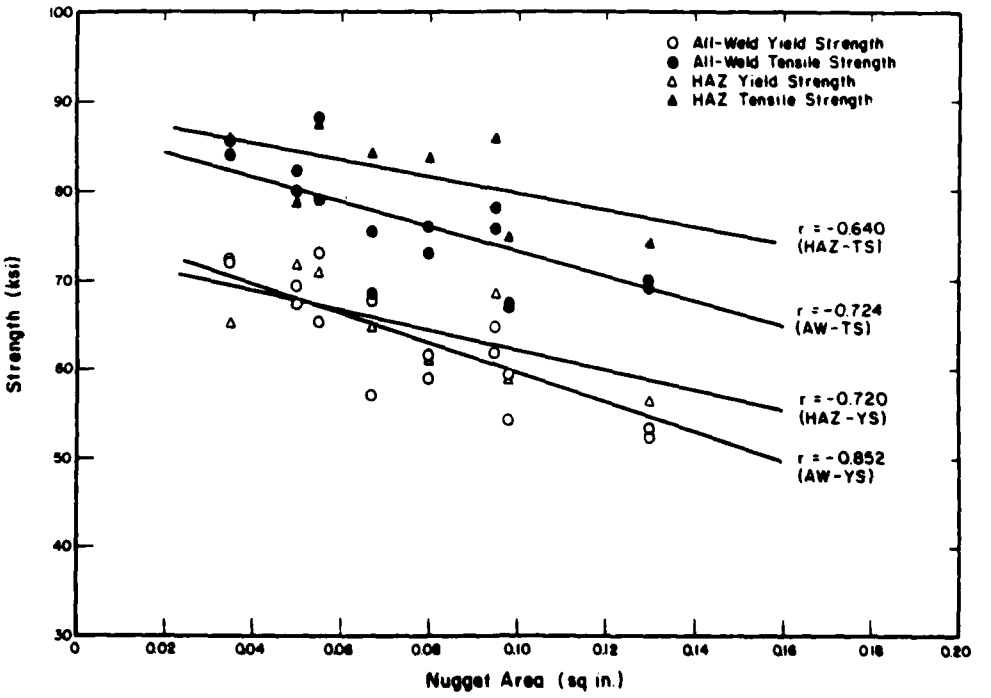

Figure 65. Weld and HAZ tensile and yield strength versus nugget area for A516 GMA weldments.

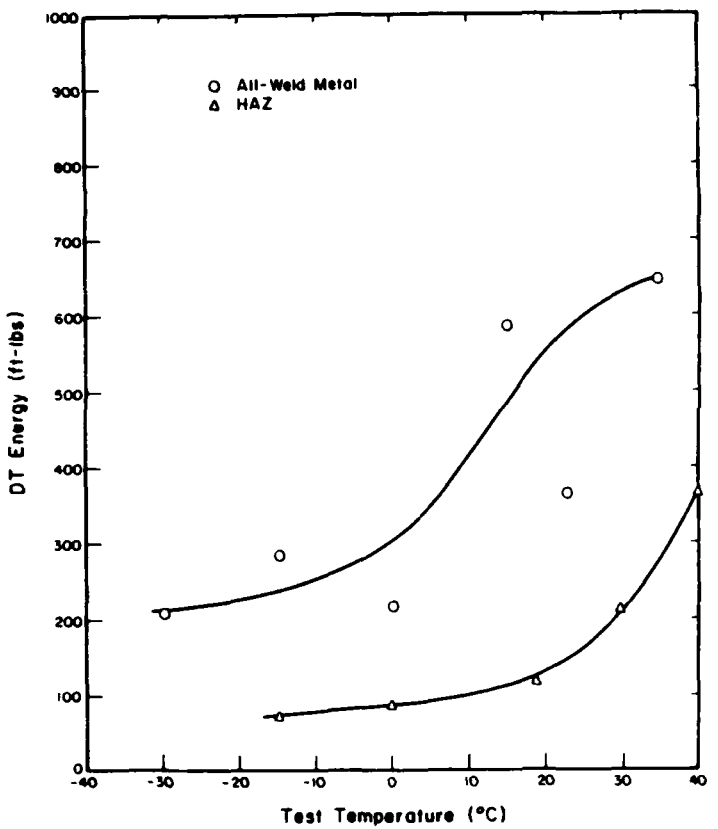

Figure 66. Dynamic tear impact energy versus test temperature for A516 GMA weldment B30.

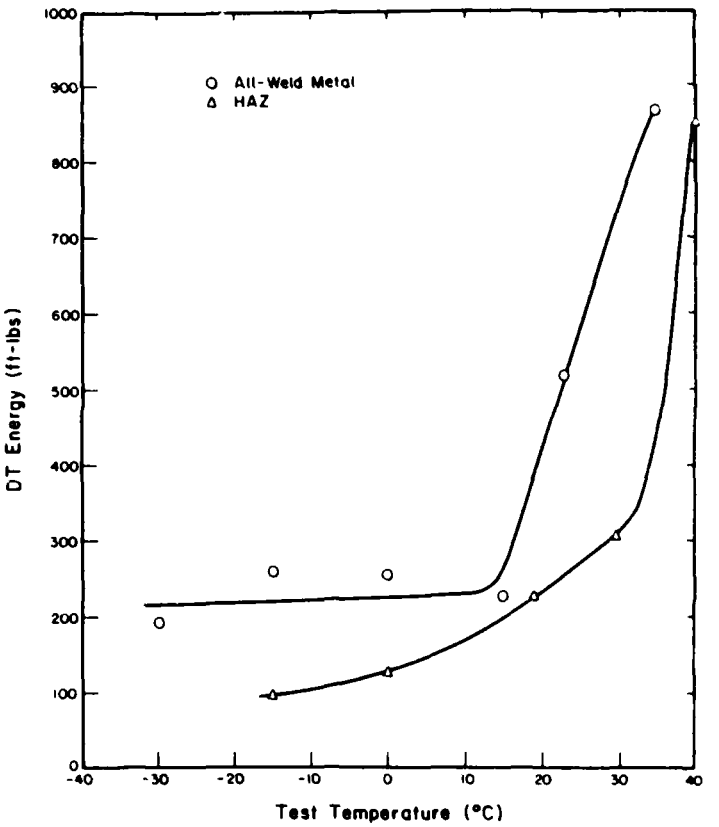

Figure 67. Dynamic tear impact energy versus test temperature for A516 GMA weldment B29.

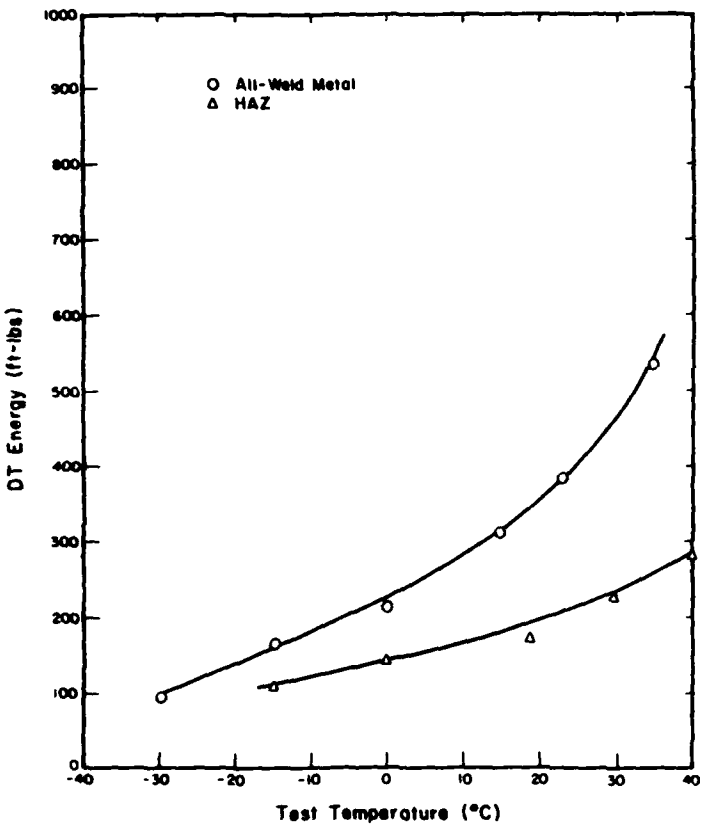

Figure 68. Dynamic tear impact energy versus test temperature for A516 GMA weldment B31.

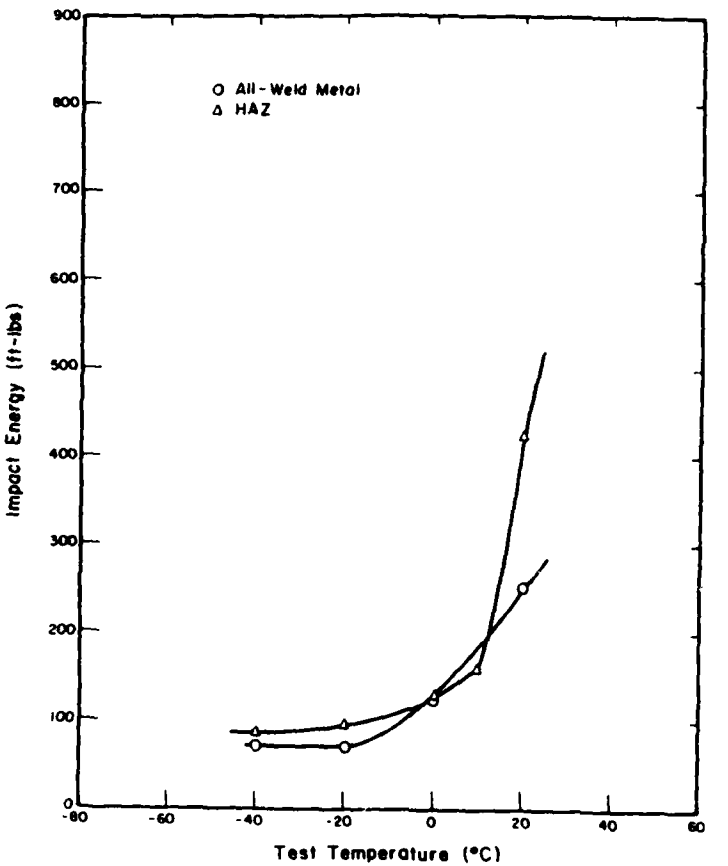

Figure 69. Dynamic tear impact energy versus test temperature for A516 GMA weldment D3.

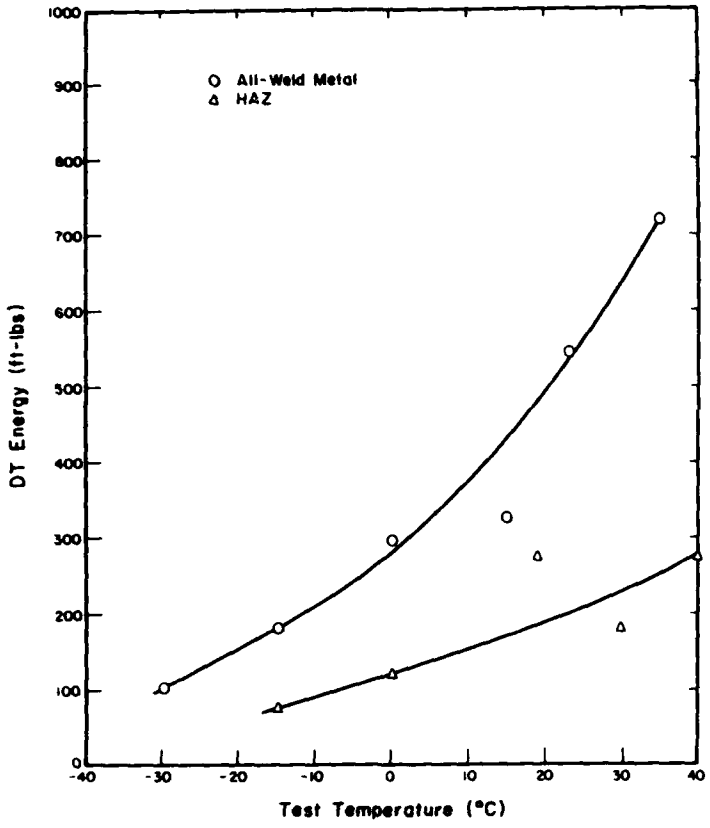

Figure 70. Dynamic tear impact energy versus test temperature for A516 GMA weldment B32.

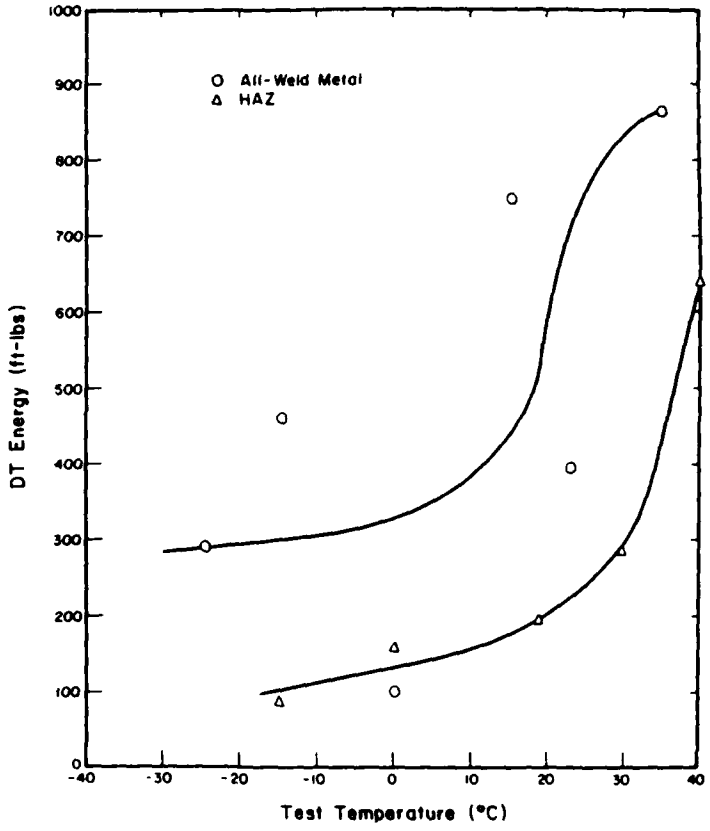

Figure 71. Dynamic tear impact energy versus test temperature for A516 GMA weldment B28.

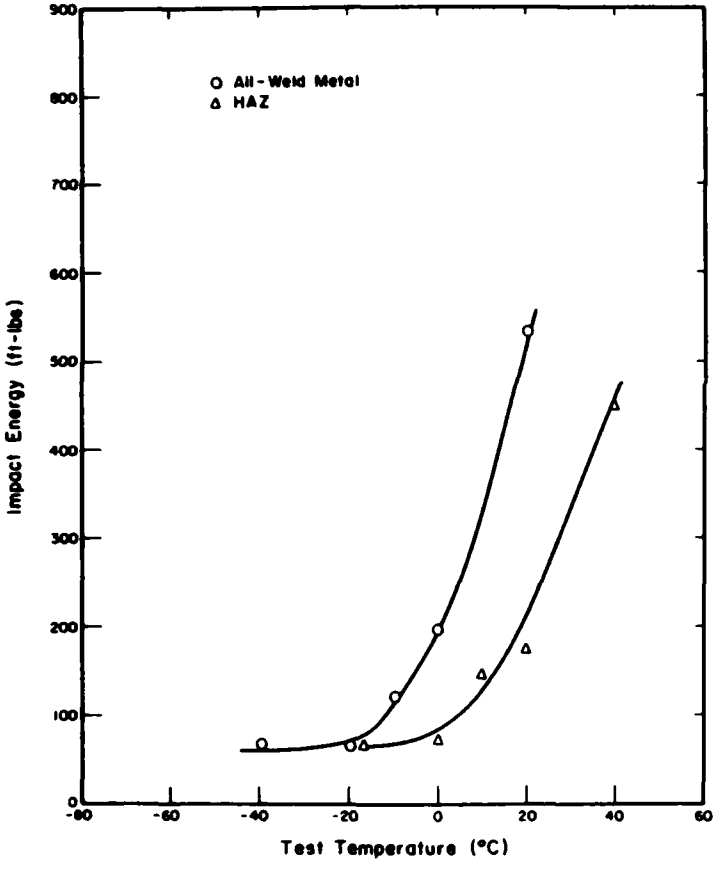

Figure 72. Dynamic tear impact energy versus test temperature for A516 GMA weldment D2.

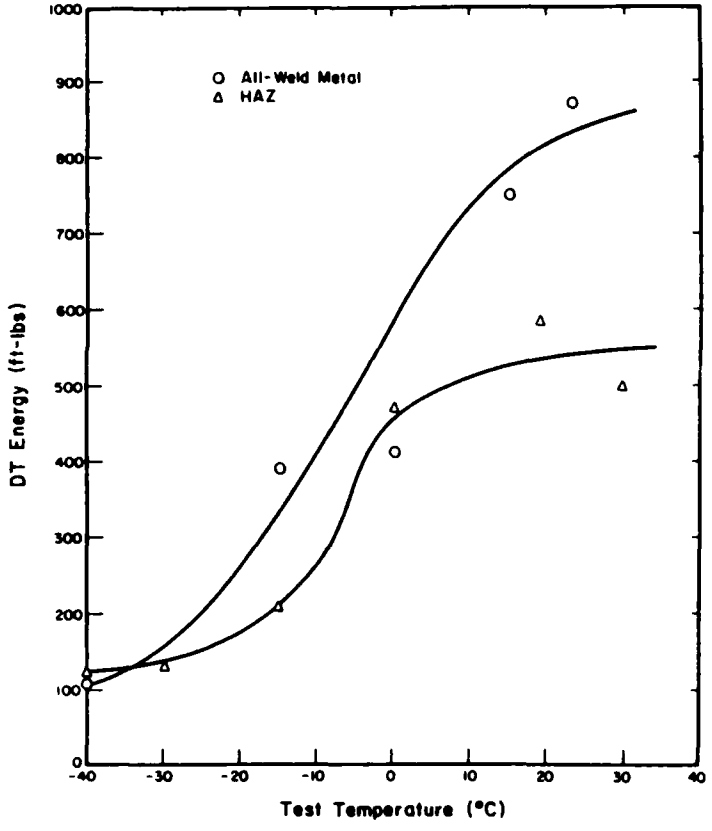

Figure 73. Dynamic tear impact energy versus test temperature for A516 GMA weldment B33.

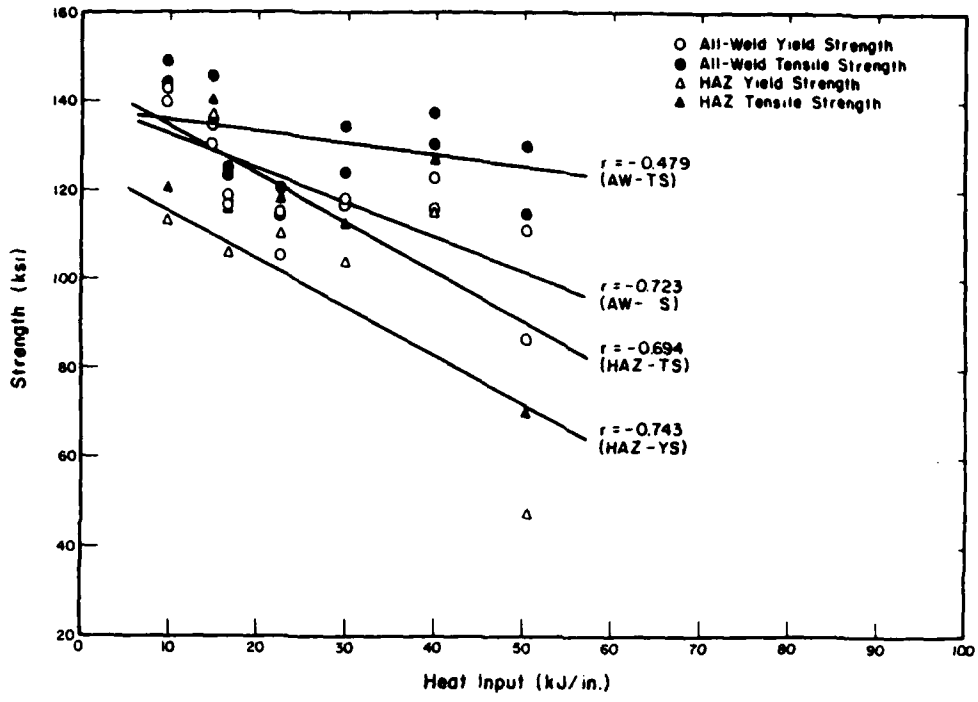

Figure 74. Weld and HAZ tensile and yield strength versus heat input for A514 GMA weldments.

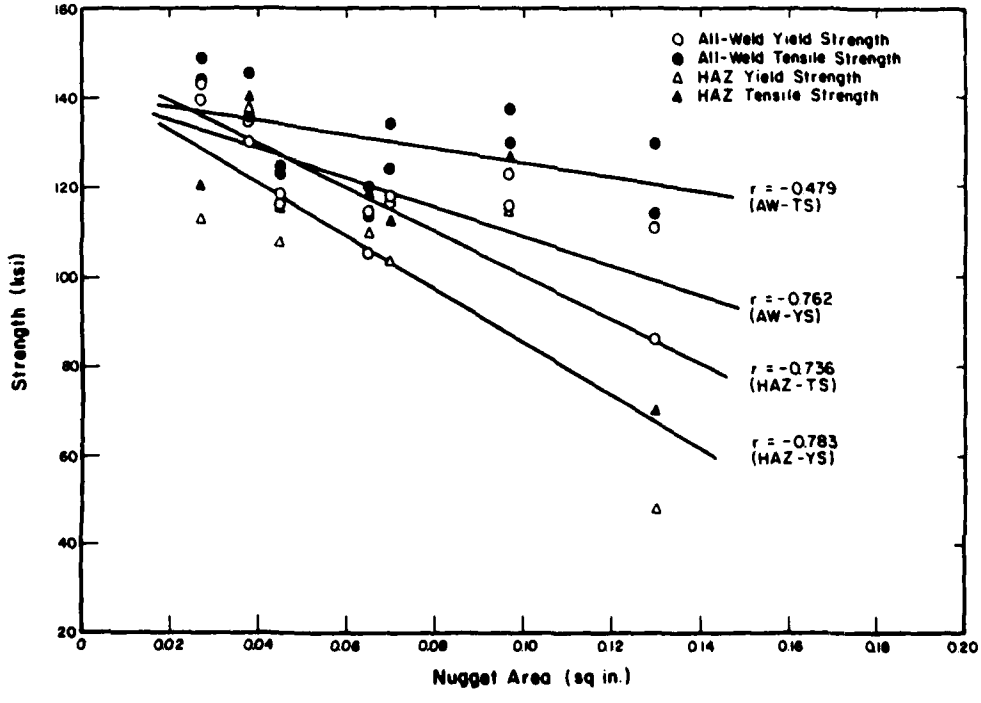

Figure 75. Weld and HAZ tensile and yield strength versus nugget area for A514 GMA weldments.

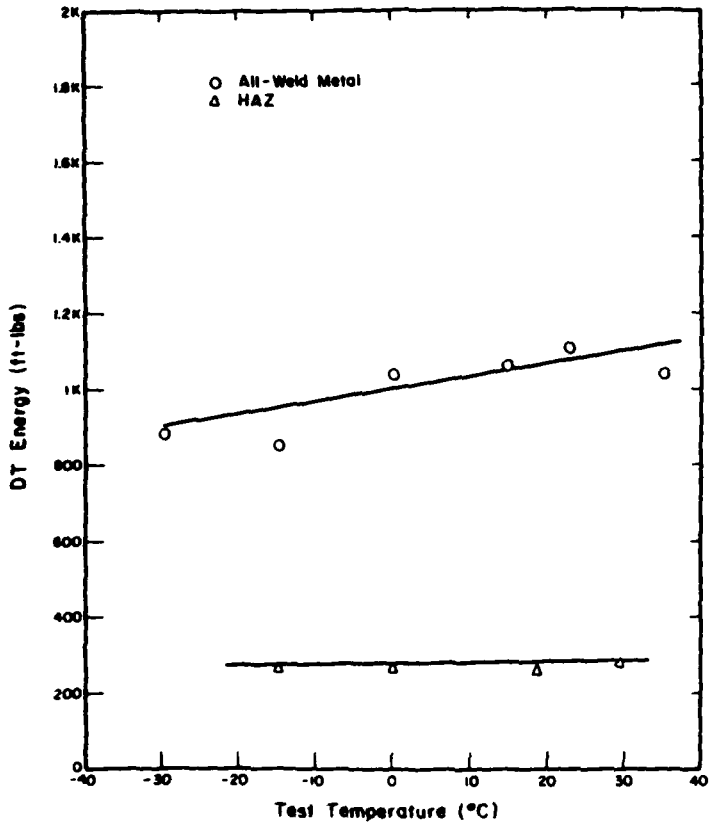

Figure 76. Dynamic tear impact energy versus test temperature for A514 GMA weldment B39.

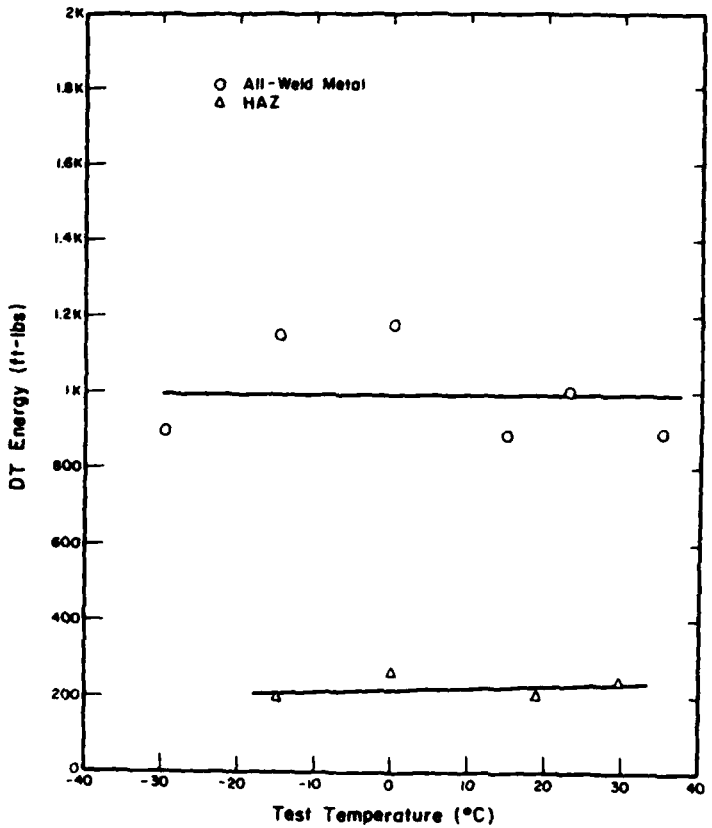

Figure 77. Dynamic tear impact energy versus test temperature for A514 GMA weldment B38.

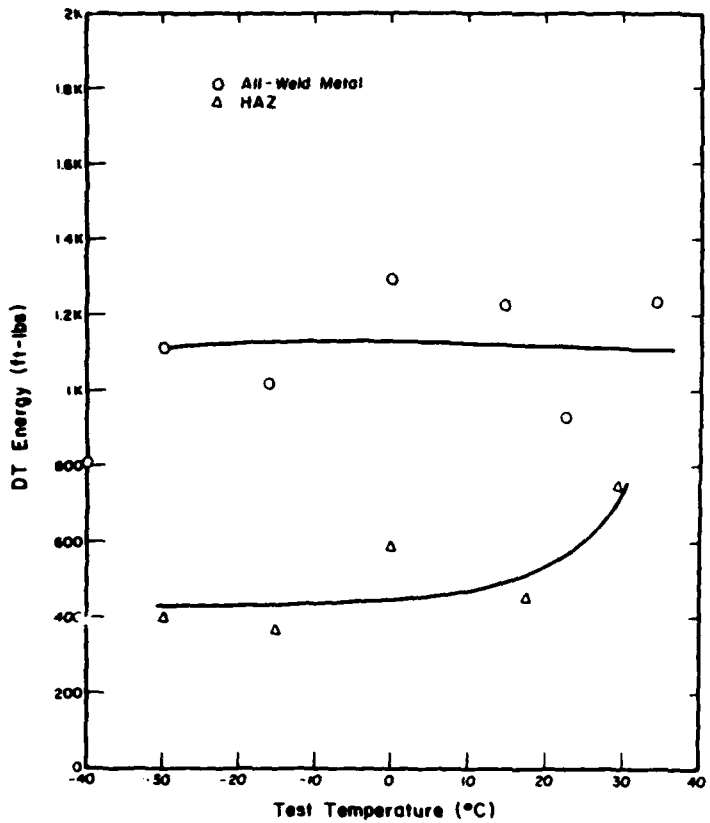

Figure 78. Dynamic tear impact energy versus test temperature for A514 GMA weldment B36 (nugget area: 0.045 sq in. [30 mm^2]).

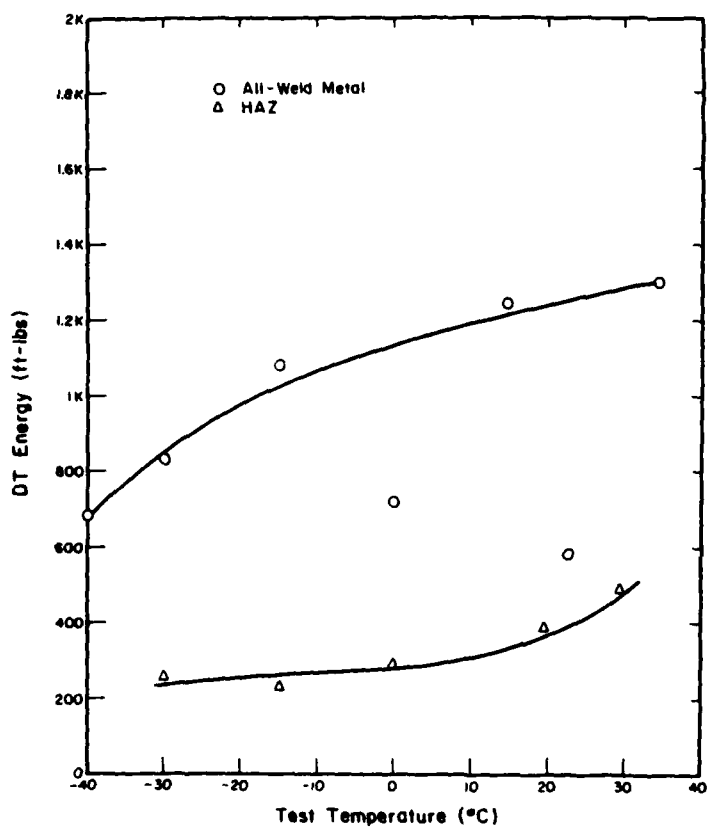

Figure 79. Dynamic tear impact energy versus test temperature for A514 GMA weldment B35.

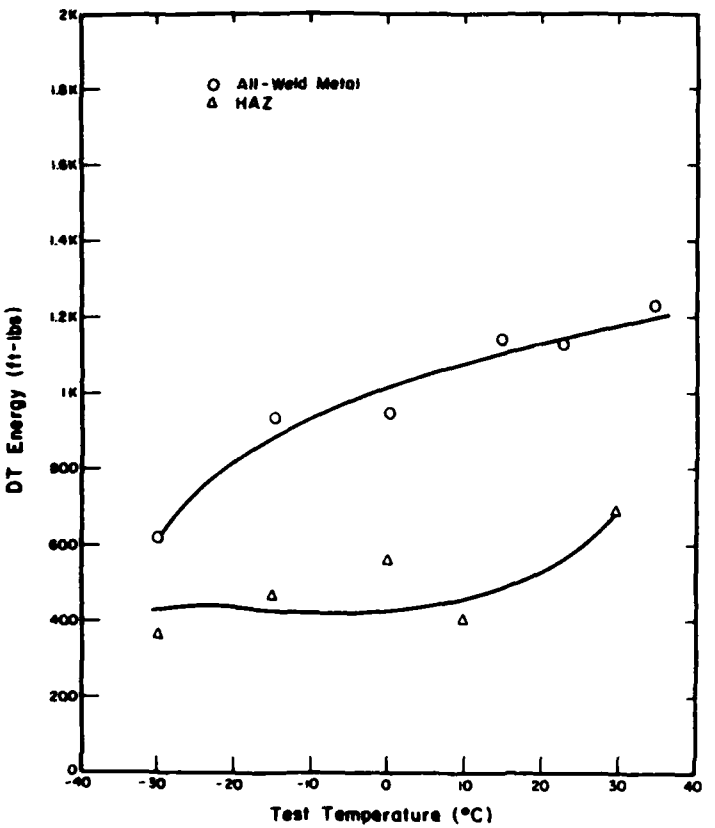

Figure 80. Dynamic tear impact energy versus test temperature for A514 GMA weldment B37.

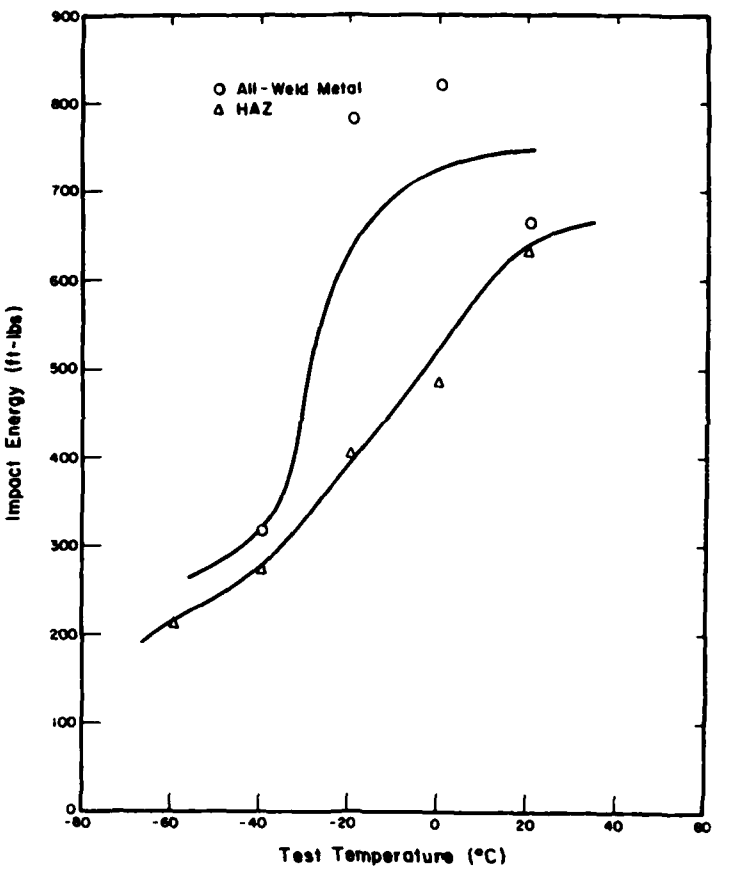

Figure 81. Dynamic tear impact energy versus test temperature for A514 GMA weldment D1.

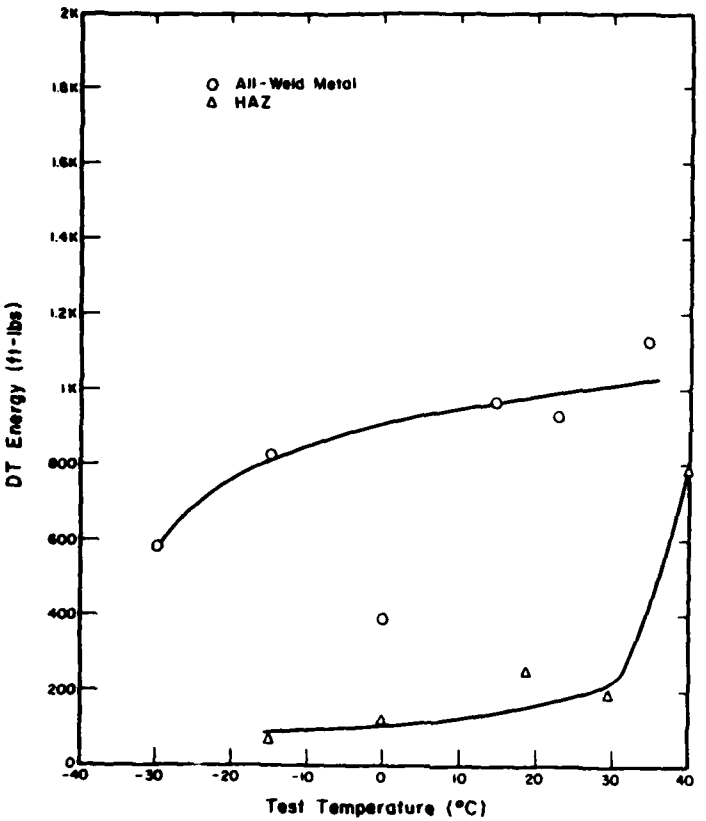

Figure 82. Dynamic tear impact energy versus test temperature for A514 GMA weldment B34.

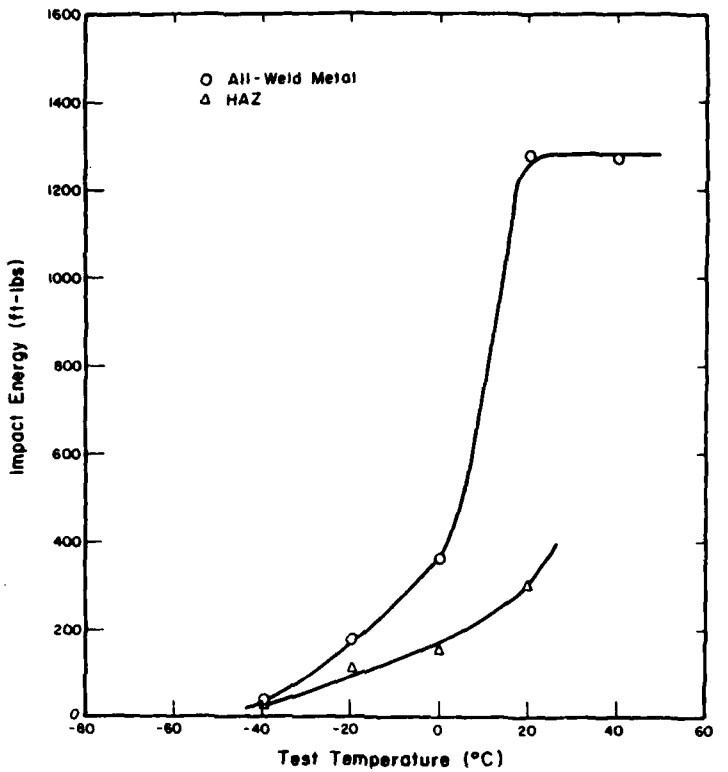

Figure 83. Dynamic tear energy versus test temperature for A36 SMA weldment T.

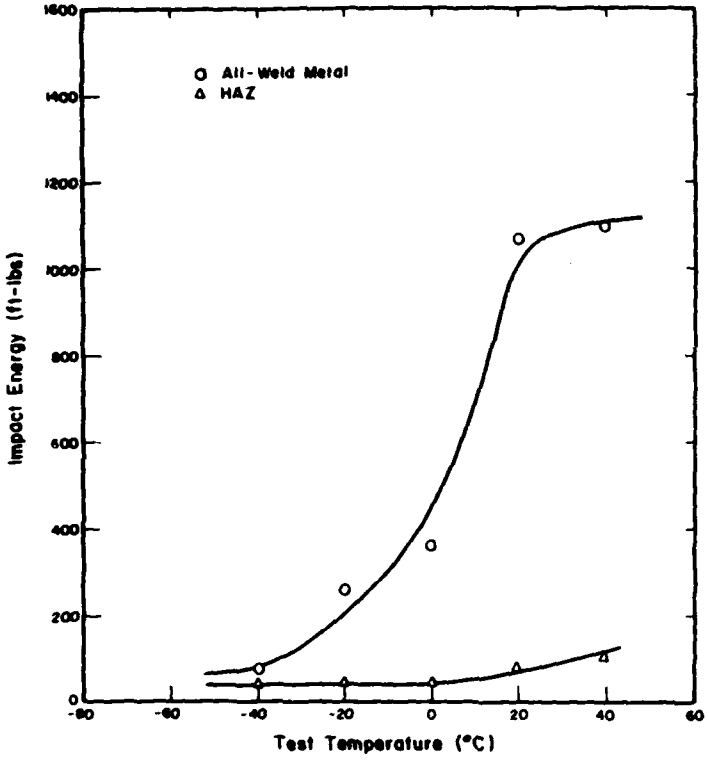

Figure 84. Dynamic tear energy versus test temperature for A36 SMA weldment M.

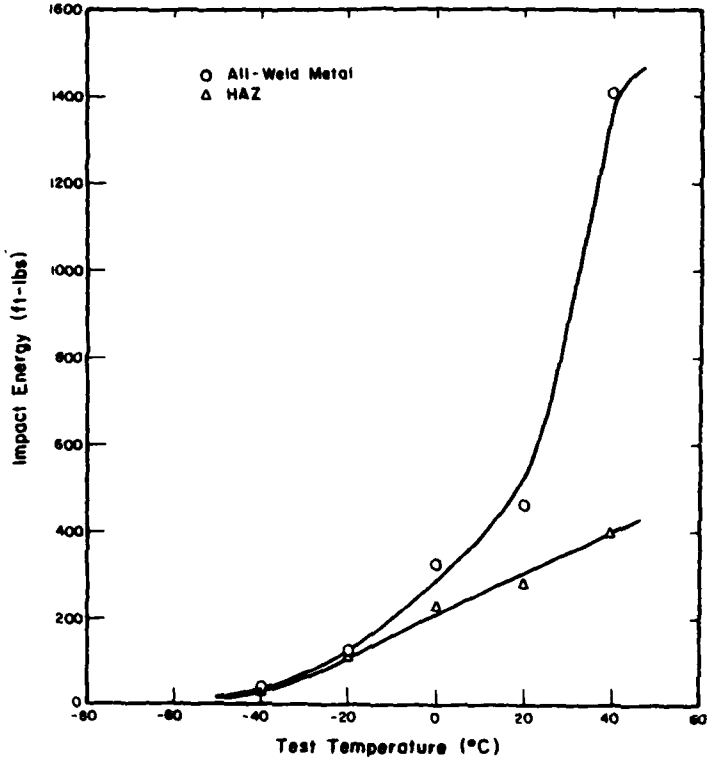

Figure 85. Dynamic tear energy versus test temperature for A516 SMA weldment R.

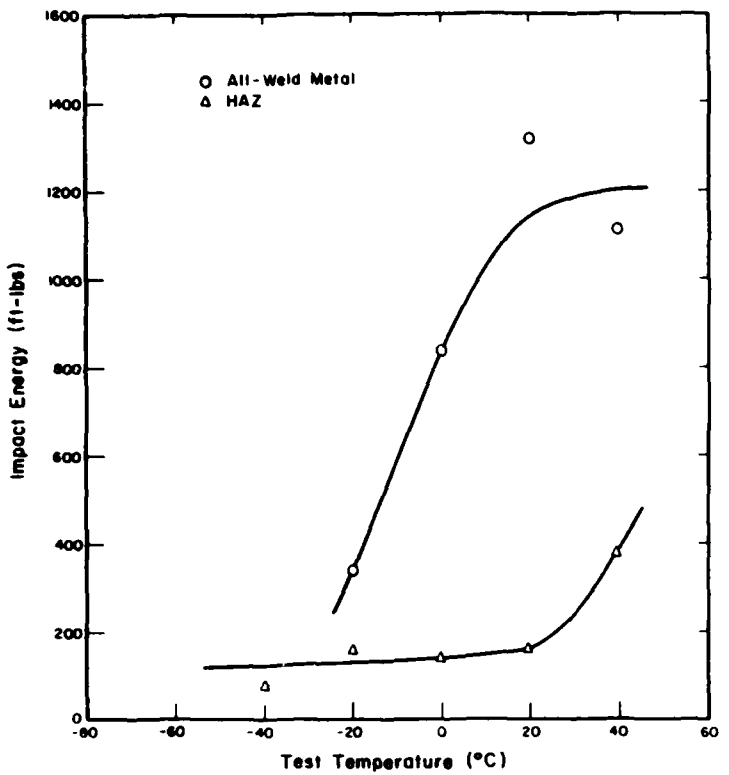

Figure 86. Dynamic tear energy versus test temperature for A516 SMA weldment Q.

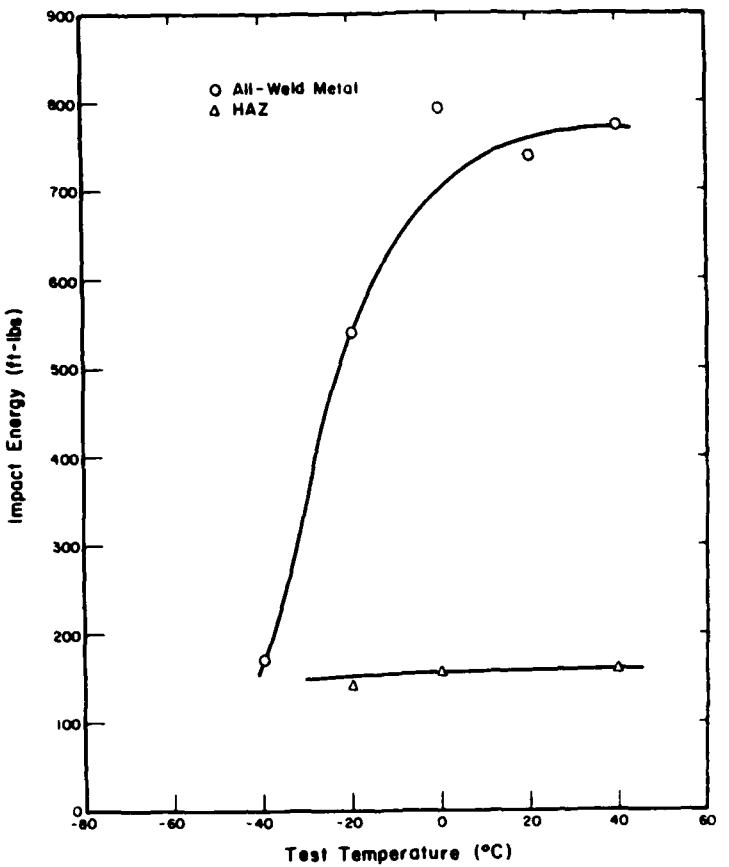

Figure 87. Dynamic tear energy versus test temperature for A514 SMA weldment P.

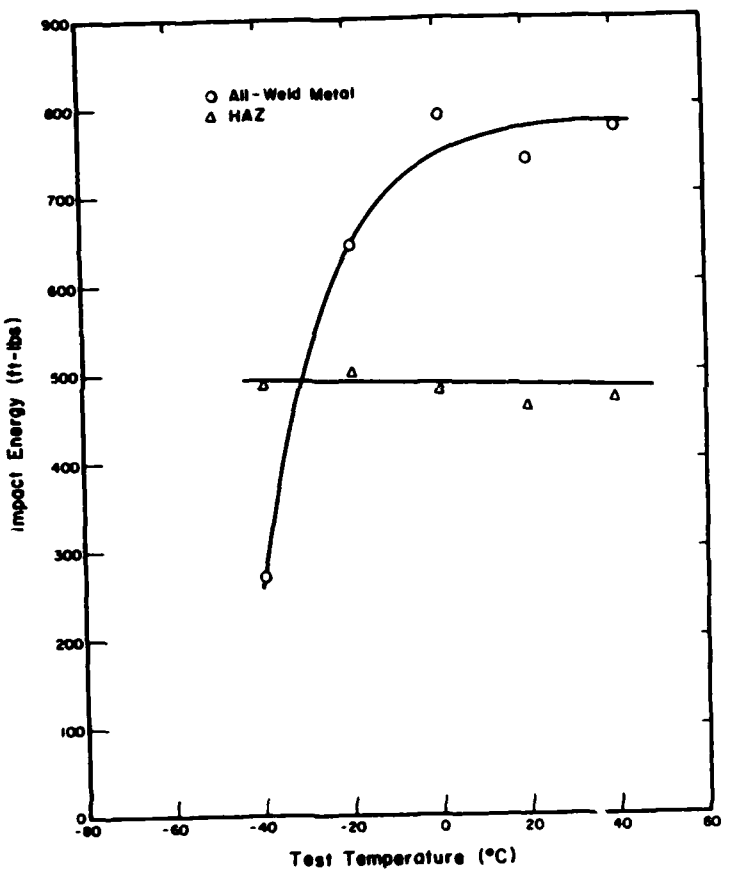

Figure 88. Dynamic tear energy versus test temperature for A514 SMA weldment O.

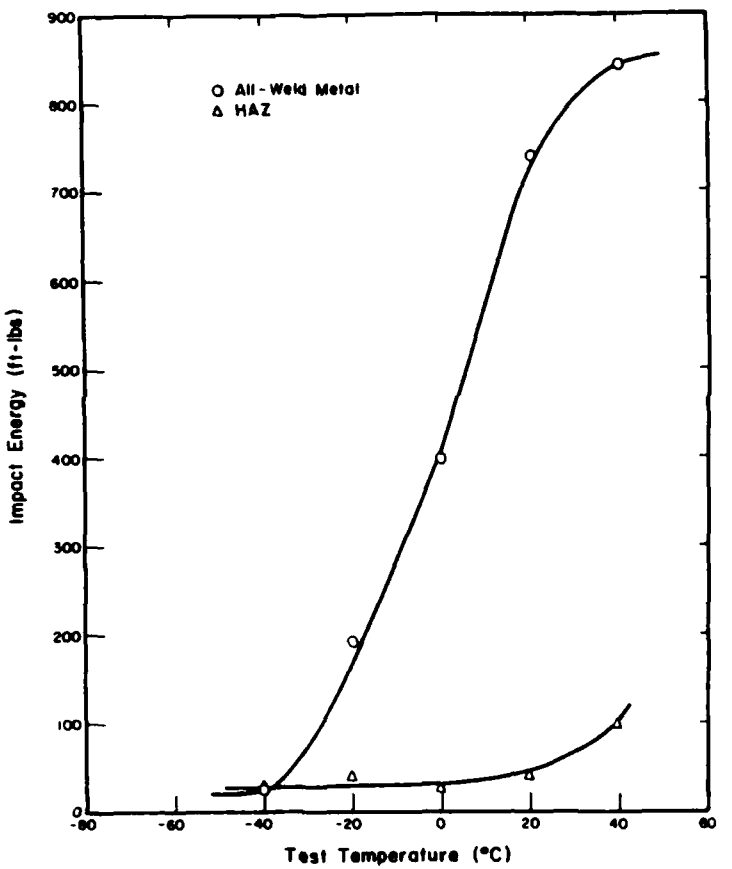

Figure 89. Dynamic tear energy versus test temperature for A36 GMA weldment K.

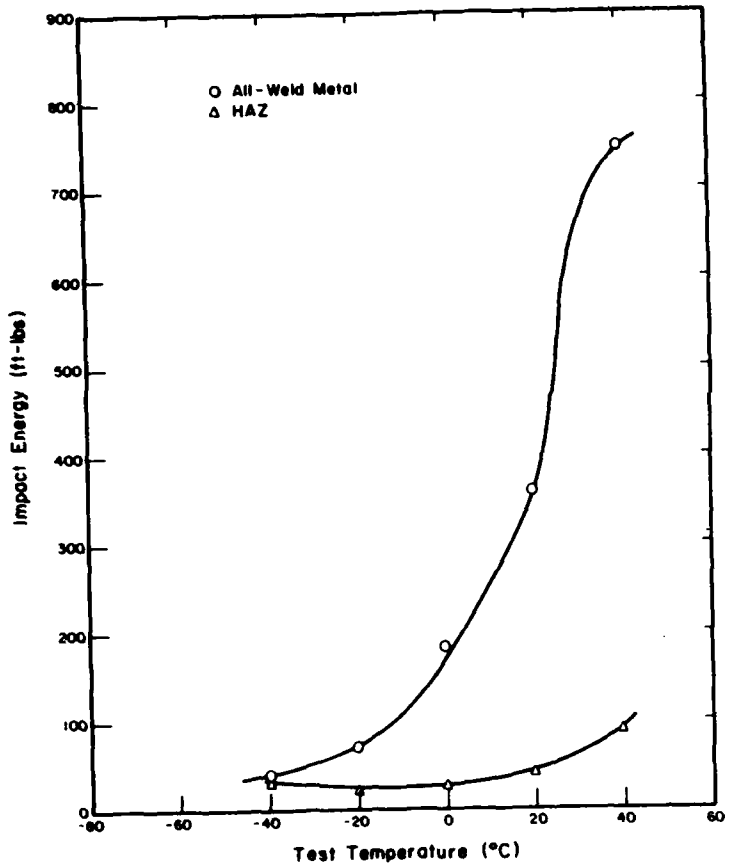

Figure 90. Dynamic tear energy versus test temperature for A36 GMA weldment L.

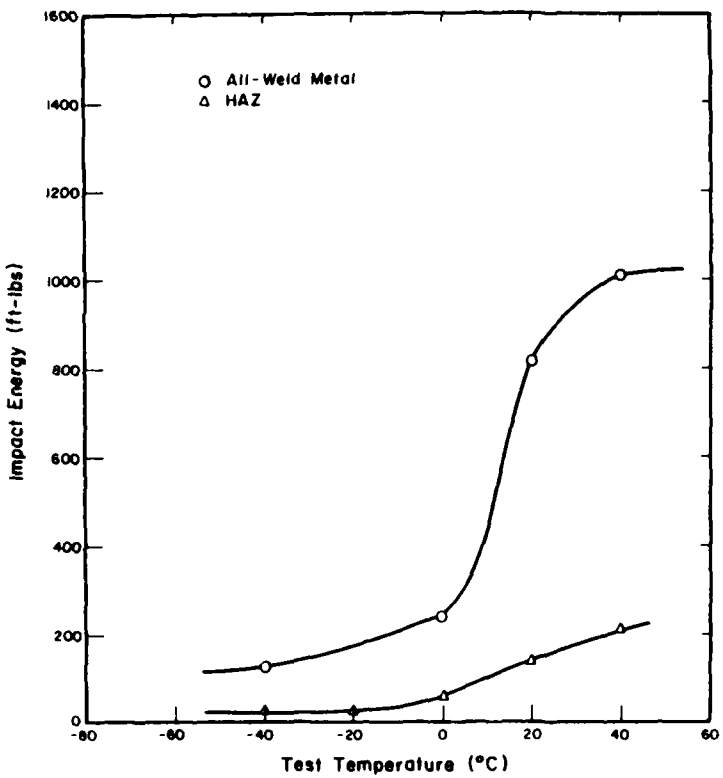

Figure 91. Dynamic tear energy versus test temperature for A516 GMA weldment I.

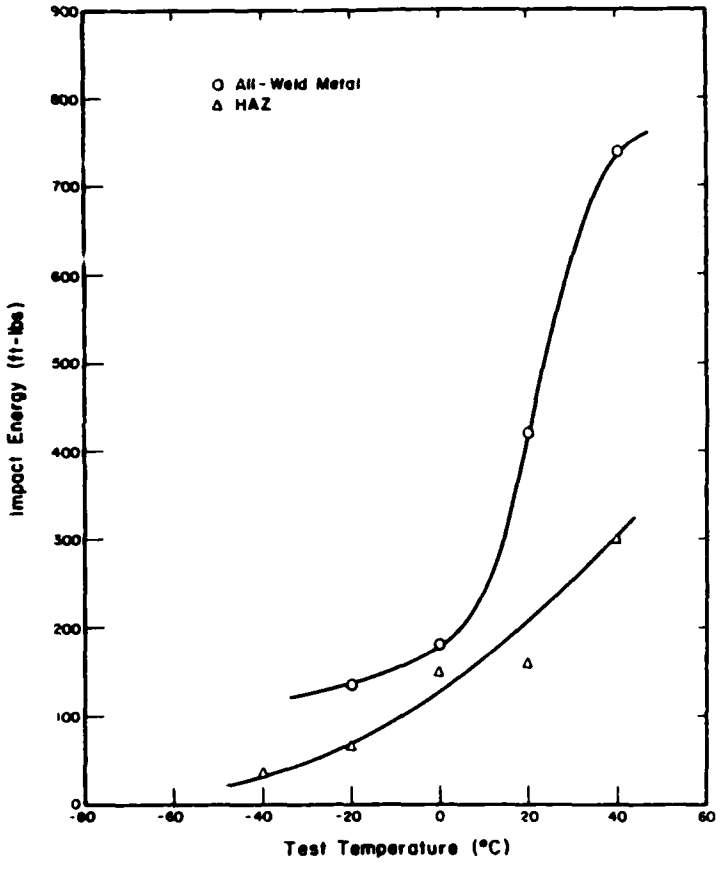

Figure 92. Dynamic tear energy versus test temperature for A516 GMA weldment W.

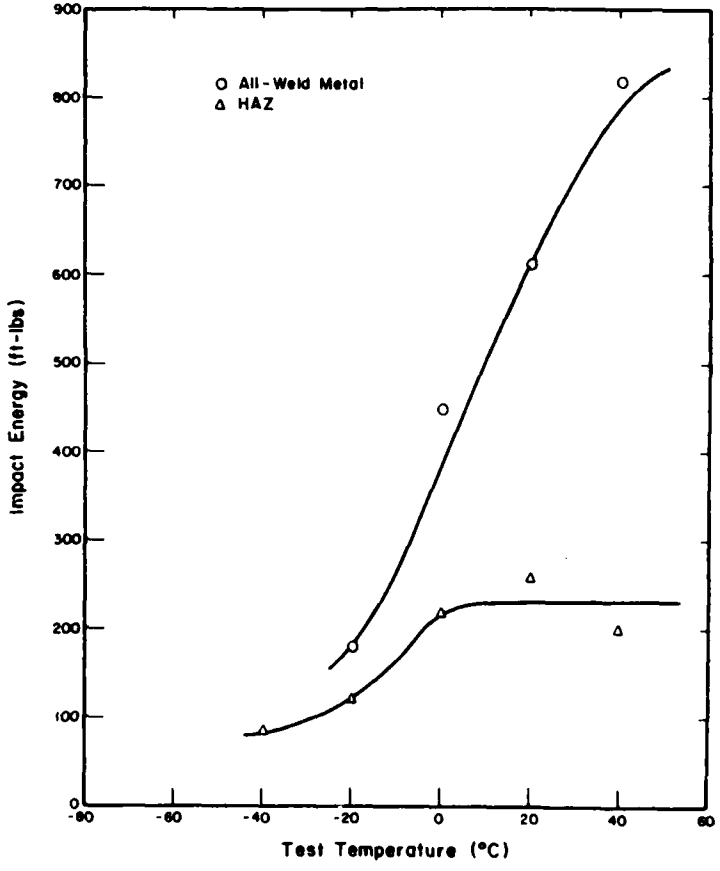

Figure 93. Dynamic tear energy versus test temperature for A514 GMA weldment V.

AD-A111 886 CONSTRUCTION ENGINEERING RESEARCH LAB (ARMY) CHAMPAIGN IL F/G 11/6
WELDABILITY CHARACTERISTICS OF CONSTRUCTION STEELS A36, A514, A--ETC(U)
DEC 81 R A WEBER
UNCLASSIFIED CERL-TR-M-302 NL

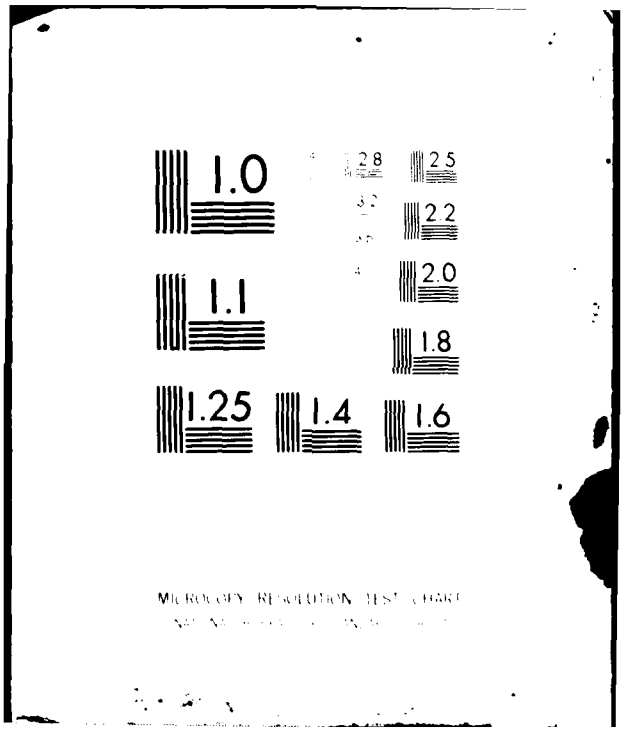
1.0
1.1
1.25
1.4
1.6
1.8
2.0
2.2
2.5
2.8
3.2
3.6
4
MICROCOPY RESOLUTION TEST CHART

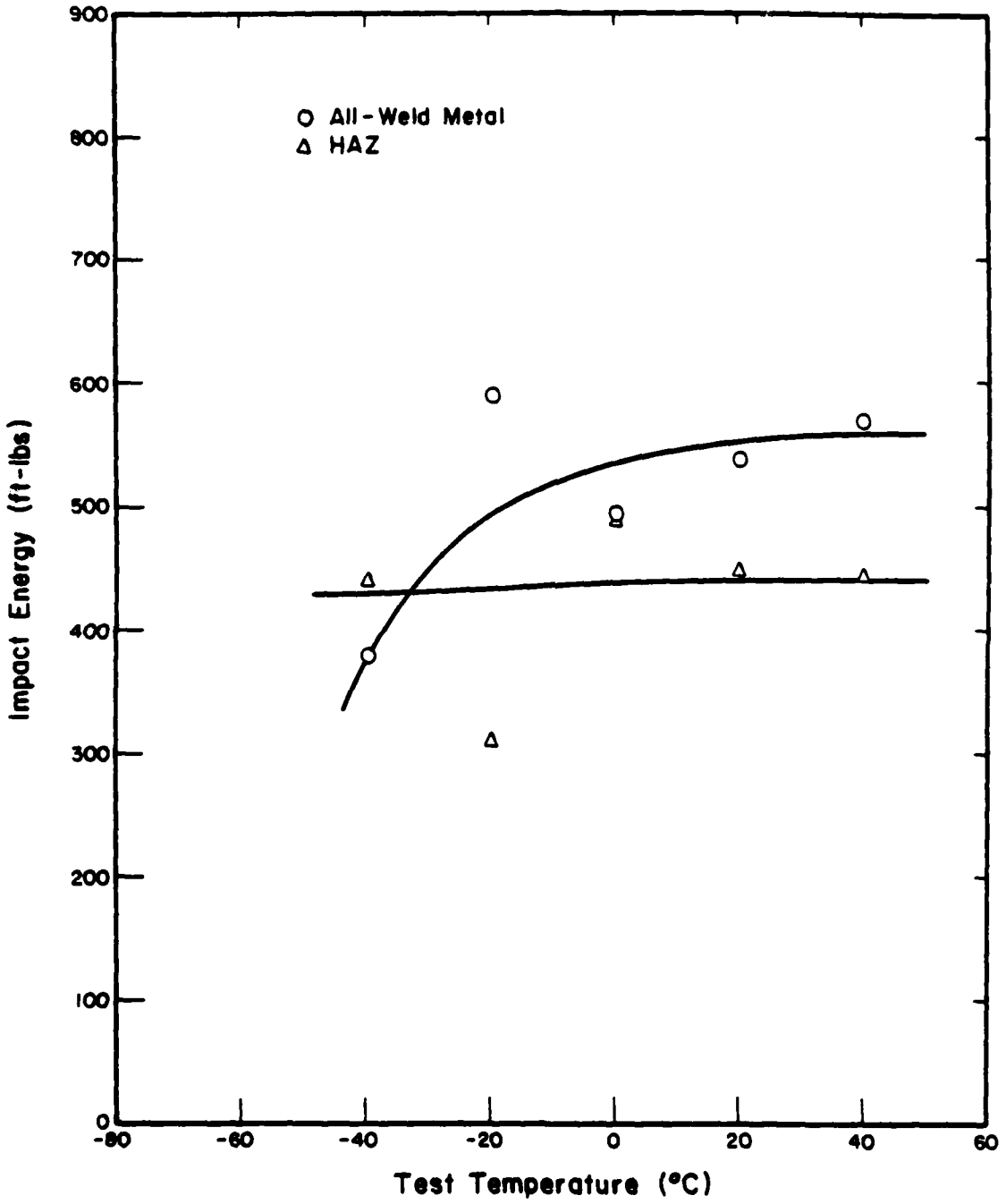

Figure 94. Dynamic tear energy versus test temperature for A514 GMA weldment J.

REFERENCES

"ASTM Proposed Method for 5/8-In. (16-mm) Dynamic Tear Test of Metallic Materials," *1980 Annual Book of ASTM Standards*, Part 10 (American Society for Testing and Materials [ASTM], 1980).

Dorschu, K. E., "Control of Cooling Rates in Steel Weld Metal," *Welding Journal*, Vol 47 (February 1968), Research Supplement.

Military Standard, *Mechanical Tests for Welded Joints*, MIL-STD-418C (June 1972).

Operator Manual: Welding Theory and Application, Technical Manual (TM) 9-237 (Headquarters [HQ], Department of the Army [DA], October 1976).

Schultz, B. L. and C. E. Jackson, "Influence of Weld Bead Area on Weld Mechanical Properties," *Welding Journal*, Vol 53 (June 1974), Research Supplement.

Specification for Mild Steel Covered Arc Welding Electrodes, American Welding Society (AWS) A5.1 (1969).

Steel, Structural, ASTM A36 (14 August 1979).

Structural Welding Code, D1.1 (AWS, 1979).

Weber, R. A., *Determination of Arc Voltage, Amperage, and Travel Speed Limits by Bead-on-Plate Welding*, Technical Report M-197/ADA033684 (U.S. Army Construction Engineering Research Laboratory [CERL], December 1976).

Weber, R. A., *Determination of the Effect of Current and Travel Speed of Gas Metal-Arc Welding on the Mechanical Properties of A36, A516, and A514 Steels*, Technical Report M-278/ADA085342 (CERL, May 1980).

Welding: Design, Procedures, and Inspection, TM 5-805-7 (HQ, DA, March 1968).

Welding, Mechanical, Corps of Engineers Guide Specification (CEGS) 15116 (DA, Office of the Chief of Engineers [OCE], October 1974).

Welding, Structural, CEGS 05141 (DA, OCE, April 1975).

CERL DISTRIBUTION

Chief of Engineers
ATTN: Tech Monitor
ATTN: DAEN-ASI-L (2)
ATTN: DAEN-CCP
ATTN: DAEN-CW
ATTN: DAEN-CWE
ATTN: DAEN-CWM-R
ATTN: DAEN-CWO
ATTN: DAEN-CWP
ATTN: DAEN-MP
ATTN: DAEN-MPC
ATTN: DAEN-MPE
ATTN: DAEN-MPO
ATTN: DAEN-MPR-A
ATTN: DAEN-RD
ATTN: DAEN-RDC
ATTN: DAEN-RDM
ATTN: DAEN-RM
ATTN: DAEN-ZC
ATTN: DAEN-ZCE
ATTN: DAEN-ZCI
ATTN: DAEN-ZCM

US Army Engineer Districts
ATTN: Library
Alaska
Al Batin
Albuquerque
Baltimore
Buffalo
Charleston
Chicago
Detroit
Far East
Fort Worth
Galveston
Huntington
Jacksonville
Japan
Kansas City
Little Rock
Los Angeles
Louisville
Memphis
Mobile
Nashville
New Orleans
New York
Norfolk
Omaha
Philadelphia
Pittsburgh
Portland
Riyadh
Rock Island
Sacramento
San Francisco
Savannah
Seattle
St. Louis
St. Paul
Tulsa
Vicksburg
Walla Walla
Wilmington

US Army Engineer Divisions
ATTN: Library
Europe
Huntsville
Lower Mississippi Valley
Middle East
Middle East (Rear)
Missouri River
New England
North Atlantic
North Central
North Pacific
Ohio River
Pacific Ocean
South Atlantic
South Pacific
Southwestern

Waterways Experiment Station
ATTN: Library

Cold Regions Research Engineering Lab
ATTN: Library

US Government Printing Office
Receiving Section/Depository Copies (2)

Defense Technical Information Center
ATTN: DDA (12)

Engineering Societies Library
New York, NY

FESA, ATTN: Library

ETL, ATTN: Library

Engr. Studies Center, ATTN: Library

Inst. for Water Res., ATTN: Library

SHAPE
ATTN: Survivability Section, CCB-OPS
Infrastructure Branch, LANDA

HQ USEUCOM
ATTN: ECJ 4/7-LOE

Army Instl. and Major Activities (CONUS)
DARCOM - Dir., Inst., & Svcs.
ATTN: Facilities Engineer
ARRADCOM
Aberdeen Proving Ground
Army Matls. and Mechanics Res. Ctr.
Corpus Christi Army Depot
Harry Diamond Laboratories
Dugway Proving Ground
Jefferson Proving Ground
Fort Monmouth
Letterkenny Army Depot
Natick Research and Dev. Ctr.
New Cumberland Army Depot
Pueblo Army Depot
Red River Army Depot
Redstone Arsenal
Rock Island Arsenal
Savanna Army Depot
Sharpe Army Depot
Seneca Army Depot
Tobyhanna Army Depot
Tooele Army Depot
Watervliet Arsenal
Yuma Proving Ground
White Sands Missile Range

FORSCOM
FORSCOM Engineer, ATTN: AFEN-FE
ATTN: Facilities Engineers
Fort Buchanan
Fort Bragg
Fort Campbell
Fort Carson
Fort Devens
Fort Drum
Fort Hood
Fort Indiantown Gap
Fort Irwin
Fort Sam Houston
Fort Lewis
Fort McCoy
Fort McPherson
Fort George G. Meade
Fort Ord
Fort Polk
Fort Richardson
Fort Riley
Presidio of San Francisco
Fort Sheridan
Fort Stewart
Fort Wainwright
Vancouver Bks.

TRADOC
HQ, TRADOC, ATTN: ATEN-FE
ATTN: Facilities Engineer
Fort Belvoir
Fort Benning
Fort Bliss
Carlisle Barracks
Fort Chaffee
Fort Dix
Fort Eustis
Fort Gordon
Fort Hamilton
Fort Benjamin Harrison
Fort Jackson
Fort Knox
Fort Leavenworth
Fort Lee
Fort McClellan
Fort Monroe
Fort Rucker
Fort Sill
Fort Leonard Wood

INSCOM - Ch, Instl. Div.
ATTN: Facilities Engineer
Vint Hill Farms Station
Arlington Hall Station

WESTCOM
ATTN: Facilities Engineer
Fort Shafter

MDW
ATTN: Facilities Engineer
Cameron Station
Fort Lesley J. McNair
Fort Myer

HSC
HQ USAHSC, ATTN: HSLO-F
ATTN: Facilities Engineer
Fitzsimons Army Medical Center
Walter Reed Army Medical Center

USACC
ATTN: Facilities Engineer
Fort Huachuca
Fort Ritchie

MTMC
HQ, ATTN: MTMC-SA
ATTN: Facilities Engineer
Oakland Army Base
Bayonne MOT
Sunny Point MOT

US Military Academy
ATTN: Facilities Engineer
ATTN: Dept of Geography & Computer Science
ATTN: DSCPER/MAEN-A

USAES, Fort Belvoir, VA
ATTN: ATZA-DTE-EM
ATTN: ATZA-DTE-SW
ATTN: ATZA-FE
ATTN: Engr. Library

Chief Inst. Div., I&SA, Rock Island, IL

USA ARRCOM, ATTN: Dir., Instl & Svc
TARCOM, Fac. Div.
TECOM, ATTN: DRSTE-LG-F
TSARCOM, ATTN: STSAS-F
NARAD COM, ATTN: DRDNA-F
AMMRC, ATTN: DRXMR-WE

HQ, XVIII Airborne Corps and Ft. Bragg
ATTN: AFZA-FE-EE

HQ, 7th Army Training Command
ATTN: AETTG-DEH (5)

HQ USAREUR and 7th Army
ODCS/Engineer
ATTN: AEAEN-EH (4)

V Corps
ATTN: AETVDEH (5)

VII Corps
ATTN: AETSDEH (5)

21st Support Command
ATTN: AEREH (5)

US Army Berlin
ATTN: AEBA-EN (2)

US Army Southern European Task Force
ATTN: AESE-ENG (5)

US Army Installation Support Activity, Europe
ATTN: AEUES-RP

8th USA, Korea
ATTN: EAFE
Cdr, Fac Engr Act (8)
AFE, Yongsan Area
AFE, 2D Inf Div
AFE, Area II Spt Det
AFE, Cp Humphreys
AFE, Pusan
AFE, Taegu

DLA ATTN: DLA-WI

USA Japan (USARJ)
Ch, FE Div
Fac Engr (Army)
Fac Engr (Navy)

ROK/US Combined Force Command
ATTN: EUSA-HHC-CFC/Engr

416th Engineer Command
ATTN: Facilities Engineering

Norton AFB
ATTN: AFRCE-MX/DEE

Port Hueneme, CA 93043
ATTN: Library (Code LOBA)

AFESC/Engineering & Service Lab
Tyndall AFB, FL 32403

Chanute AFB, IL 61868
3345 CES/DE, Stop 27

National Guard Bureau
Installation Division
WASH DC 20310

EMM Team Distribution

Director of Facilities Engineering
ATTN: AFZI-FE-E
Ft. Richardson, AK 99505

Ft. Clayton, Canal Zone 34004
ATTN: DFAE

West Point, NY 10996
ATTN: Dept of Mechanics
ATTN: Library

Chief of Engineers
ATTN: DAEN-MPO-U
ATTN: DAEN-MPZ-A
ATTN: DAEN-MPR

Fort Belvoir, VA 22060
ATTN: Canadian Liaison Officer (2)

Fort Leavenworth, KS 66027
ATTN: ATZLCA-SA

Fort McPherson, GA 30330
ATTN: AFEN-CD

Fort Monroe, VA 23651
ATTN: ATEN-AD (3)

6th US Army
ATTN: AFKC-EN

7th US Army
ATTN: AETTM-HRD-EHD

US Army Science & Technology
Center - Far East Office

US Army Engineer District
Philadelphia
ATTN: Chief, NAPEN-D
Baltimore
ATTN: Chief, Engr Div
Norfolk
ATTN: Chief, NAOEN-D
Wilmington
ATTN: Chief, SAWEN-O
Charleston
ATTN: Chief, Engr Div
Savannah
ATTN: Chief, SASAS-L
Jacksonville
ATTN: Const Div
Mobile
ATTN: Chief, SAMEN-C
ATTN: Chief, SAMEN-D
Memphis
ATTN: Chief, LMMED-DM
Vicksburg
ATTN: Chief, Engr Div
Louisville
ATTN: Chief, Engr Div
St. Paul
ATTN: Chief, ED-D
Omaha
ATTN: Chief, Engr Div
New Orleans
ATTN: Chief, LMNED-DG
Little Rock
ATTN: Chief, Engr Div
San Francisco
ATTN: Chief, Engr Div
Sacramento
ATTN: Chief, SPKED-D
Portland
ATTN: Chief, DB-6
Seattle
ATTN: Chief, NPSCO
Walla Walla
ATTN: Chief, Engr Div
Alaska
ATTN: Chief, NPASA-R

US Army Engineer Division
New England
ATTN: Chief, NEDED-T
North Atlantic
ATTN: Chief, NADEN-T
South Atlantic
ATTN: Chief, SADEN-TS
Huntsville
ATTN: Chief, HNDED-CS
ATTN: Chief, HNDED-SR
Ohio River
ATTN: Chief, Engr Div
Southwestern
ATTN: SWDED-TM
Pacific Ocean
ATTN: Chief, Engr Div
North Pacific
ATTN: Chief, Engr Div

AFESC/PRT
Tyndall AFB, FL 32403

Tinker AFB, OK 73145
2854 ABG/DEEE

Patrick AFB, FL 32925
ATTN: XRQ

Naval Air Systems Command
ATTN: Library
WASH DC 20360

Naval Facilities Engr Command
ATTN: Code 04
Alexandria, VA 22332

Washington, DC
ATTN: Transportation Research Board

ATTN: Dept of Transportation Library

National Defense Headquarters
Director General of Construction
Ottawa, Ontario
Canada K1A 0K2

Airports and Construction Services Dir
Technical Information Reference Centre
Ottawa, Ontario
Canada K1A 0N8

Weber, Robert A.
Weldability characteristics of construction steels A36, A514, and A516. -- Champaign, IL : Construction Engineering Research Laboratory ; available from NTIS, 1981.
97 p. (Technical report ; M-302)

1. Steel, structural - welding. I. Title. II. Series : U. S. Army. Construction Engineering Research Laboratory. Technical report ; M-302.

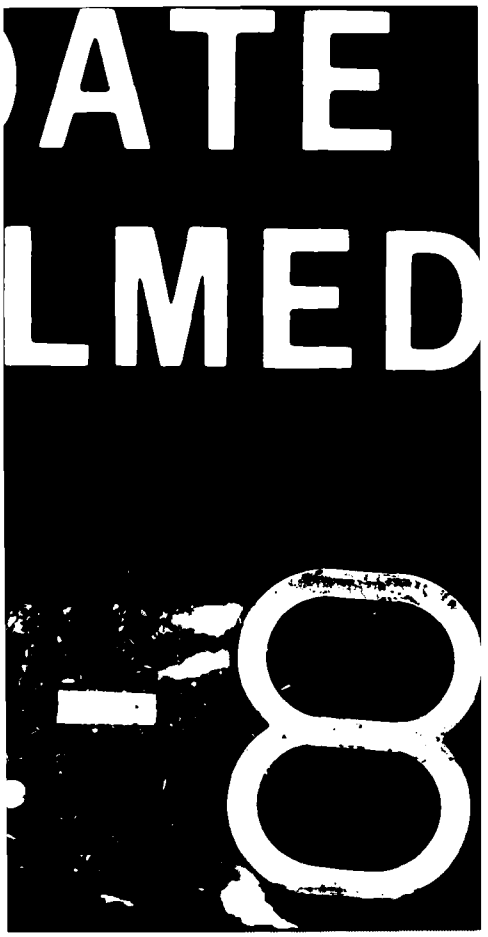
ATE
LMED
8